CNEA - NT 3/76

Progress Report
Department of Nuclear Physics
1974 - 1975

Comisión Nacional
de Energía Atómica

Area de Investigación
Desarrollo y Servicios

República Argentina

Buenos Aires - March 1976

CNEA - NT 3/76

Progress Report
Department of Nuclear Physics
1974 - 1975

Comisión Nacional
de Energía Atómica

Area de Investigación
Desarrollo y Servicios

República Argentina

Buenos Aires - March 1976

INTRODUCTION

The Nuclear Physics Department of the Comisión Nacional de Energía Atómica is not new. It already has a history of its own having gone through prosperous as well as difficult times. However, in spite of tis age, this is the first Progress Report produced by our Department. Hence it deserves a somewhat special introduction so that the present can be put in a better perspective.

The Nuclear Physics Department is one of the oldest of the CNEA. Most scientists among the first group to be incorporated in 1951 worked in the field of Nuclear Science. If one were to pick out the most important events in the development of our Department, perhaps the dedication in 1954 of the Philips Sinchrocyclotron capable of delivering 28 MeV deuterons, and the decision in 1965 to undertake a joint program with physicists from the University to study Isotopes Far off the Stability Line (IALE project), should be mentioned. But many other episodes and efforts should also be remembered, like the earliest experiments with the first "big" accelerator in Argentina, a 1.2 ME Cockcroft-Walton acquired in 1952, or the Slobodrian-Bilaniuk report on their evidence for the existence of the diproton in 1961, or the patient and careful work of the β-ray spectroscopists with their Scandinavian orange and double focussing spectrometers. The number of papers presented at the 1958 IAEA Conference on Peaceful Uses of the Atomic Energy appropriately reflects the rapid growth and vitality of the Department at that time.

In 1966, however, the massive emigration of physicists from the University of Buenos Aires represented a heavy blow for the Department, particularly in view of the fruitful joint program that had just been started. Nevertheless the IALE project survived and since the first results were obtained, a steady and considerable output has been produced.

In recent years the Department acquired a new dimension with the formation of the theoretical group. Quite fortunately for our development the interaction between theoreticians and experimentalists has been strong and fruitful to a degree rarely found in other laboratories in the world. The meritorious work on $(d,^{6}Li)$ reactions carried out at the Synchrocyclotron is a nice example in this respect. A new development has been the initiation of the (α,xn) program at the Synchrocyclotron which was accompanied by the incorporation of new physicists. This program, started in 1973, has already yielded a good number of interesting results. The activities in both this and the theoretical fields enhanced our friendly and productive contact with colleagues and institutions abroad.

Reading through the pages of this report we sense a feeling of pride. The contributors are many and they all have had to struggle against unfavourable conditions and obsolete machines.

The last years have been difficult and the general environment for research has not been stimulating. However, the work described here indicates that the Department has managed to remain as vigorous as ever. This brief account shows that there have been, as in every institution, good and bad times. If the present results spring from the latter, we should be very hopeful about the future. This Progress Report is a testimony of our faith.

Many people have worked in the Department who are not among us now. This report should also serve as a tribute to them

The responsible of the enterprise of putting together all the material in an appropriate form has been Edgardo Ventura, who for many weeks kept us on our toes, working at a hectic pace. At one time or another we all hated him, but now that it is over we deeply appreciate his work. He has done so well that we very much hope he will be at it next year!

Mario A. J. Mariscotti

SUMMARY

The programme of research of the Department of Nuclear Physics has been mostly oriented towards nuclear structure investigations, both from an experimental and theoretical point of view.

One of the major efforts over the past two years has been the use of the alpha-beam from the Synchrocyclotron in the study of (α,xn) reactions. This also involved the development of a beam energy degrader (E_{α} = 30-55 MeV) and facilities for the measurement of nuclear half-lives in the μsec, nsec and msec range. The experiments carried out mostly involved the study of odd-odd nuclei in the $64 \leq A \leq 76$ region, as well as properties of individual states in neighbouring nuclei.

The on-line facility, consisting of the cascade accelerator and the isotope separator, has continued to yield considerable information on the structure of nuclei far away from the stability line. The facility has been up-dated by the development of a new ion-source capable of producing non-gaseous fission products.

Radioactivity (off-line) studies consititute a new addition to the present facilities. A set-up for the measurement of gamma-gamma angular correlations and gamma-gamma polarized directional correlations has been completed and used to determine spins, parities and mixing ratios. This set-up is also currently being used to study radiation damage in solids by means of perturbed angular correlations.

The theoretical group has focussed its attention on problems of nuclear structure and nuclear reactions. The nuclear structure work has been highlighted by the formulation of a nuclear field theory. The theory allows the simultaneous treatment of collective and single-particle degrees of freedom and the corresponding problems of Pauli principle violations and overcompletness. In addition shape and pairing phase transitions have been studied within the framework of microscopical and phenomenological models. In the field of nuclear reactions the efforts were mainly concentrated in the study of isospin dependence of the optical parameters and coupled-channel calculations.

The Department has always been involved in activities supporting other areas of research and development of the C.N.E.A. To such extent a program to evaluate the utilization of thorium in power reactors has been initiated. In addition, a group to study the utilization of solar energy has been created.

Many of the achievements of this Department could not have been carried out without the continuous and efficient support of the former and present heads of

the Research and Development Branch of the C.N.E.A., Dr. E.Pérez Ferreira and Dr. R.Cabrini, respectively. It is there a pleasure to acknowledge their help and understanding.

This Progress Report is our first venture in this field. Many thanks are offered to the authors who so willingly contributed to write the reports; to Mrs. J.Corvalán and Mrs. M.Neufeld for their enormous patience and skills in the preparation of the manuscript; and to Mr. A.Binda for his valuable help in the printing of this work.

Edgardo Ventura

TABLE OF CONTENTS

PART B - THEORETICAL PHYSICS

V. NUCLEAR STRUCTURE.

VI. NUCLEAR REACTIONS.

APPENDIX

PART A

EXPERIMENTAL PHYSICS

I. TRANSFER REACTIONS

I.1. The (d,^{6}Li) Reaction in the f-p Shell at E_d = 27.25 MeV.

A.E.Ceballos, H.J.Erramuspe, A.M.J.Ferrero, M.J.Sametband*, J.E.Testoni**, D.R.Bes, E.E.Maqueda, R.P.J.Perazzo and S.L. Reich.

As early as 1970, as a consequence of a study[1] of the T = 1 pairing force, it was suggested that whenever the transfer of two nucleons coupled to $J^{\pi}T = 0^{+}1$ is favoured, an enhancement of the α-particle transfer, may also be expected. Thus, a formalism for the (d,^{6}Li) reaction was developed[2] and a set of experiments was started[3,4] using the 27.25 MeV deuteron beam from the Buenos Aires Synchrocyclotron on targets in the Ni-Zn region, where a detailed nuclear structure study was possible.

Previous arguments[5] casted some doubts on the viability of (d,^{6}Li) reactions on targets heavier than Ca at bombarding energies of the order of 30 MeV. In spite of this, it was possible to measure angular distributions corresponding to the population of the lowest two states in the reactions ^{64,66,68}Zn(d,^{6}Li) ^{60,62,64}Ni. Later,measurements were also made on targets of ^{56}Fe and ^{58}Ni, and the theoretical analysis was performed throughout this region.

The measurements described here have been performed by bombarding self-supporting metallic foils with the external 27.25 MeV deuteron beam of the Synchrocyclotron of the CNEA. The targets used in the experiment were enriched foils of ^{56}Fe(99.95%) and ^{58}Ni(99.96%), 0.800 mg/cm^2 and 1.13 mg/cm^2 thick respectively.

The experimental set-up consisted of two independent (E - ΔE) detector telescopes, operating simultaneously and placed in a symmetrical arrangement off the azimuthal plane; they were mounted on a moving plate whose position could be determined to within 0.05° relative to the zero direction. The telescopes consisted of two sets of (100 - 50) μm and (90 - 55) μm fully depleted surface barrier Si detectors. They allowed the ^{6}Li ions to be completely stopped, whereas the lighter products of the reaction and the involved pile-up were well identified or did not interfere significantly with the nuclear levels studied. The overall energy resolution was estimated in 400 keV FWHM.

The electronic set-up consisted of two conventional chains functionally identical. The events were registered in a 4096-channel Intertechnique analyzer working in two 32 x 64 channel bidimensional mode.

As a typical example, Fig. I.1.1 shows the spectrum of the ^{6}Li ions produced in the ^{64}Zn(d,^{6}Li)^{60}Ni reaction at 30° in the lab. system. The 0^+ ground state and the 1.33 MeV 2^+ level of the residual nucleus are clearly resolved. Because of the Q-value the ^{59}Ni states populated in the ^{64}Zn(d,^{7}Li)^{59}Ni reaction are at least 4.13 MeV below the 0^+ ground state of ^{60}Ni. Similar kinematic effects occur in almost all nuclei in the medium mass region, allowing the separation of the lowest states of the different isotopes.

Figures 1.1.2 and 1.1.3 show the angular distributions of the differential cross sections corresponding to the 0^+ ground state and the lowest 2^+ state of the residual nuclei for the reactions ^{56}Fe(d,^{6}Li)^{52}Cr, ^{58}Ni(d,^{6}Li)^{54}Fe and ^{64,66,68}Zn(d,^{6}Li)^{60,62,64}Ni. The data are given in the c.m. system.

The patterns and magnitudes of the angular distributions in the zone close to the doubly magic ^{56}Ni are quite similar to those obtained in the Zn region. This fact suggests the pick-up of a superficial α-cluster through a mechanism independent of the progressive filling of the shell. They all show the diffraction structure and forward peaking characteristics of a direct reaction mechanism. This fact may be simply expected by the small probability of a ^{6}Li emission in a compound nucleus reaction. The magnitudes of the measured cross sections range approximately between 1 μb/sr and 20 μb/sr, the higher values corresponding to the lower mass number. These results are consistent with the ones reported for lighter nuclei and in particular with those obtained on Ca[7] at 19.5 MeV. A DWBA calculation indicates that the Zn(d,^{6}Li)Ni cross-sections are about the same for an incident energy of 19.5 MeV, in spite of the fact that in such case the Li ions are emitted with an energy corresponding to about the Coulomb barrier height.

The DWBA analysis of the experimental results has been performed by using the DWUCK code[8] under the assumption that the (d,^{6}Li) reactions proceed through a direct interaction mechanism and in a pick-up process a cluster α moving in the averaged potential of the core is transferred to the incoming deuteron to form the ^{6}Li ion.

It is assumed that the transferred α particle is a point ($m = 4$) mass; thus we can construct a phenomenological form factor using the wave function of an α particle moving in a Woods-Saxon potential whose radius,diffusenes and depth are calculated such to bind the nuclear states described by a radial wave function with orbital quantum numbers $N = 0$-7 and $N = 0$-6 for angular momentum $L = 0$ and $L = 2$ respectively.

The optical parameters for the entrance channel has been taken from ref. 9, the Li parameters were chosen within reasonable ranges in order to yield good agreement with the experimental data. Both sets of optical parameters are shown in Table 1.1.1. Only the real potential V presents some variation with the mass of the target nucleus; the Coulomb radius in large in the outgoing channel as a consequence of the finite size of the ^{6}Li ions.

In order to check the validity of the structure factors extracted from the experimental data, an extensive survey of the influence of the different Li optical parameters has been performed.

The form factor has been constructed according to the formalism proposed by Dragún et al[2] as a coherent sum over the allowed quantum number N.

Solid lines in Figs. I.1.2 and I.1.3 correspond to the DWBA calculations, computed with the structure factors G_{NL} obtained from the different theoretical approximations[6]. Each curve is normalized with the corresponding value of $D_o^2 = \sigma_{exp}/\sigma_{DWUCK}$.

The analysis of the α-transitions populating the $J^{\pi} = 0^+$ states has been made under the assumption that the main component of the residual nuclear interaction which is relevant in this process is the T = 1 part of the pairing force.

The calculation of the microscopic form factor has been performed in four different ways:

a) through an exact diagonalization of the residual pairing force in a four-level shell model basis[1,10].
b) considering a simple shell model pure configuration.
c) assuming that the (d,^{6}Li) reaction leading to the 0^+ ground states of the residual nuclei are transitions between vibrational states described in terms of addition and removal phonons[1,11].
d) through a description in terms of the pairing-plus-quadrupole model, which are treated within the BCS and RPA approximation [12,13].

For the analysis of the transitions leading to the $J^{\pi} = 2^+$ final states, the experimental results have been divided in two groups according to whether they take place around A = 56 or on the ^{A}Zn region. For the first group it is easy to perform a calculation with almost pure configurations; in the case of the ^{A}Zn targets the final $J^{\pi} = 2^+$ states of the $^{A-4}$Ni isotopes are described in terms of the pairing-plus-quadrupole model which are treated within the BCS and RPA approximation as in the case d) for $J^{\pi} = 0^+$.

Conclusions

They are considered in refs. 2, 3, 4, 6 and they point essentially:

a) the good agreement of the experimental results with the calculations performed under the assumption of a direct interaction mechanism.
b) the agreement between the magnitudes of the measured experimental differential cross-sections and those obtained for the four particle transfer in lighter nuclei.

c) the validity of the optical parameters used for the DWBA calculations, allowing the relative strength of the 0^+ and 2^+ states to be determined within an error of 20%.
d) the validity of the theoretical assumptions formulated to account for the transitions leading to the final nuclear states $J^\pi = 0^+$ and $J^\pi = 2^+$.

The relationship between the cross sections for the (d,^{6}Li) reactions and the pairing degree of freedom was again pointed out in a recent paper by Becchetti et al[14].

---

* Present address: Departamento de Combustibles Nucleares (CNEA).

** Present address: Departamento de Reactores (CNEA).

1 G.G.Dussel, E.E.Maqueda and R.P.J.Perazzo, Nucl. Phys. A153 (1970) 469.
2 O.Dragún, G.G.Dussel, E.E.Maqueda and R.P.J.Perazzo, Nucl. Phys. A167 (1971) 529.
3 A.E.Ceballos, H.J.Erramuspe, A.M.J.Ferrero, M.J.Sametband and J.E.Testoni, Phys. Rev. C4 (1971) 1959.
4 A.E.Ceballos, H.J.Erramuspe, A.M.J.Ferrero, M.J.Sametband, J.E.Testoni, D.R. Bes and E.E.Maqueda, Nucl. Phys. A208 (1973) 617.
5 W.W.Daehnick and L.J.Denes, Phys. Rev. 136 (1964) 1325.
6 A.E.Ceballos, H.J.Erramuspe, A.M.J.Ferrero, M.J.Sametband, J.E.Testoni, D.R. Bes, E.E.Maqueda, R.P.J.Perazzo and S.L.Reich, Nucl. Phys. A228 (1974) 216.
7 H.Gutbrod, H.Yoshida and R.Bock, Nucl. Phys. A165 (1971) 240.
8 P.D.Kunz, University of Colorado, rep. COO-535-606 (unpublished).
9 P.E.Hodgson, Adv. in Physics, Phil. Mag. Suppl. 15 (1966) 321.
10 D.R.Bes, E.E.Maqueda and R.P.J.Perazzo, Nucl. Phys. A199 (1973) 193.
11 A.Bohr, Proc. Int. Symp. on Nuclear Structure, Dubna, 1968 (IAEA, Vienna, 1968) p. 179.
B.Bayman, D.R.Bes and R.A.Broglia, Phys. Rev. Lett. 23 (1969) 1299.
12 L.S.Kisslinger and R.Sorensen, Rev. Mod. Phys. 35 (1963) 910.
13 D.R.Bes and R.Sorensen, Adv. in Nucl. Phys., vol. 2 (Plenum Press, 1969) p. 129.
14 F.D.Becchetti, L.T.Chua, J.Jaenecke and A.M.Vander Molen, Phys. Rev. Lett. 34 (1975) 225.

Table I.1.1

The optical parameters for the deuteron and lithium channels and the parameters for the bound α-particle well

	d-channel	Li channel	α-particle well
V (MeV)	71.9	310 for ^{56}Fe 312 for ^{58}Ni 328 for ^{64}Zn 321 for ^{66}Zn 310 for ^{68}Zn	Adjusted to get the binding energy
W (MeV)	56.0	75.0	
r_{ov} (fm)	0.96	1.50	1.25
a_v (fm)	0.99	0.65	0.65
r_{ow} (fm)	1.35	1.50	
a_w (fm)	0.75	0.65	
r_{oc} (fm)	1.25	2.50	1.25
a_c (fm)	0.00	0.00	0.00

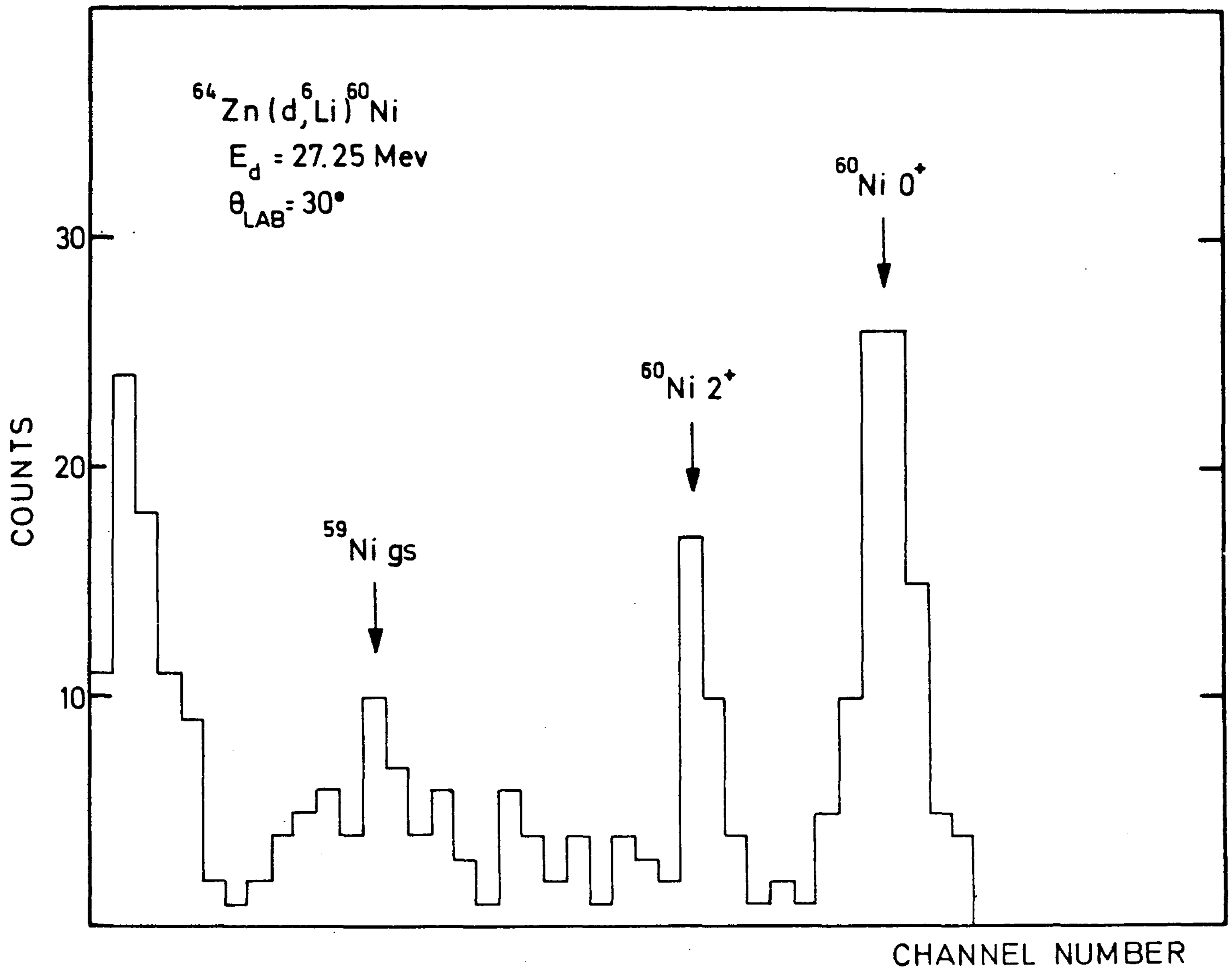

<u>Fig. I.1.1</u> The spectrum of Li ions obtained in reactions on ^{64}Zn induced by 27.25 MeV deuterons, at $\theta_{lab} = 30°$.

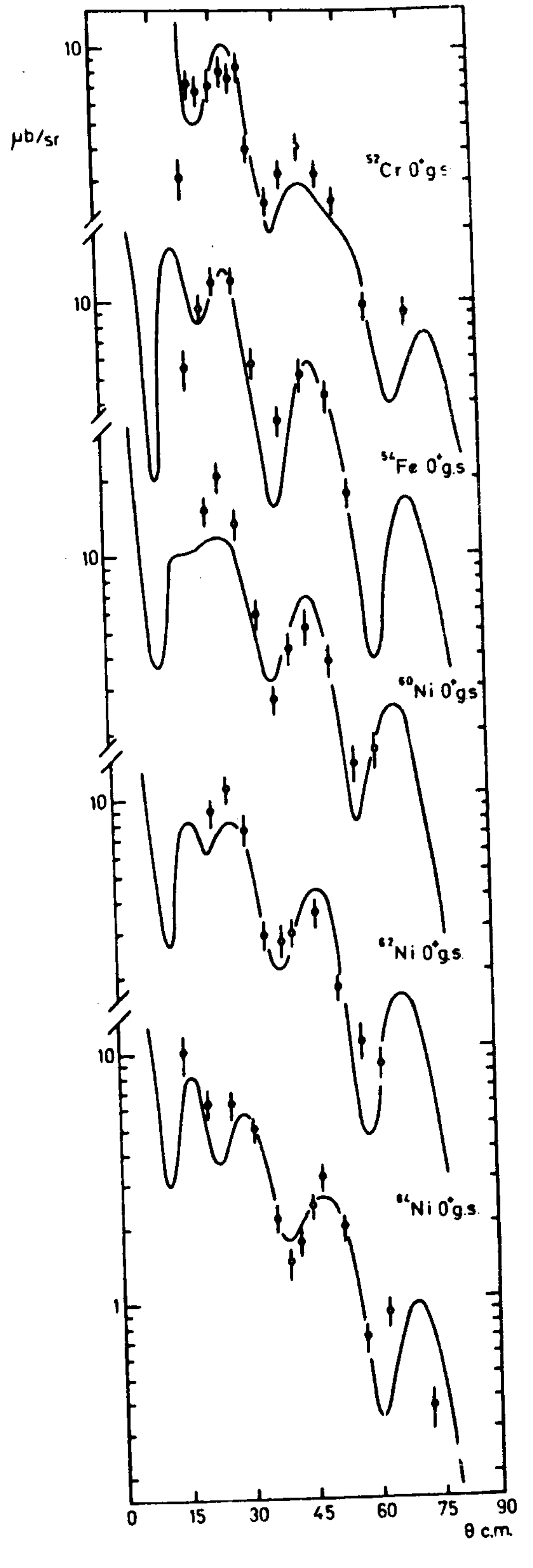

Fig. 1.1.2 The differential cross sections of the reactions $^{56}Fe(d,{}^{6}Li)^{52}Cr$, $^{58}Ni(d,{}^{6}Li)^{54}Fe$ and $^{64,66,68}Zn(d,{}^{6}Li)^{60,62,64}Ni$, leading to the 0^+ ground state at E_d = 27.25 MeV. Solid lines represent DWBA calculations.

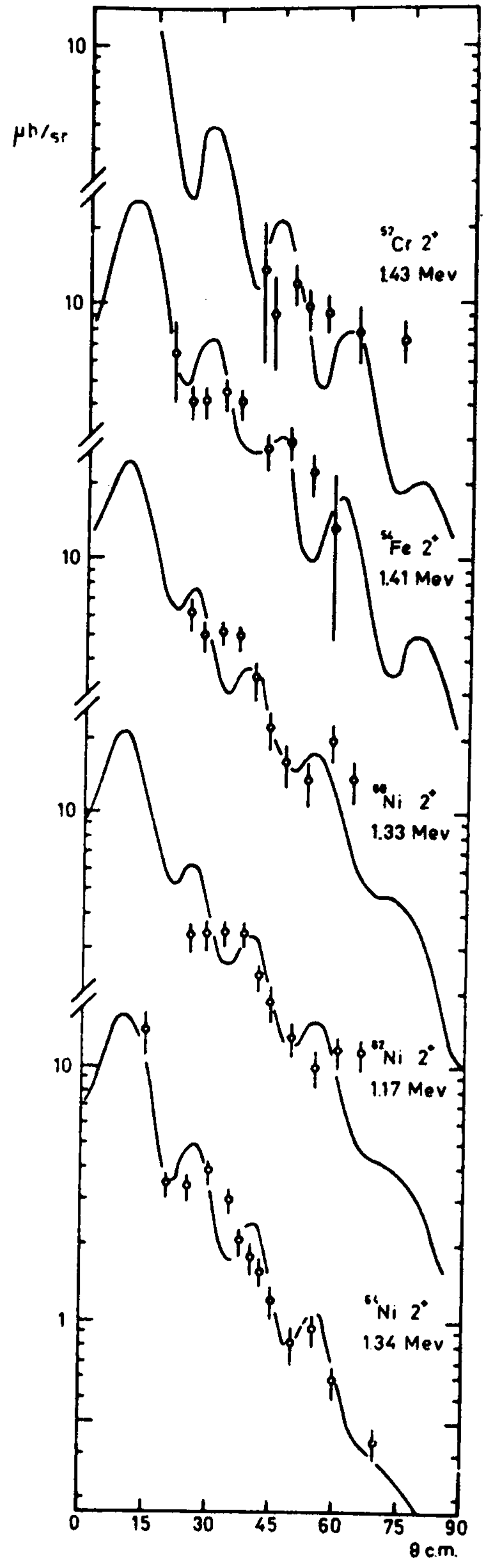

Fig. 1.1.3 The differential cross sections of the reactions $^{56}Fe(d,{}^{6}Li)^{52}Cr$, $^{58}Ni(d,{}^{6}Li)^{54}Fe$ and $^{64,66,68}Zn(d,{}^{6}Li)^{60,62,64}Ni$, leading to the 2^+ first excited state at E_d = 27.25 MeV. Solid lines represent the DWBA calculations.

II. GAMMA RAY SPECTROSCOPY BY MEANS OF (α,xnyp) REACTIONS

II.1. Possible K = 1/2 Quasirotational Band in ^{73}Se.

M.Behar, A.Filevich, G.García Bermudez, A.M.Hernández and M.A.J. Mariscotti.

Our knowledge of the ^{73}Se level scheme was until now limited to the study of the decay of ^{73}Br[1]. Little is known about spins and other properties of the levels populated in these decays, namely that the ground and first excited states are $7/2^+$ and $1/2^-$, respectively[2].

The fact that the ground state is $7/2^+$ instead of $9/2^+$, is an indication of an anomalous coupling. Recently, Kuriyama et al.[3] have developed a new theory and were successful in reproducing the experimental trend in the systematics of the excitation energies. In the framework of this theory, when the excitation energy of the mode with spin J-1($7/2^+$ in the present case) becomes equal or smaller than the energy of the one-quasiparticle state with spin J($9/2^+$), an instability of the spherical shape may occur and the onset of deformation should be expected. If the existence of the anomalous $7/2^+$ state implies a deformed structure, this should give rise to a rotational structure. In order to explore this possibility we have investigated the (α,3n) reaction leading to levels in ^{73}Se which is well suited for this purpose.

An 82% enriched ^{72}Ge target was bombarded with the α-particle beam from the Buenos Aires Synchrocyclotron. Excitation functions were measured in the energy range 30 to 55 MeV; and γ-γ coincidences and angular distributions were obtained at 35 MeV. The results of these measurements are summarized in the decay scheme shown in Fig. II.1.1.

As mentioned above, the ground state of ^{73}Se is $7/2^+$ and therefore one expects some indication of nuclear deformation. However in the present work we have not obtained evidence for a rotational band built on this state as should be expected if it were deformed. On the other hand, the levels observed here decaying to the 25 keV $J^\pi = 1/2^-$ state actually exhibit a spin sequence, energy spacing, and decay pattern consistent with a rotational structure. In order to further explore this point we have adjusted the energy sequence to the expression

$$E_{IK} = \varepsilon_K + \frac{\hbar^2}{2J}\left[I(I+1) - \frac{1}{2} + a\,(-1)^{I+1/2}\,(I+1/2)\right]^2 \qquad (1)$$

which is characteristic of a K = 1/2 rotational band. The results are summarized in Fig. II.1.2. The moment of inertia used in the calculation

(j = 0.01 $\hbar^2$) is about three times smaller than those typically found in the well deformed rare-earth nuclei; and comparable to those of nuclei with N = 88-90, that is just where the transition between spherical and deformed shapes takes place. Because transitional nuclei exhibiting small ground state moments of inertia are soft (i.e. moment of inertia increases with spin I), a least squares fit was carried out allowing the moment of inertia to vary linearly with I. The result of this improved fit is indicated in Fig. II.1.2 with solid triangles.

A second test for the rotational band picture of this level scheme is to compare the experimental branching ratio for each level with the single particle and unified models predictions. This comparison, shown in Table II.1.1 again supports the hypothesis of a rotational band built on the $1/2^-$ state of ^{73}Se.

---

[1] G.Murray, W.J.White, J.C.Willmott and R.F.Entwistle, Nucl. Phys. A142 (1970) 21.

[2] G.Murray, W.J.White, J.C.Willmott and R.F.Entwistle, Phys. Lett. 28B (1968) 35.

[3] A.Kuriyama, T.Marumori and K.Matsyuanagi, Prog. Theor. Phys. 47 (1972) 498.

Table II.1.1

Comparison of Experimental Branching Ratios with Theoretical Predictions

Level Energy (keV)	I	$T(M1 + E2, I \rightarrow I - 1) / T(E2, I \rightarrow I - 2)$		
		Single particle	Strong coupling	Experiment
505.1	5/2	1000	> 6	3.4 ± 0.6
804.4	7/2	100	> 0.06	0.78 ± 0.10
1178.1	9/2	100	> 0.30	1.13 ± 0.20

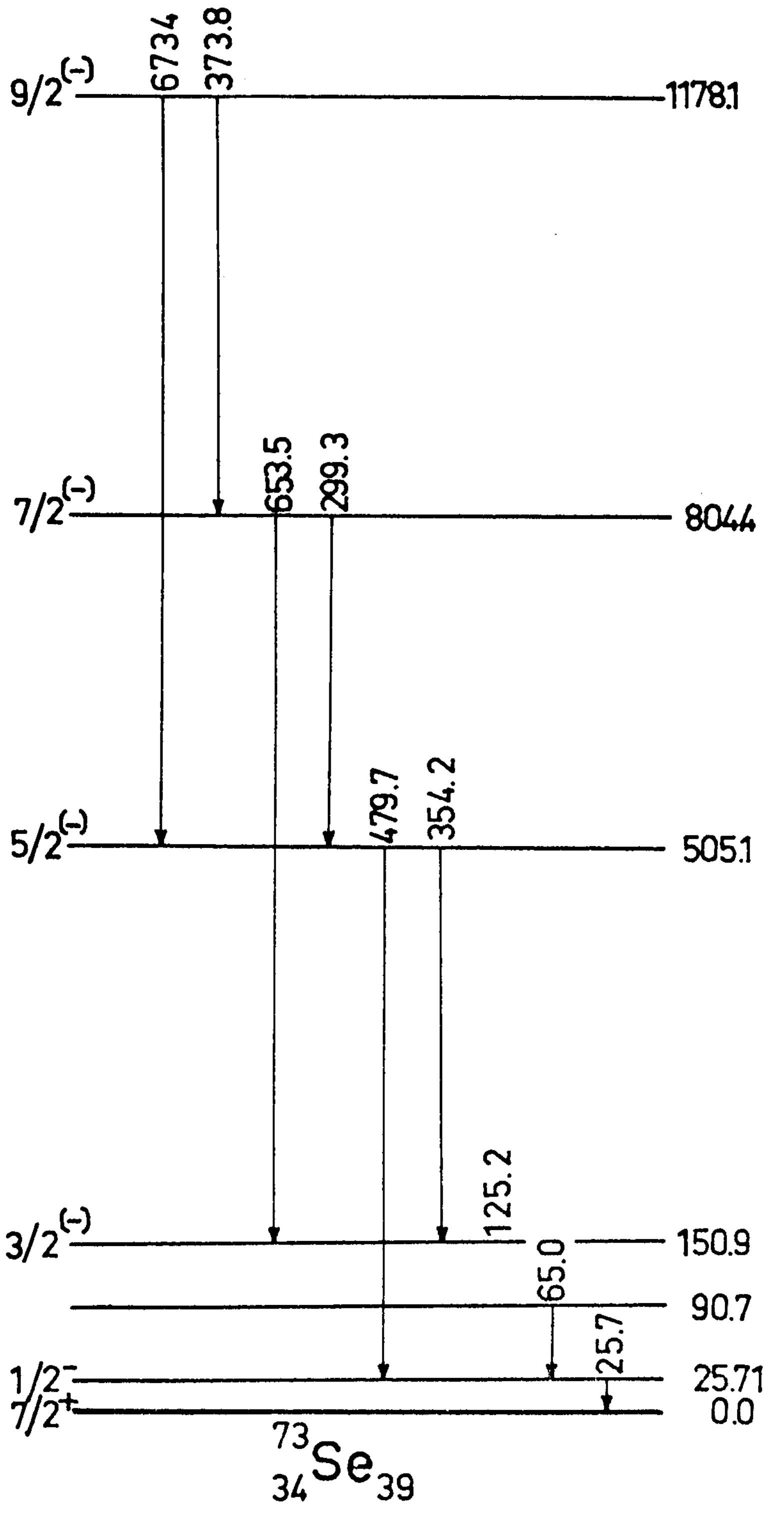

Fig. II.1.1 Level scheme of ^{73}Se obtained in the present work.

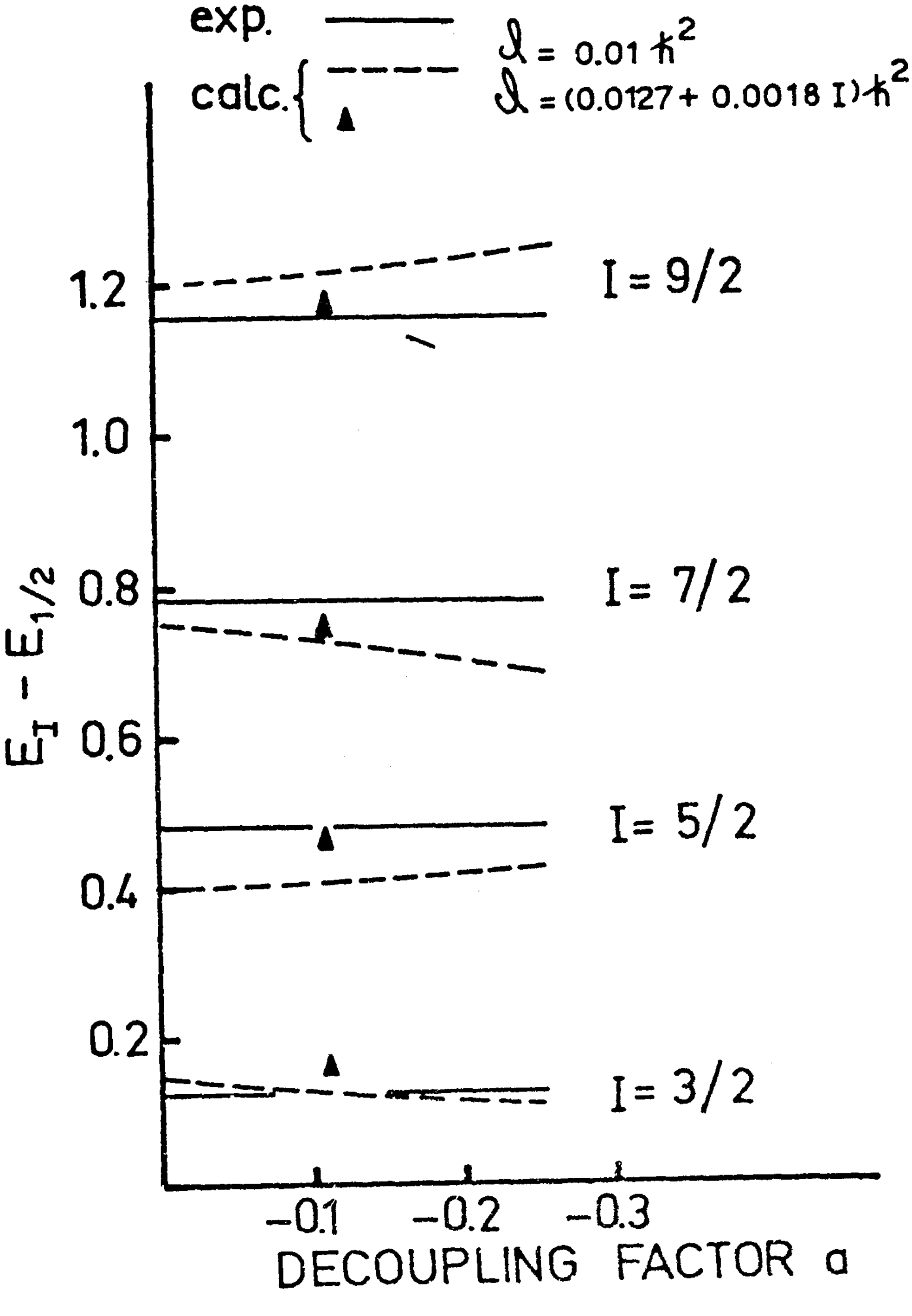

Fig. II.1.2 Comparison of experimental and calculated energies for ^{73}Se. The dashed lines, obtained from the rigid rotor model, are shown as a function of the decoupling parameter α. The triangles indicate the results obtained by assuming a linear variation of the moment of inertia with angular momentum I.

II.2. Structure of ^{70}As Studied with the $^{70}Ge(\alpha,3np)^{70}As$ Reaction.

A.Filevich, M.Behar, G.García Bermudez and M.A.J.Mariscotti.

The level structure of the odd-odd nucleus $^{70}_{31}As_{39}$ has up to now only been investigated by ten Brink et al.[1] by means of the radioactive decay of ^{70}Se. Since no reaction studies of this nucleus have been made, we have investigated the $^{70}Ge(\alpha,3np)^{70}As$ reaction with the idea of populating high-spin states whose subsequent decay would add new nuclear structure information. The existence of relative high-spin states in ^{70}As at low excitation energies can be expected because the spin and parity of its ground state is $J^{\pi} = 4^{+}$.

The experiment consisted of several runs in which single γ-ray spectra at different bombarding energies were measured. From the excitation functions so obtained, it was possible to identify five different γ-rays (75.9, 81.2, 134.6, 318.8, 320.2 keV) as belonging to ^{70}As. In order to confirm these assignments and build up a level-scheme for this nucleus, γ-γ coincidences were measured with gates set on the above mentioned γ-rays. The results enabled us to construct the level scheme shown in Fig. II.2.1. The order of the 318 keV and 134 keV γ-rays has been adopted on the basis of their intensities. In addition, the measurement of the half-life of the 81 keV γ-ray yielded a value of $T_{1/2} = 9.2 \pm 4$ nsec, (see Fig. II.2.2), which allowed us to make an assignment of J = 5 to the 81.2 keV level of ^{70}As.

The errors in the measurement of the γ-ray angular distributions do not allow the determination of the γ-ray multipolarities. However, in the case of the 81.2 keV γ-ray the experimental angular distribution suggests a $\Delta I = 1$ transition with large mixing ratio implying a strong M1/E2 mixture, and hence a positive parity assignment for this state. The absence of cross-over transitions suggests assignments of J = 6 and J = 7 for the 400.0 and 534 keV states, respectively.

The results obtained in the present work indicate a strong selectivity of the $(\alpha,3np)$ reactions to excite only a few levels in the product nucleus. This fact is in good agreement with the results in other odd-odd neighboring nuclei (see following sections). It is interesting to note that the levels observed in ^{70}As show a remarkable similarity with those in ^{72}As and ^{74}As having level sequences with spin J = 4,5,6,7 and level spacings of approximately 55, 200 and 120 keV, respectively (see Sects. II.2.3 and II.2.4).

Further experiments are planned in order to improve the precission of these measurements.

---

[1] B.O.ten Brink, R.D.Vis, A.W.B.Kalshoven and H.Verheul, Z. Phys. 270 (1974) 83.

[2] A.P.de Ruiter, H.Verheul and J.Konijn, Nucl. Phys. A116 (1968) 473.

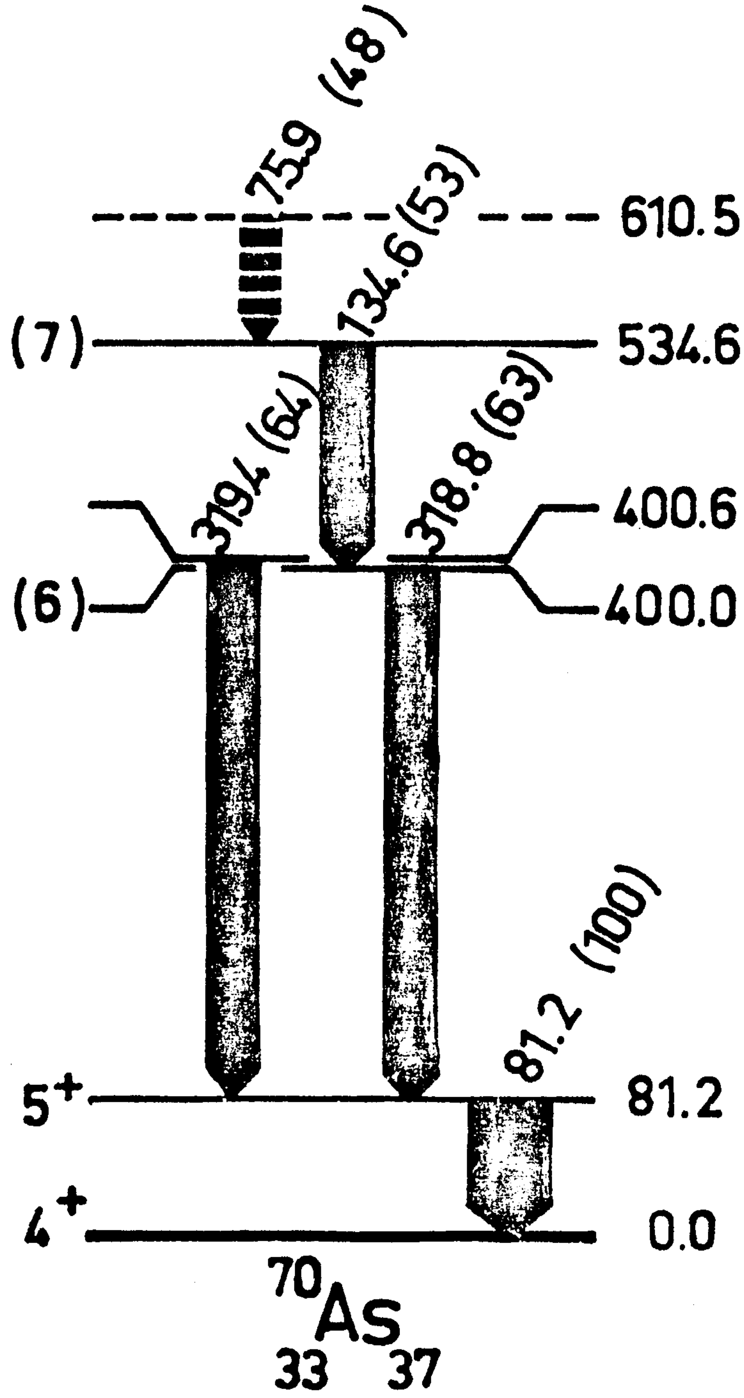

Fig. II.2.1 Preliminary level scheme for ^{70}As.

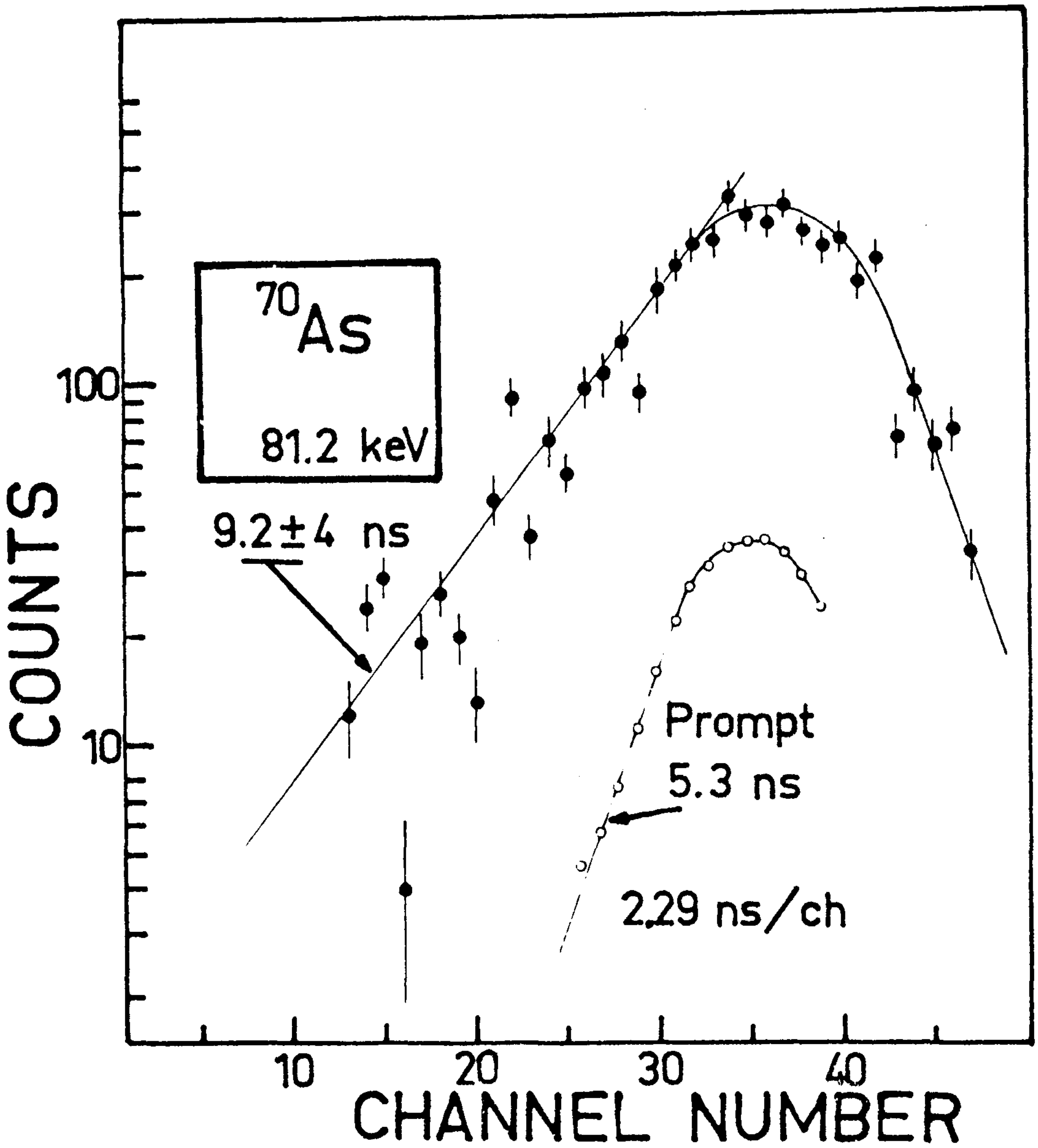

Fig. II.2.2 Decay of the 81.1 keV γ-ray in ^{70}As. A pure prompt peak is shown for comparison.

II.3. Level Structure of ^{72}As from the $^{70}Ge(\alpha,np)$ Reaction.

M.A.J.Mariscotti, M.Behar, A.Filevich, G.García Bermudez and A.M.Hernández.

The low-spin levels of ^{72}As have been previously studied[1,2] by means of the (p,n) reaction at $E_p \simeq 5$ MeV. As part of a research program to study high spin states in odd-odd nuclei we have investigated the $^{70}Ge(\alpha,pn)^{72}As$ reaction and the $^{72}Ge(\alpha,3np)^{72}As$ reaction.

A preliminary γ-ray identification was obtained by means of excitation functions using as reference those γ-rays previously assigned[1,2] to ^{72}As (see Chapter X).

With a fixed bombarding energy $E_\alpha = 35$ MeV, the (α,np) reaction was used to measure γ-γ coincidences, angular distributions and time distributions in the nsec range. As a result of these measurements the level scheme shown in Fig. II.3.1(c) was produced. This is compared to previous results shown in Figs. II.3.1(a) and II.3.1(b).

Except for the 414.1 keV level (which can be identified with the 413 keV level of Mordechai et al.[2]) all the levels observed in the present work above $E_x = 320$ keV are different from those observed in the (p,n) reaction. The new levels have spin assignments up to J = 7. Our measurements confirm the assignment[1] of $J^\pi = 3^+$ to the 213.8 keV state.

The time distributions allowed us to establish a halflife $T_{1/2} = 17 \pm 3$ nsec for the 309.8 keV state and $T_{1/2} < 3.7$ nsec for the 362.8 keV level. The proposed spin and parity assignments for these levels are $J^\pi = 4^-$ and J = 5, respectively. In addition the dipole moment of the ground state[3] is explained assuming a $\{\pi f_{5/2} \nu g_{9/2}\}_{2^-}$ configuration for this state. The existence of an isomeric state with $T_{1/2} > 100$ nsec at $E_x > 362.8$ keV was also observed.

---

1 H.Bertschat et al., Int. Conf. Nuclear Moments and Nuclear Structure, Osaka, Japan, p. 171, (1972).

2 S.Mordechai et al., Nucl. Phys. A230 (1974) 343.

3 E.A.Phillips et al., Bull. Am. Phys. Soc. 14 (1968) 944.

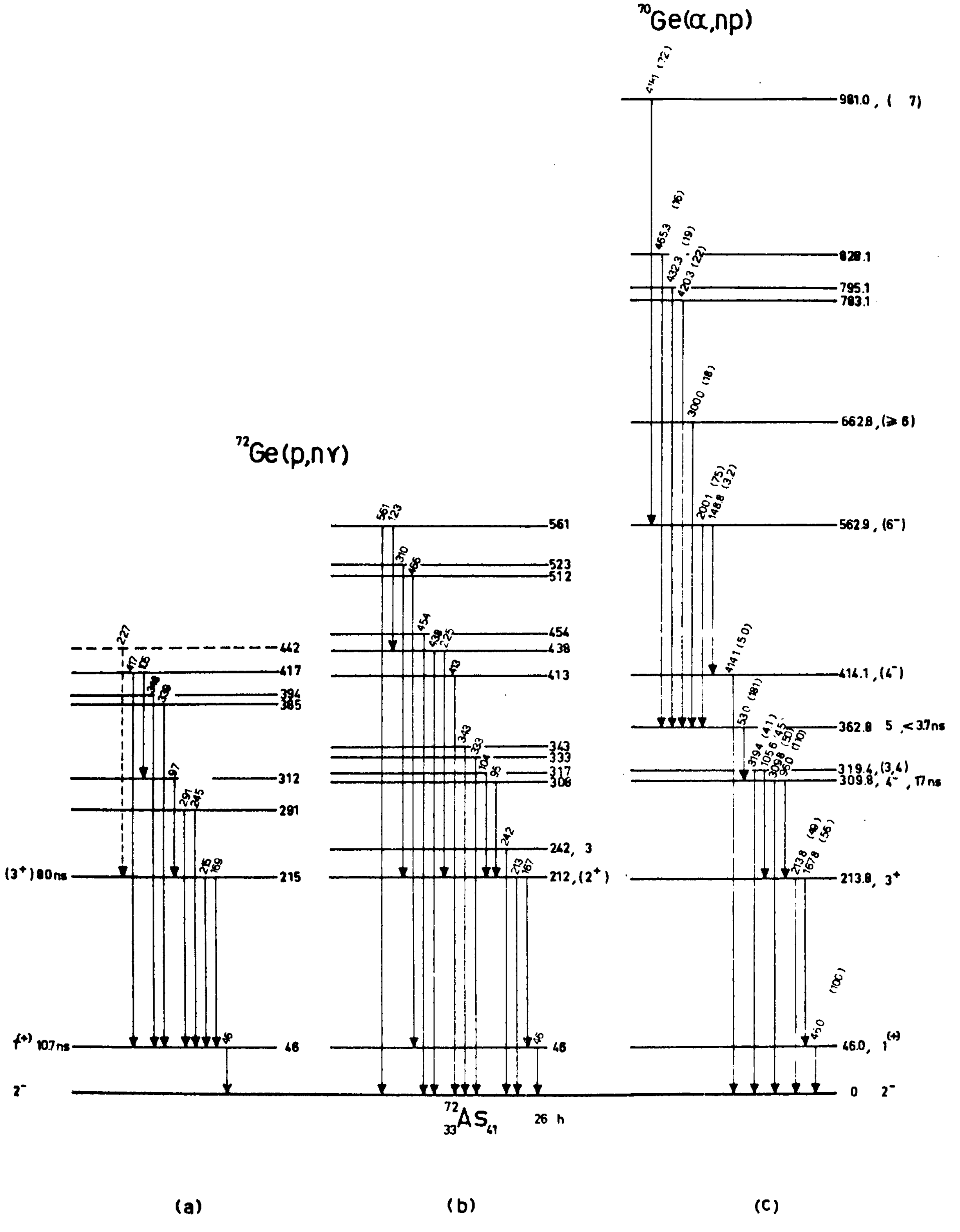

Fig. II.3.1 Level Scheme of ^{72}As. Parts (a) and (b) have been determined from the ^{72}Ge(p,nγ) reaction (Refs. 1 and 2). Part (c) is obtained from the present work.

II.4. Level Structure of ^{74}As from the ^{72}Ge(α,npγ) Reaction.

G.García Bermudez, M.Behar, A.Filevich and M.A.J.Mariscotti.

The odd-odd nucleus ^{74}As has been previously studied by means of the (p,nγ), (^{3}He,d) and (p,d) reactions. The most recent and comprehensive investigation is that of Kimura[1] who, from measurements of conversion electrons and cross sections, determined spins, parities and γ-ray multipolarities corresponding to levels up to 470 keV. In addition Christiansen et al.[2] determined the lifetime and g-factor of a level proposed at 273.8 keV.

We have studied the level structure of this nucleus by means of the ^{72}Ge(α,npγ) reaction in the energy range E_α = 30 - 55 MeV. This reaction predominantly populates high spin levels and therefore new information is obtained.

From the study of:(a) excitation functions, (b) γ-γ coincidences, (c) angular distribution and (d) γ-time distributions with respect to the beam bursts in the nsec range, we obtain the level scheme shown in Fig. II.4.1. The γ-ray transitions with E_γ < 100 keV have been detected in a high resolution X-ray detector. Three states at 183.0 keV, 259 keV and 271.6 keV are identified with levels previously observed with the (p,n) reaction[1]. In addition six new levels are incorporated into the level scheme.

From the timing measurements we observe that all the γ-rays with E_γ < 100 keV assigned to ^{74}As exhibit a prompt distribution except for the 76.2 keV γ-ray. The latter shows a half-life of 28 ± 2 nsec, in good agreement with the value of 26.8 ± 0.5 nsec previously measured[2]. These authors[2], however, associate the 76.2 keV γ-ray with a different level from the one proposed in both Kimura's and the present work. The regularities observed in ^{70}As, ^{72}As and ^{74}As are intriguing and stimulate further studies.

---

[1] K.Kimura, Nucl. Phys. A213 (1973) 61.

[2] J.Christiansen, H.E.Mahnke, E.Recknagel, D.Riegel, and W.Witthuna, Nucl. Phys. A164 (1971) 367.

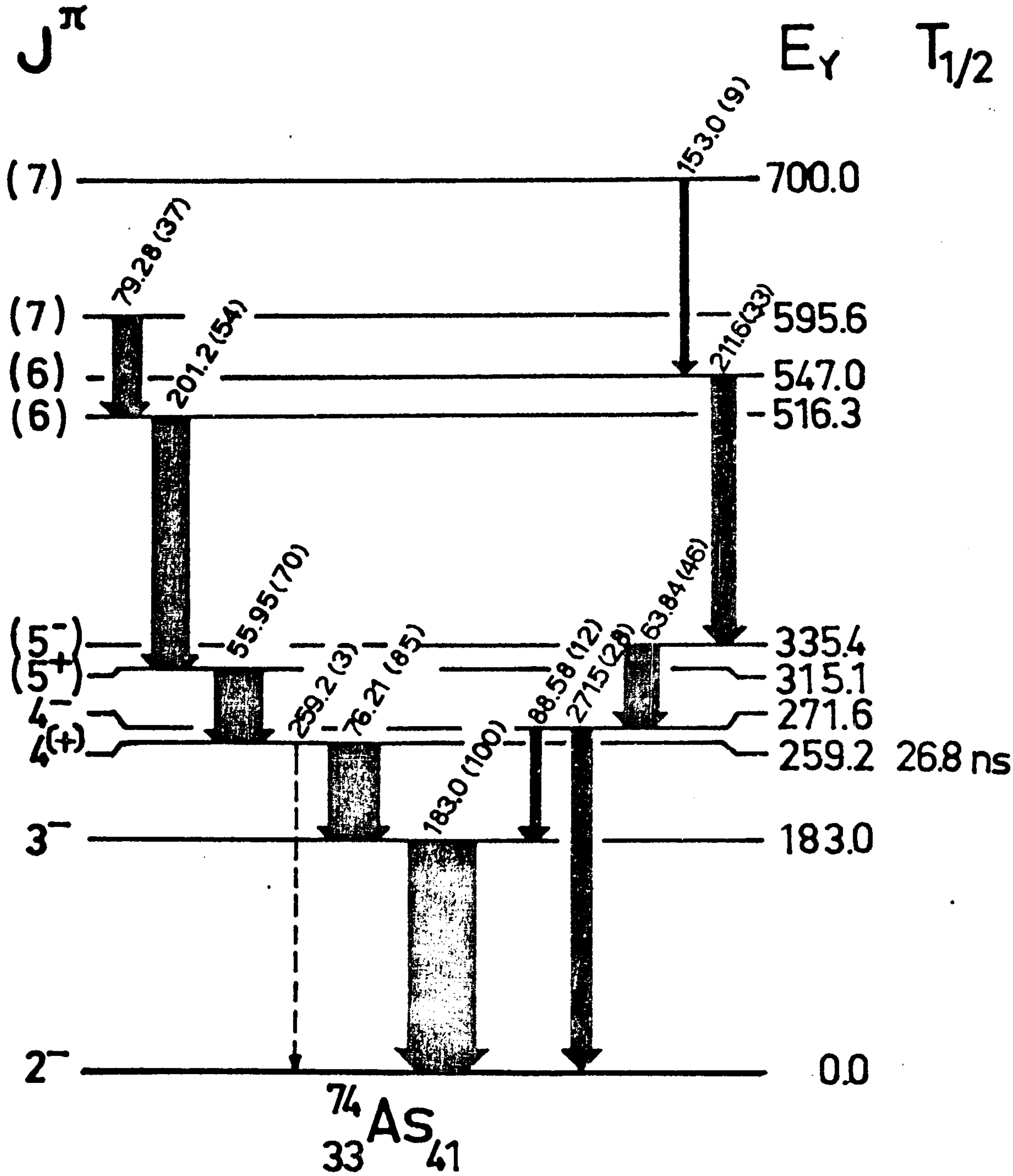

Fig. II.4.1 Level scheme of ^{74}As.

II.5. Level Schemes of ^{66}Ga and ^{68}Ga.

C.Pomar, M.A.J.Mariscotti, P.Kleinheinz*, R.M.Lieder* and O.W.B.Schult*.

The nuclei ^{66}Ga and ^{68}Ga have been studied by means of the (α,np) reaction at E_α = 30 to 50 MeV on targets of ^{64}Zn and ^{66}Zn, respectively. These experiments have been carried out in a combined effort between the Buenos Aires Synchrocyclotron and the Jülich Isochronous Cyclotron groups.

The excitation functions obtained for the γ-rays corresponding to ^{66}Ga are shown in Fig. II.5.1. Angular distributions and γ-γ coincidences are shown in Figs. II.5.a and II.5.3, respectively. The coincidence measurements were taken over a period of 30 hours per nucleus. The data were accumulated in an event by event mode with the information corresponding to four different parameters; (a) the gamma ray energies detected with one and (b) another Ge(Li) diodes, (c) the time interval between the pulses and (d) the time interval between γ-ray pulses and beam bursts. The results are summarized in the level schemes shown in Fig. II.5.4.

The nucleus ^{66}Ga has been previously studied by the radioactive decay[1-5] of ^{66}Ge and also by means of the ^{66}Zn(p,n)^{66}Ga reaction[6]. Our results show the presence of four new levels at 493.5 keV, J = 3; 840.6, J = 4; 1327.4 keV, J = 4 and 1440.9 keV, J = 6. The parities of the 1327 and 1440 keV levels are the same but opposite to that of the 840 keV level. Furthermore, half-lives of $T_{1/2} \simeq 100$ nsec and $T_{1/2} = 5 \pm 2$ nsec have been measured for the states at 1440.9 and 139.9 keV, respectively.

The nucleus ^{68}Ga has recently been investigated by Harms-Ringdahl et al.[7] using the ^{65}Cu(α,n) reaction at E_α = 14.2 MeV. Our results, which are in general good agreement with theirs, allow us to determine that the spins for the 805.9 and 1323.0 keV levels are J = 4 and J = 6, respectively. Furthermore the present work also indicates J(1219.6 keV) = 7 and J(1103.3 keV) = 5. The first of these states is isomeric and its halflife has been confirmed[8] to be $T_{1/2}$ = 85 nsec.

---

* Institüt für Kernphysik der Kernforschungsanlage, Jülich, West Germany.

1 H.H.Bolotin, Bull. Am. Phys. Soc. 8, N° 7, 524, 13 (1963).
2 R.A.Ricci, R.K.Girgis and R. van Lieshout, Nucl. Phys. 21 (1960) 177.
3 H.H.Bolotin and D.A.Mc Clure, Phys. Rev. 180 (1969) 987.
4 H.B.Bakhru and I.M.Ladenbauer-Bellis, Phys. Rev. 184 (1969) 1142.
5 D.G.Sarantites and S.Gronemeyer, Nucl. Phys. A130 (1969) 97.
6 N.R.Najam, W.F.Davidson, W.M.Zuk, L.E.Carlson and M.A.Awal, Nucl. Phys. A173 (1971) 577.

[7] L.Harms-Ringdahl, J.Sztarkier and Z.P.Sawa, Annual Report 1973 Research Institute for Physics, Stockolm, Sweden.

[8] W.Zeitz, private communication.

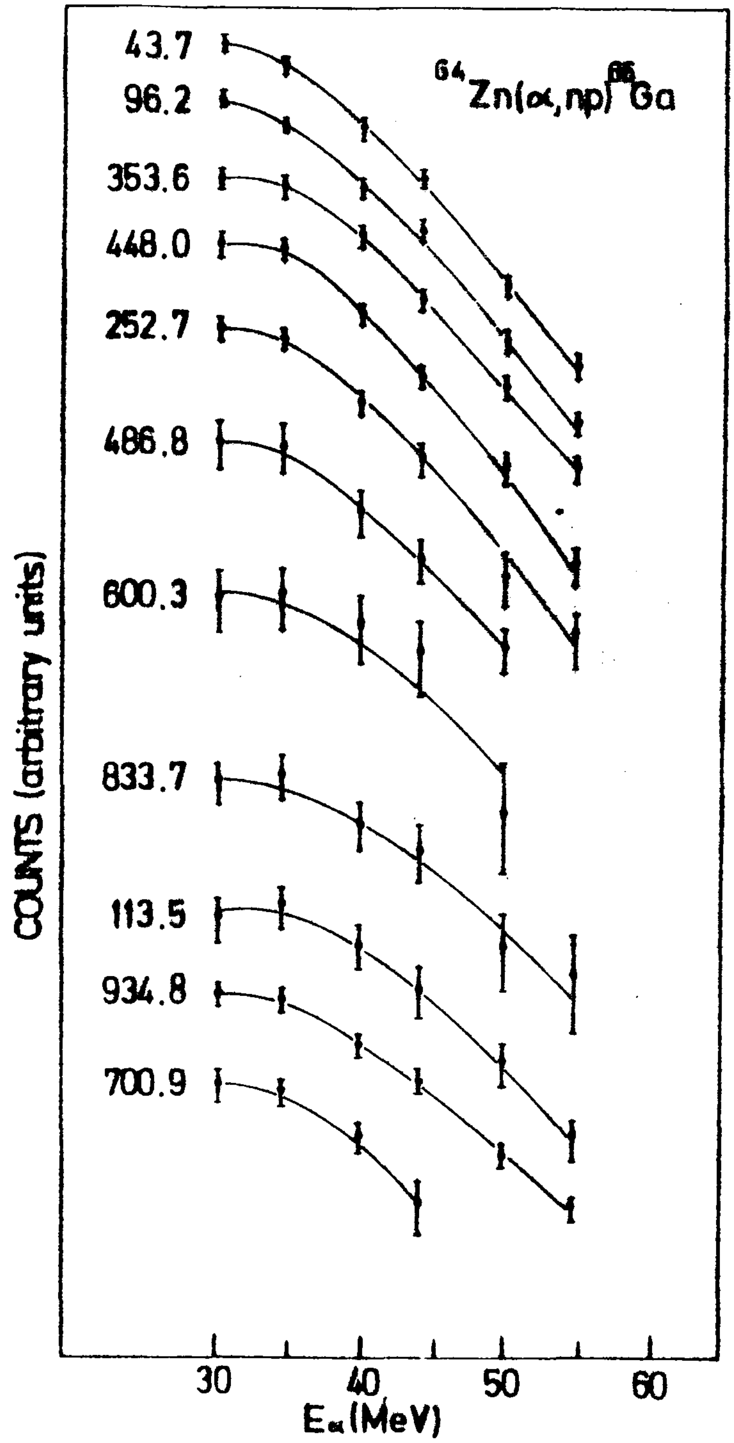

Fig. II.5.1 Excitation functions of γ-rays following the $^{64}Zn(\alpha,np)^{66}Ga$ reaction.

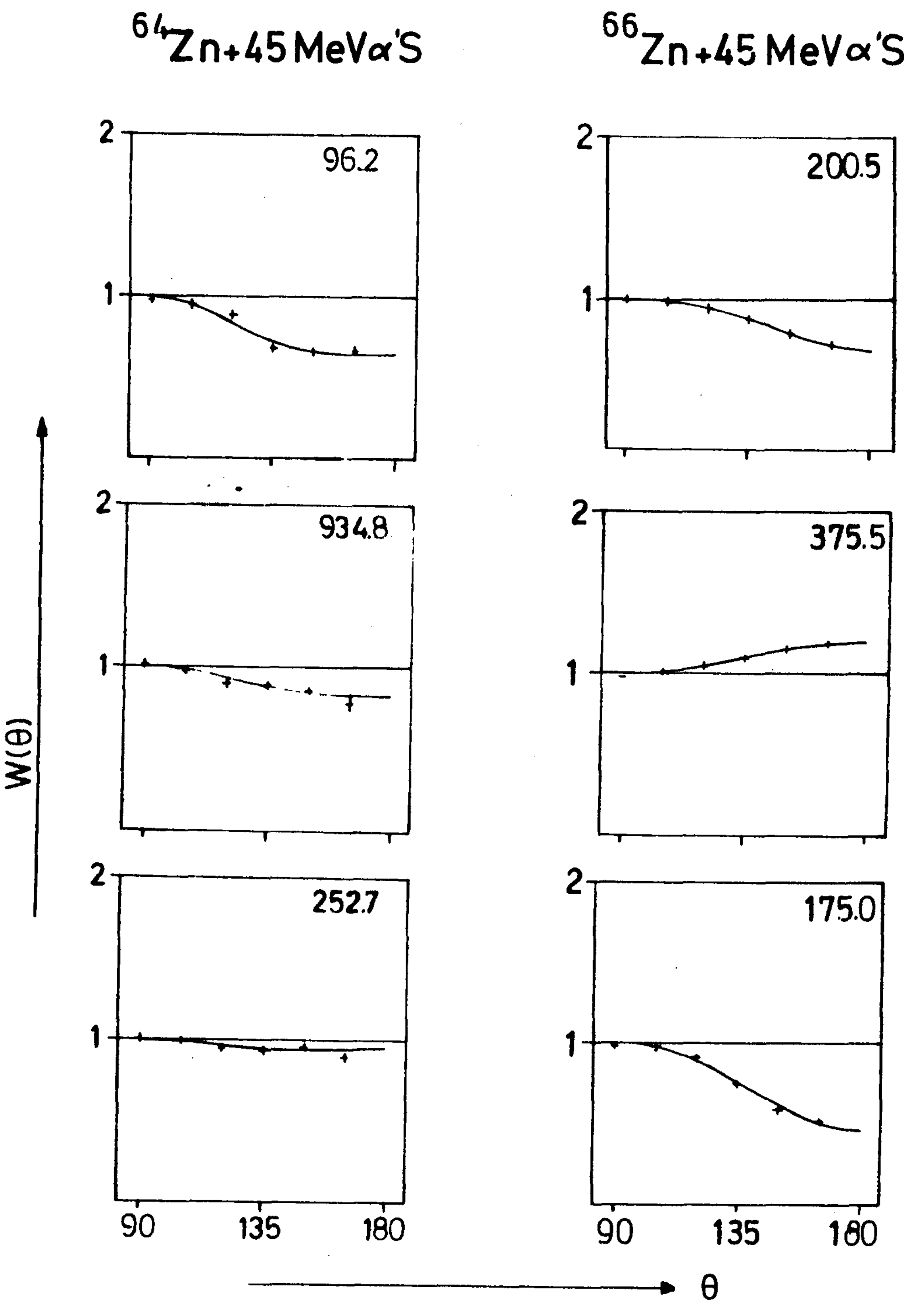

Fig. II.5.2 Gamma-ray angular distributions following the $^{64}Zn(\alpha,np)$ and $^{66}Zn(\alpha,np)$ reactions.

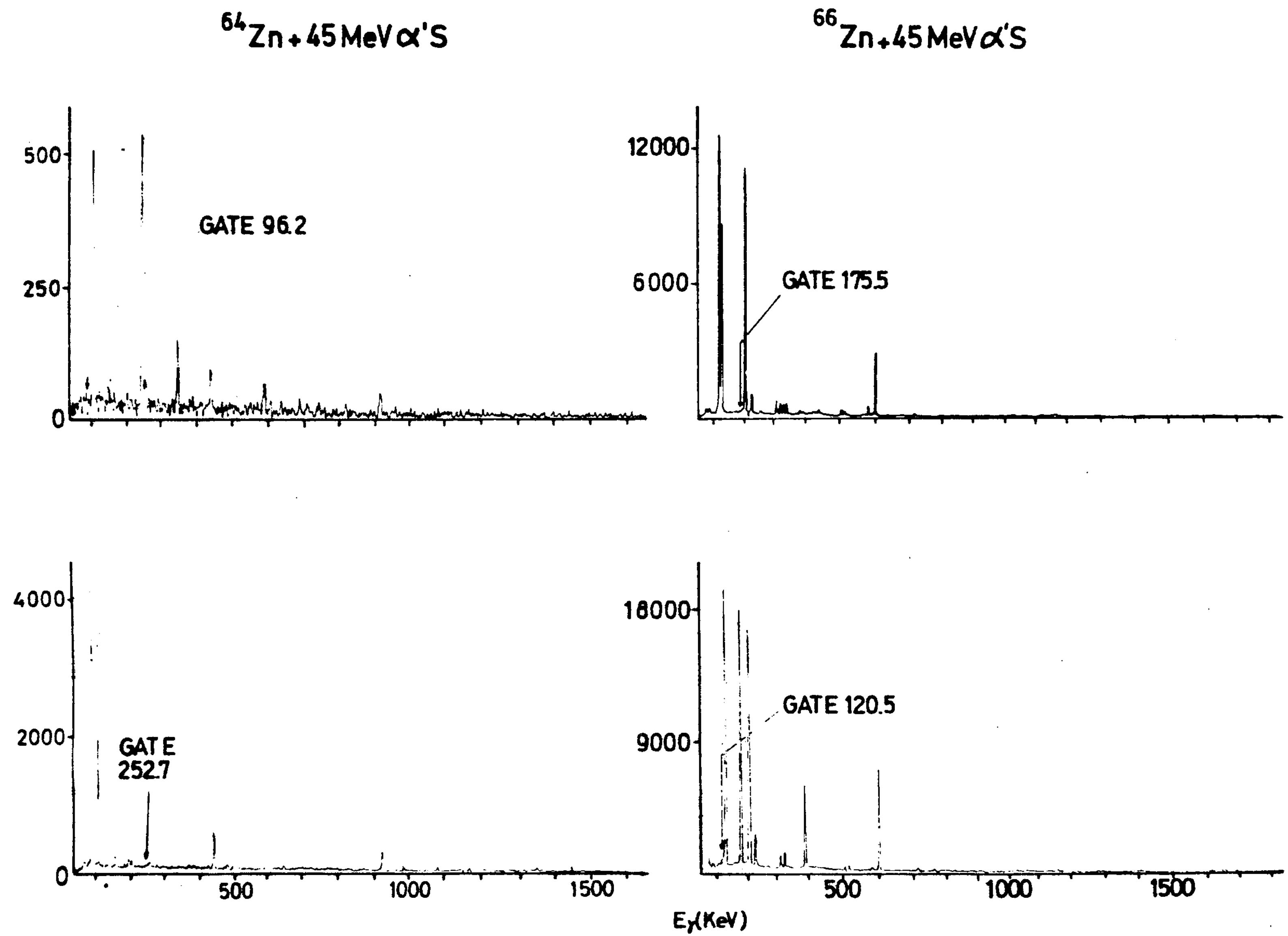

<u>Fig. II.5.3</u> γ-γ coincidence spectra observed in this work.

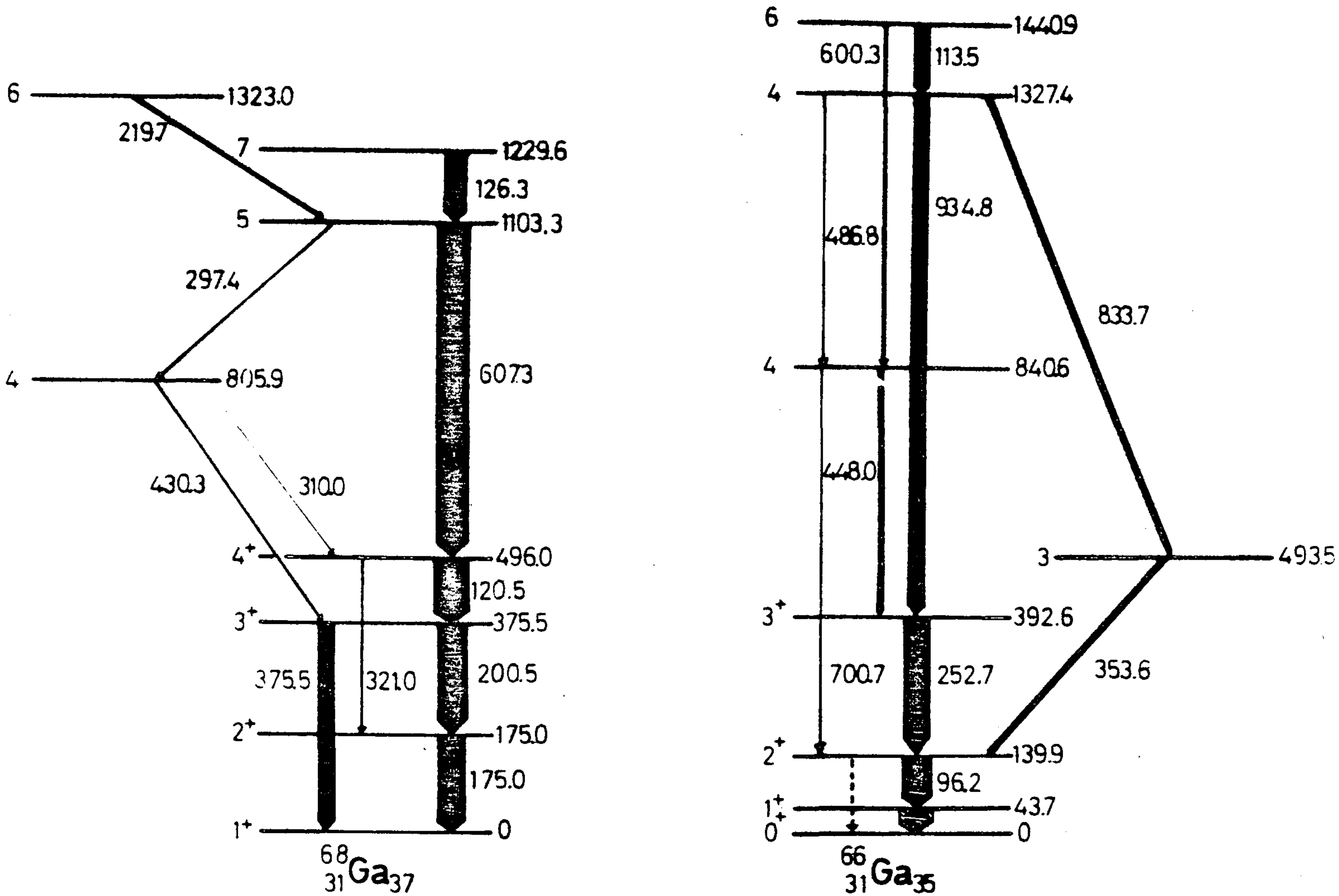

<u>Fig. II.5.4</u> Level schemes of ^{66}Ga and ^{68}Ga.

II.6. Trends in (α,xnyp) Reaction Cross Sections.

C.Pomar and M.A.J.Mariscotti.

Reactions of the type (α,xn) are clearly predominant in the rare earth region. For lighter nuclei, however, proton emission also becomes important. This circumstance usually precludes a straightforward identification of the product nucleus through the study of γ-ray excitation functions. Frequently reactions such as the (α,3n) and (α,2np) exhibit similar excitation functions. However, both the bombarding energy at which these reactions reach their maxima $E_\alpha(\sigma_{max})$ and their maximum cross sections, σ_{max}, vary according to the degree of neutron deficiency of the target.

The knowledge of the behavior of these two quantities is useful to assist in the identification procedure and also serves as a guide to make preliminary estimates on the feasibility of different reactions for a given target.

The study of the trend shown by $E_\alpha(\sigma_{max})$ and σ_{max} is the aim of the present work for the case of the Zn isotopes with A = 64, 66, 67 and 68.

The different reactions (α,xnyp) which could be observed in the interval E_α = 30 - 55 MeV were investigated. Excitation functions for most of the observed γ-rays were obtained in 5 MeV steps. These γ-rays were in turn assigned to a product nucleus through the identification of certain lines with transitions hitherto known from other processes (e.g. radioactive decay or (p,n) reactions in most cases).With this information it was possible to determine $E_\alpha(\sigma_{max})$ for the different reactions on the different targets, that is, $E_\alpha(\sigma_{max})$ as a function of A. The results concerning this quantity are shown in Fig. II.6.1. The $E_\alpha(\sigma_{max})$ values indicated with a "shadowed" symbol represent extrapolations estimated from the shape of the excitation curve. Some of the cases shown below the 29.5 MeV limit correspond to data reported by other authors[1]. Each thin dashed line corresponds to a given γ-ray produced in different reactions according to the target. Thick lines join the experimental values corresponding to the same reaction. The plot shows how the reactions involving protons require, as a trend, more energy as we move towards the stability line (increasing A) while the opposite applies to reactions involving only neutrons.

To study σ_{max} as a function of A it is necessary to have some knowledge of the level schemes of the product nuclei, at least regarding the lowest states. The value σ_{max} was thus obtained from the total intensity which feeds the ground state of the product nucleus and it was normalized in all cases to the total number of counts accumulated in the spectrum. Fig. II.6.2 shows σ_{max} as a function of A for the (α,p), (α,np), (α,2np), (α,n), (α,2n) and

(α,3n) reactions. For ^{64}Zn, the isotope farthest from the stability line, the (α,np) and (α,2np) reactions predominate. Again, the trend observed for these reactions is opposite to that of reactions involving neutrons only. For ^{68}Zn the (α,2n) reaction is the most intense.

These results show that both $E_\alpha(\sigma_{max})$ and σ_{max} exhibit a regular behavior. The knowledge of these trends greatly helps the γ-ray identification in those cases where other information is lacking. This information is particularly useful when dealing with medium and light nuclei. Presently the study of $E_\alpha(\sigma_{max})$ and σ_{max} is being extended to the Ni isotopes. The preliminary results suggest that trends similar to those obtained for the Zn isotopes can be expected.

---

[1] Harms et al., Phys. Scr. 9 (1974) 15.

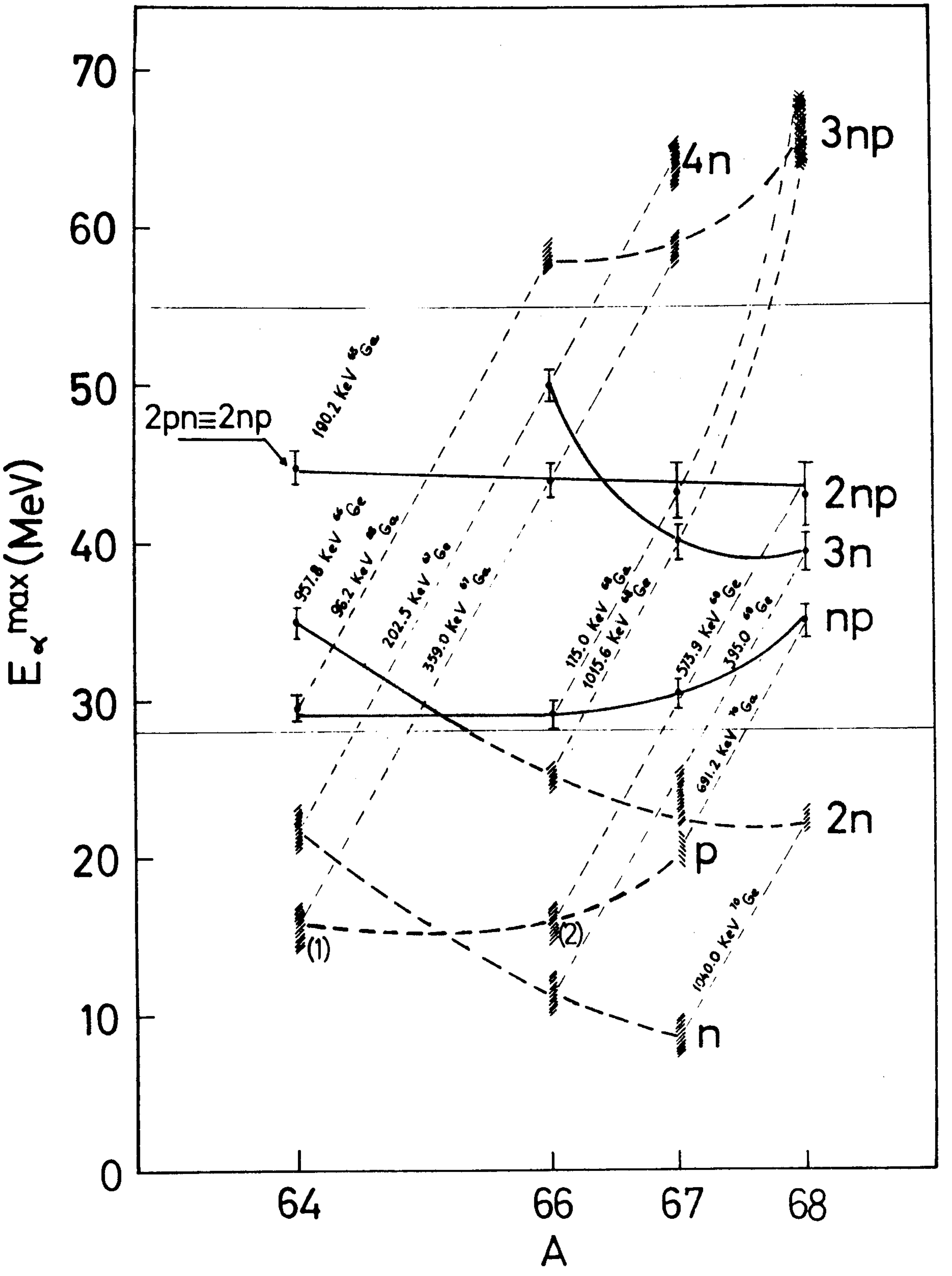

Fig. II.6.1 Bombarding energy at which the (α,xnyp) reaction reaches its maximum versus A for the Zn isotopes. Each thin dashed line corresponds to a given γ-ray observed through different reactions on different targets. Shadowed symbols indicate extrapolations beyond the energy range of the machine from the shapes of the excitation curves. Points labelled (1) and (2) are results from other authors (see Text).

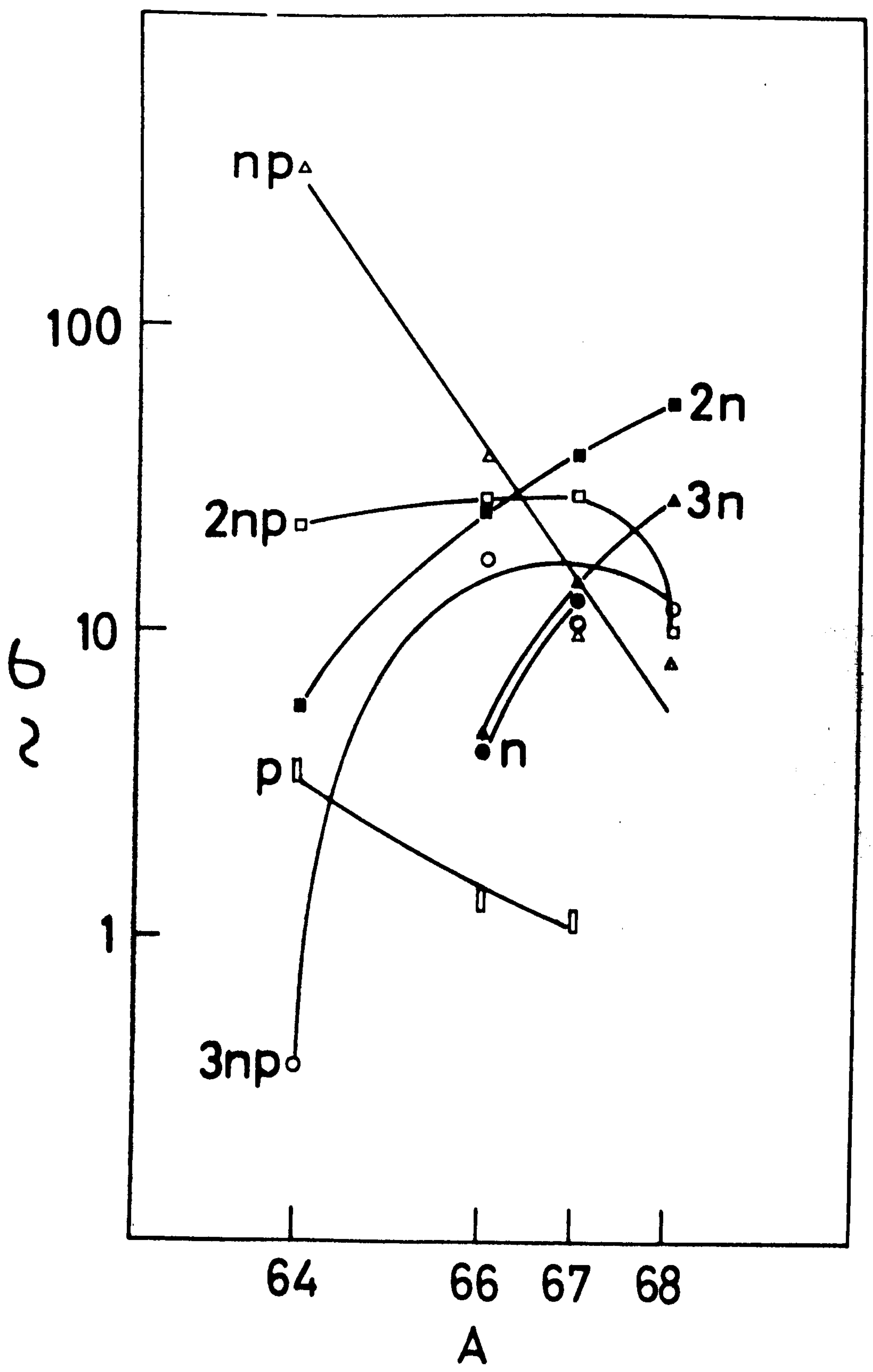

Fig. II.6.2 Cross sections (in arbitrary units) as function of A for the Zn isotopes.

II.7. Smooth Variation of the Critical Angular Momentum Throughout the Periodic Table.

M.A.J.Mariscotti.

Energy spacings $\Delta E_I = E_I - E_{I-2}$ in ground state bands of deformed even-even nuclei normally increase with spin. In some cases, however, this is not so and this phenomenon, known as the "backbending" effect, can be identified with the existence of a critical value of the nuclear angular momentum $I_c \sim 12 - 14\ \hbar$, for which the derivative $d\Delta E_I/dI$ becomes negative. The case of ^{158}Er is shown in Fig. II.7.1.

The existence of a critical angular momentum defined in this way is not, however, an exclusive characteristic of ground state bands in deformed nuclei. It is well known that in some spherical nuclei a "collapse" of levels occurs for $4\hbar \lesssim I_c \lesssim 8\hbar$. This fact is interpreted as due to the predominance of an $(1j)^2_I$ configuration (characteristic of magic nuclei) for levels with $I \sim I_c$. Fig. II.7.2 shows the case of ^{86}Sr with $I_c = 4\hbar$, as well as a comparison between the experimental levels of ^{210}Po and the calculated ones assuming two $h_{9/2}$ protons interacting through a delta force.

Although the existence of a critical angular momentum I_c, both in deformed nuclei and nuclei near closed shells, is interpreted in quite unrelated terms; it is interesting to explore, from a phenomenological point of view, whether the effects involved in these two cases are indeed independent. A justification for such a search is strengthened by the recently reported data on Hg and Pt isotopes which contribute to close the gap between well deformed ($E4/E2 \sim 3.3$) and spherical nuclei ($E4/E2 \sim 2$).

Fig. II.7.3 shows that when I_c is plotted versus the ratio E4/E2, (possibly the best classifier of even-even nuclei), a clear correlation emerges. Magic and semi-magic nuclei, for which the ambiguity $I_c = 0$ or $I_c = 2$ remains, are also included.

In recent years several models have been proposed to explain the backbending effect in deformed nuclei. The observation of a smooth variation of I_c versus E4/E2 may contribute to clarify the nature of such a phenomenon.

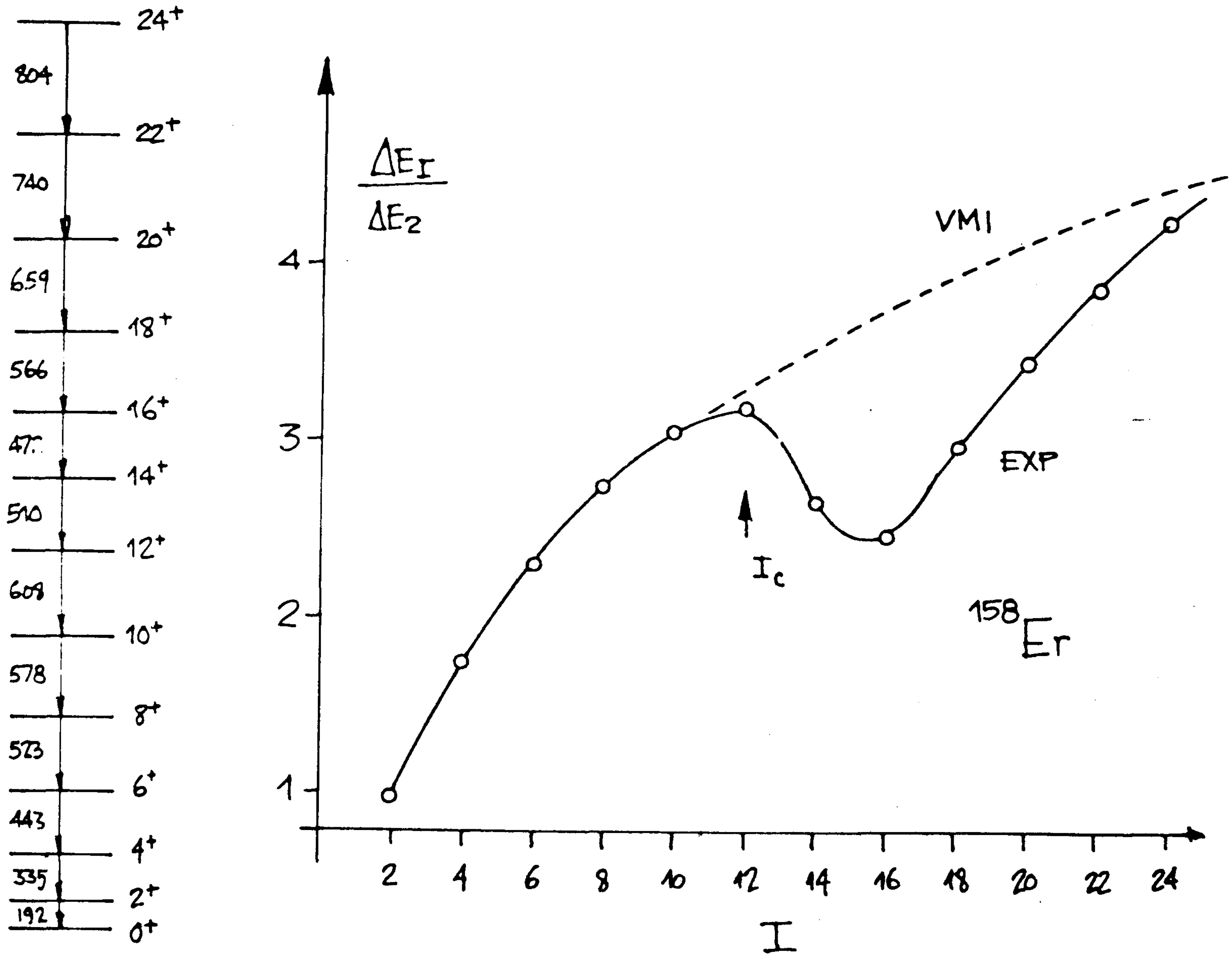

Fig. II.7.1 Ground state energy spacings as a function of angular momentum in ^{158}Er compared to the VMI prediction.

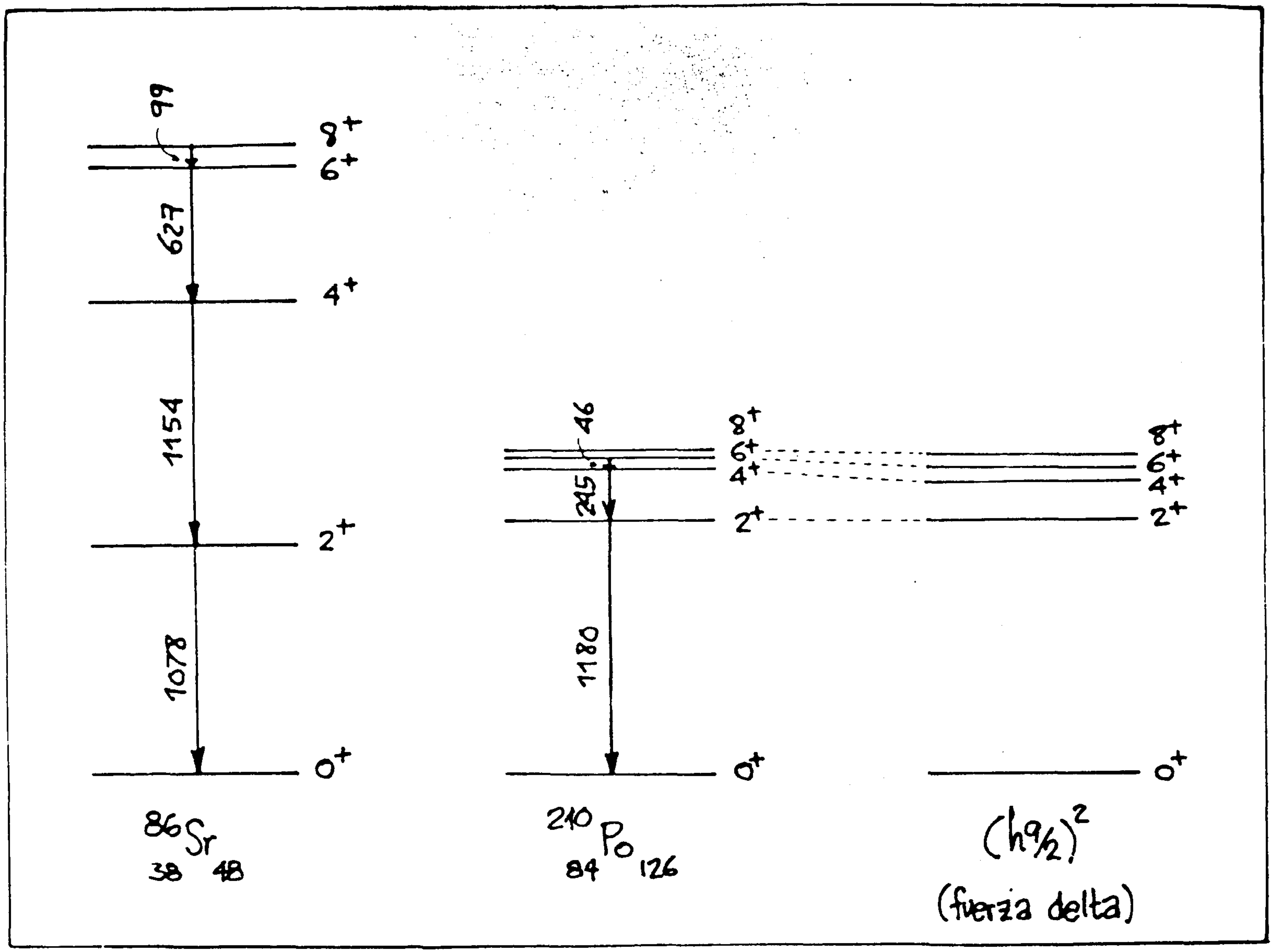

Fig. II.7.2 Ground state bands in ^{86}Sr and ^{210}Po. For the latter, the experimental values are compared to a calculation assuming two $h_{9/2}$ protons interacting through a delta force.

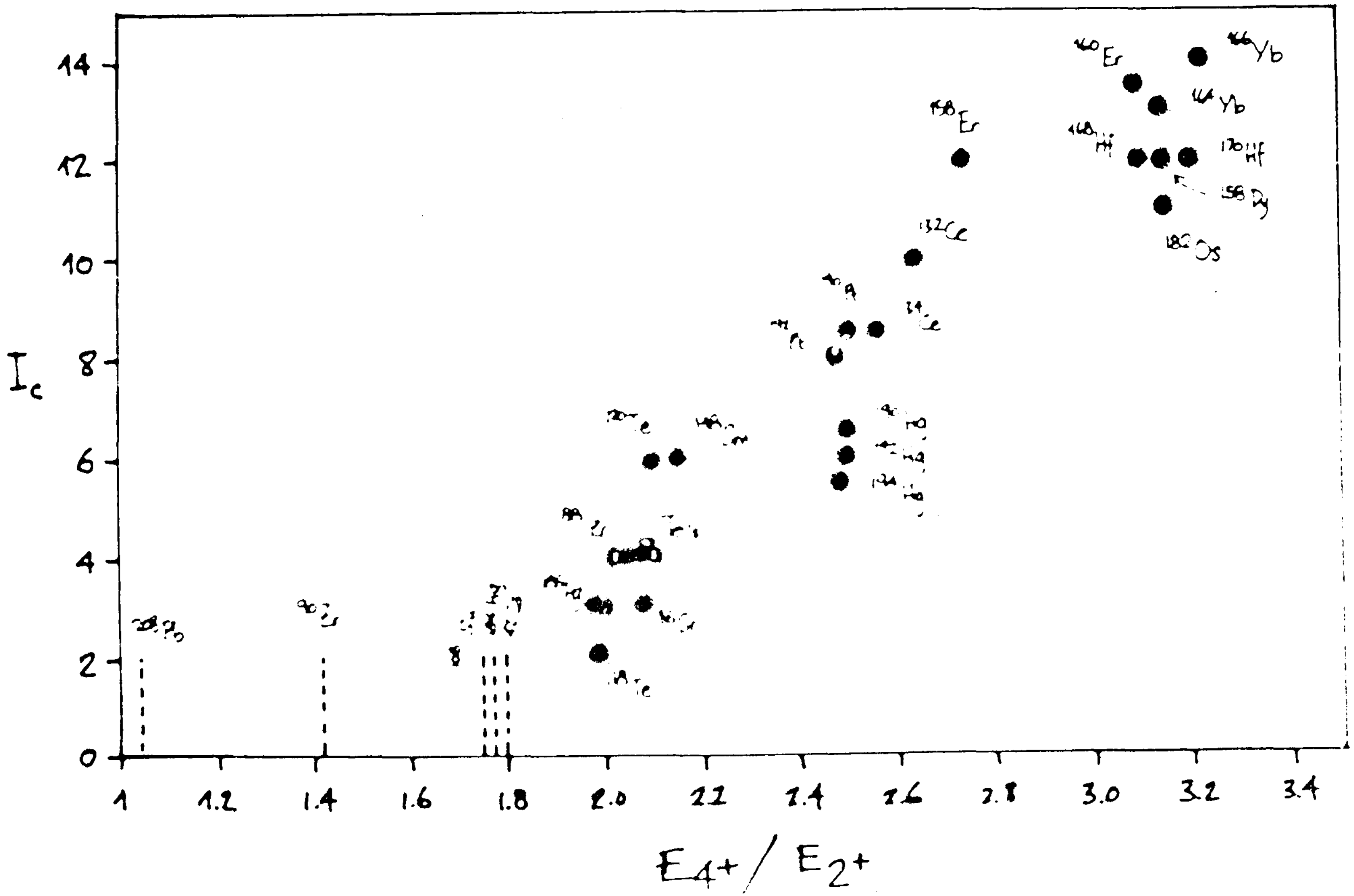

Fig. II.7.3 Plot of the critical angular momentum I_c as a function of E4/E2 showing a correlation between these two quantities.

III. ON-LINE STUDIES OF FISSION FRAGMENTS

III.1. General Techniques Used in the IALE† Facility.

E.Achterberg, F.C.Iglesias*, A.E.Jech**, J.A.Moragues, D.Otero, M.L.Pérez, A.N.Proto, J.J.Rossi and W.Scheuer.

The studies presented in this section have been made using similar techniques, which for convenience are summarized here.

The samples are produced in the Buenos Aires On-Line facility, which is described in detail in Ref. 1. Briefly, an uranyl-stearate target containing ∿ 10 grs of ^{235}U is placed in a thermal neutron flux obtained, after moderation through paraffin, from the Li(d,n) reaction. The deuteron beam is produced by a 1 MeV Cockcroft-Walton accelerator. The rare gases from the ^{235}U fission are fed into the ion source of an electromagnetic mass separator and the mass of interest is deposited on an appropriate collector. Different types of collectors are used including aluminized-mylar moving tapes, 0.5 mm thick detachable Be-plates, 0.03 mm thick detachable Al-plates and some special arrangements to measure conversion electrons[2].

Measurements of γ-ray spectra are carried out with Ge(Li) detectors of variable resolution and efficiency (between 2 and 3 keV at the ^{60}Co lines)and about 40 c.c. Conversion electron spectra are determined with a Si(Li) detector (6.0 keV resolution at 250 keV), and β-ray spectra with a thick Si(Li) detector. Low energy radiation is observed with an X-ray Si(Li) spectrometer (290 keV resolution at 5.9 keV).

The data are recorded in an analyzer system provided with two 4096-channel analog-to-digital converters and several read-out peripherals under control of a 16K memory HP 2116B computer.

The analysis of gamma-ray spectra is performed with a specially developed program ANPIK[3] using a non-linear least-squares iterative technique to fit a phenomenological function to the peaks and background. This program was developed to run on the HP 2116 minicomputer. The memory size and speed limitations of the hardware led to a rather slow program which can handle only 400 channels of the spectrum at a time, while the actual fitting procedure is restricted to a region of no more than 150 channels, which however may contain up to 10 peaks. The error assignments produced by the program appear to be realistic, leading to consistent energy values for the peaks observed in runs taken with different gain settings.

---

† Isotopes Far From the Line of Stability.

In order to assign transitions to each number of a given mass-chain, identification through half-life differences is made, using the moving-tape collector with an appropriate cycling.

The coincidence measurements are made in the 4096 x 4096 bidimensional mode, using our HP 2116 computer-based data acquisition system. The addresses generated by the digital-to-analog converters (ADC) are stored in an internal buffer, which is dumped onto a 7-track magnetic tape when filled and then reset to zero to start a new accumulation. Using a specially developed software package a singles γ-ray spectrum can be accumulated simultaneously with the coincidence events in another part of the computer memory. This is very useful in establishing gates for the scanning of the coincidence spectra, for the analysis of random coincidences and to ensure that no gain shifts occur during the data accumulation.

---

* Departamento de Combustibles Nucleares (CNEA).

** Universidad Nacional de Luján, Pcia. de Buenos Aires, Argentina.

1 E.Achterberg et al., Nucl. Instr. and Methods, 101 (1972) 555.

2 E.Achterberg et al., Phys. Rev. C5 (1972) 1759.

3 E.Achterberg, Private Communication.

III.2. Decay of ^{139}Xe (40 sec).

E.Achterberg.

As part of the ongoing investigation of the low-energy properties of the short-lived ^{235}U fission products at the Buenos Aires ISOL set-up, some additional measurements were made to complement those performed earlier on the decay of ^{139}Xe (40 sec). These included mainly a new run of γ-γ coincidences using an improved experimental set-up, as well as a run of β-γ coincidences and the exploration of the low-energy γ-ray region using a Si(Li) X-ray detector. Due to the great complexity of the γ-ray spectra, showing more than 200 transitions, it was necessary to emphazise the precise energy determination of the transitions in order to increase the reliability of the placement of γ-ray transitions in the ^{139}Cs level scheme when using the energy sum technique. This involved special calibration runs with a number of well known standard calibration sources, as well as a careful peak position analysis of the γ-ray spectra.

Since the intense neutron-induced background made the analysis of the low-energy γ-ray spectra accumulated in the on-line measurements difficult, spectra were also taken using a Si(Li) X-ray detector. Calibrations were performed using sources of ^{241}Am and ^{207}Bi.

The construction of the level scheme for ^{139}Cs using the described facilities is presently in progress.

III.3. Levels of ^{90}Rb Observed in the β-Decay of ^{90}Kr.

M.L.Pérez and J.J.Rossi.

As part of a study of the energy levels in the Rb isotopes[1], an investigation of the level scheme of ^{90}Rb using the IALE facility, was undertaken. In this work, single γ-ray, conversion electron, β-ray and both X-ray and low energy γ-ray-spectra were recorded. Measurements of γ-γ and β-γ coincidences were also carried out. The half-lives of the ground states of ^{90}Kr and ^{90}Rb and that of the isomer ^{90m}Rb were measured by conveniently modulating the production of ^{90}Kr and the time intervals. Precise values of γ-ray energies and intensities were determined for 94 transitions assigned to the ^{90}Kr decay. On the basis of the γ-γ and β-γ coincidences, as well as energy combinations, a level scheme involving 15 levels was constructed. Gamma-ray transition multipolarities were deduced from the conversion electron coefficients and log ft values were obtained from the intensity balance for each level. These data, together with the measured Q-value allow us to assign spin and parities to some levels.

The completion of the upper part of the level scheme (based only on energy sums and γ-ray intensities) and the theoretical interpretation of the observed structure of ^{90}Rb is in progress.

---

[1] E.Achterberg, F.C.Iglesias, A.E.Jech, J.A.Moragues, D.Otero, M.L.Pérez, A.N. Proto, J.J.Rossi and W.Scheuer, Phys. Rev. C9 (1974) 299 and Phys. Rev. C10 (1974) 2526.

III.4. Conversion Coefficients of the 13.8 and 38.3 keV Transitions in ^{140}Cs.

G.R.Kalberman*, D.Otero and A.N.Proto.

A Si(Li) detector with a thin Be window was used to determine the conversion coefficients of the 13.8 and 38.3 keV transitions in ^{140}Cs, by means of the X-ray peak to γ-ray peak method using L- and K- transitions, respectively.

Fig. III.4.1 shows the spectrum obtained. To compute the conversion coefficients, the contribution from γ-rays with $E > 80$ keV, known from other measurements[1], was subtracted. In order to evaluate the contribution of the 50.6 keV line, it was assumed that its multipolarity was limited to M1 and/or E2 character.

From these measurements we conclude that the 13.8 keV transition is M1 while the 38.3 keV transition is M1/E2.

---

* Research Student.

1 J.P.Adams, F.K.Wohn, W.L.Talbert Jr., W.C.Schick Jr., and J.R.Mc Connell, Phys. Rev. C10 (1974) 1467.

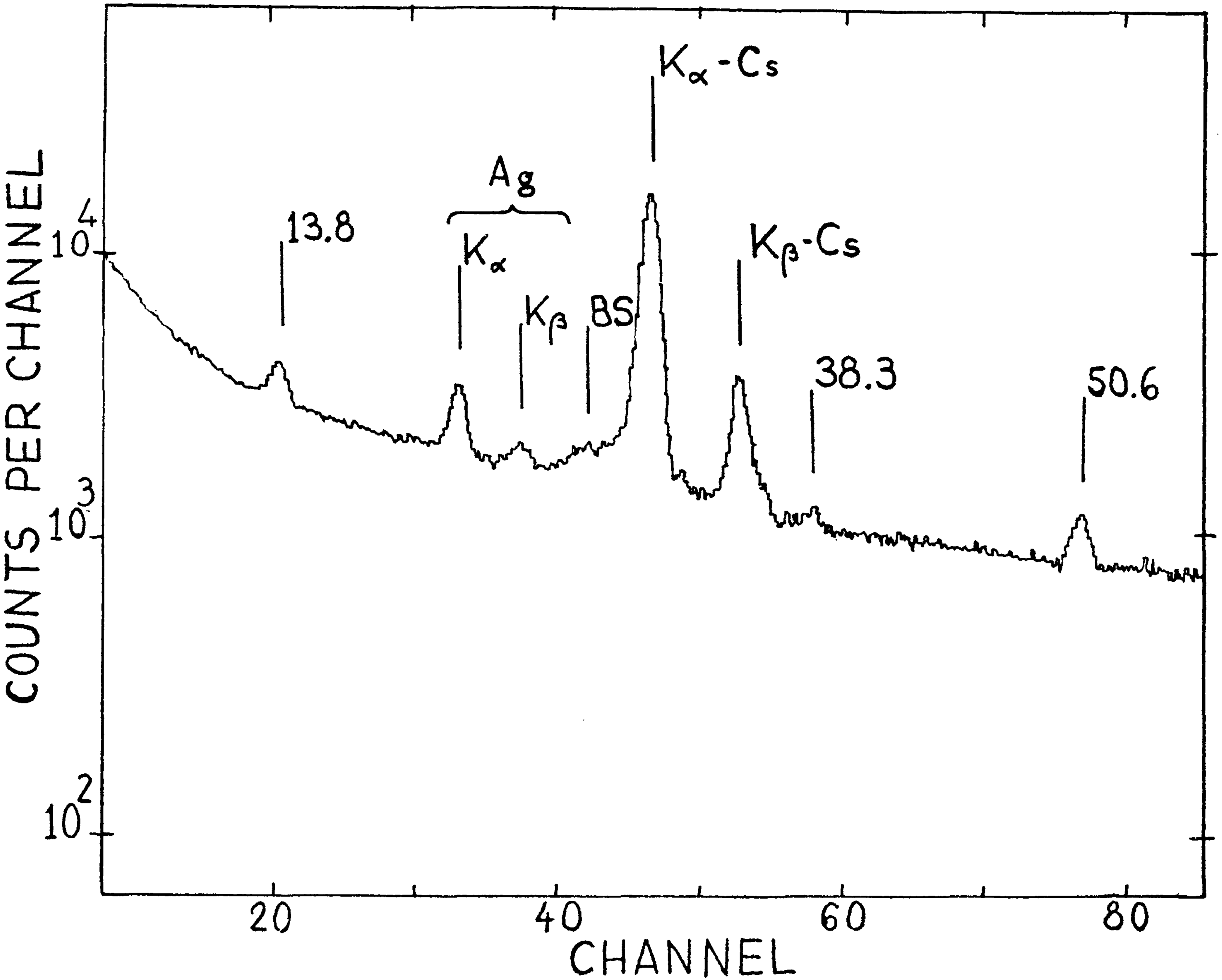

Fig. III.4.1 Low-energy spectrum of transitions observed in ^{140}Cs.

III.5. Levels of ^{141}Cs and ^{141}Ba Observed in the Decays of ^{141}Ce and ^{141}Cs.

D.Otero, A.N.Proto and F.C.Iglesias*.

We were able to assign unambiguously 209 γ-transitions to the ^{141}Xe decay. The half-life for the ^{141}Xe ground-state decay was determined to be 1.72 ± 0.03 sec. This value was obtained as a weighted average of those of the 68.98-, 81.81-, 100.76-, 105.96-, and 118.71- keV transitions. Using the Si(Li) X-ray detector the half-life of the ^{141}Cs($K_\alpha + K_\beta$) lines was also measured giving a value of 1.7 ± 0.1 sec, thus ensuring that the γ-rays which follow the 1.73-sec half-life belong to the ^{141}Xe decay.

A special run was made to determine the β^- feeding to the ^{141}Cs ground-state. The activity of the 141 mass-chain was collected for about 10 hours: this means that the ^{141}Xe, ^{141}Cs, and ^{141}Ba activities were in equilibrium and only the ^{141}La activity had to be slightly corrected for half-life. Through the 1354.52-keV transition of the ^{141}La decay, whose intensity in percent of β^- disintegrations is well known[1], it is possible to establish: (a) the total number of β^- decay in the mass-chain and (b) the intensity of the γ transitions belonging to the ^{141}Xe decay per unit of β^- disintegration. From our level scheme (see Fig. III.5.1(a), (b) and (c)) we were able to determine the β^- feedings to excited levels of ^{141}Cs and from (a) we obtained a value of 49.5% for the β^- branch to the ^{141}Cs ground-state.

Eight K-conversion coefficients were obtained through the Normalized-K-conversion-Peak-to-Gamma peak method. A special moving collector system to measure electrons, particularly suitable for short half-lives, was used in this case. We assigned multipolarities by comparing our experimental values with the theoretical ones given in Ref. 2.

A value of 24.94 ± 0.06 sec was found for the ^{141}Cs ground-state decay, through the half-lives of the 48.48, 554.74, 561.51, and 588.55 keV γ-rays. The half-lives of the ($K_\alpha + K_\beta$) lines of ^{141}Ba were also measured in order to ensure the assignment in Z, giving a value of 24.9 ± 0.7 sec.

For the intensity of the β^- branch to the ^{141}Ba ground-state we obtained a value < 5.9% disintegrations, using the same procedure as for the ^{141}Cs ground-state feeding, and considering a pure M1 multipolarity for the 48.48 keV transition (see below).

The internal conversion coefficient for the 48.48 keV transition was determined by the X-ray-peak-to-γ-ray-peak method, and a value of α_K = 6.6 ± 0.9 was found. Since theoretical α_K values for M1 and E2 multipolarities are covered by the experimental error of the measured α_K, the amount of E2 admixture cannot be obtained in this way. However, from the ground-state intensity balance the total-conversion coefficient for the 48.48 keV transition is < 8.5, establishing an M1(< 9% E2) multipolarity for this low-energy transition.

The level scheme proposed for ^{141}Cs is shown in Figs. III.5.1(a), (b) and (c). It contains 166 transitions (91% of the total observed γ intensity) within a frame of 38 levels. The levels established by γ-γ coincidences are at an excitation energy of: 68.98, 105.96, 187.72, 206.69, 467.93, 557.10, 644.26, 946.01, 961.98, 977.53, 979.86, 1097.26, 1234.82, 1245.11, 1518.28 and 1556.71 keV. In this set of 16 levels, we can place 72% of the total γ-ray intensity observed.

Recently, Morman et al.[3] published the low-energy part of the level scheme of ^{141}Cs, which is a partial reproduction of that proposed in Ref. 1. From the eight levels proposed by these authors we have not confirmed those at 492.8 and 646.8 keV. Our experimental results did not show evidence enough to establish a level at 492.8 keV and for the transitions that Morman et al.[3] used in support of the 646.8 keV level, we were able to establish (from our coincidence results) that the 89.74 keV γ-ray is placed between the levels at 467.93 and 557.10 keV, and that the 459.93 keV transition connects the levels at 1097.26 keV and 1556.71 keV, thus leaving this presumed level unsupported. In view of our disagreement with the scheme adopted by Morman et al.[3] a limit of 2.4 nsec for the half-life for the proposed level at 646.8 keV should in fact correspond to the level at 557.04 keV.

The level scheme proposed for ^{141}Ba is shown in Figs. III.5.2(a) and (b). It contains 78 transitions in frame of 27 levels. The levels at 558.55, 1194.17 and 1748.92 keV are supported by γ-γ coincidences.

Regarding the proposed scheme for ^{141}Ba, its more relevant characteristic is the existence of a 48.48 keV transition which carries an intensity of 69.9% of the total decay, and depopulates the first excited level. From the data of Morman et al. the upper limit for the half-life of the 48.48 keV first excited state should be 3.4 nsec.

---

* Present address: Departamento de Combustibles Nucleares (CNEA).

[1] R.L.Auble, Nucl. Data A10 (1973) 175.

[2] R.S.Hager and E.C.Seltzer, Nuclear Data A10 (1971) 206.

[3] J.A.Morman, W.C.Schick and W.L.Talbert,Jr., Phys. Rev. C11 (1975) 913.

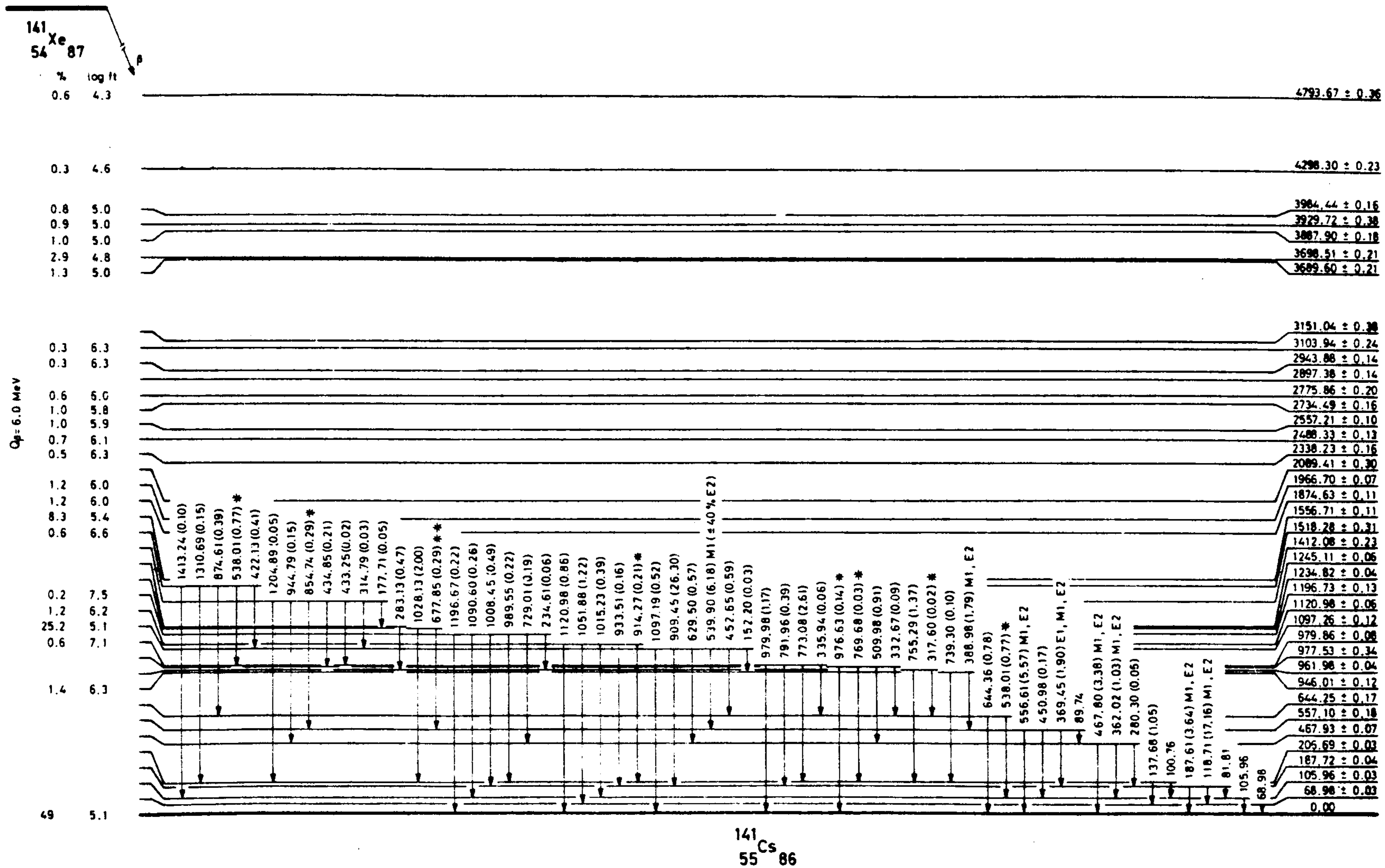

Fig. III.5.1(a) Level scheme of ^{141}Cs (low energy part). Intensities per 100 disintegrations are given in parenthesis. Doubly placed γ-rays are marked with asterisks.

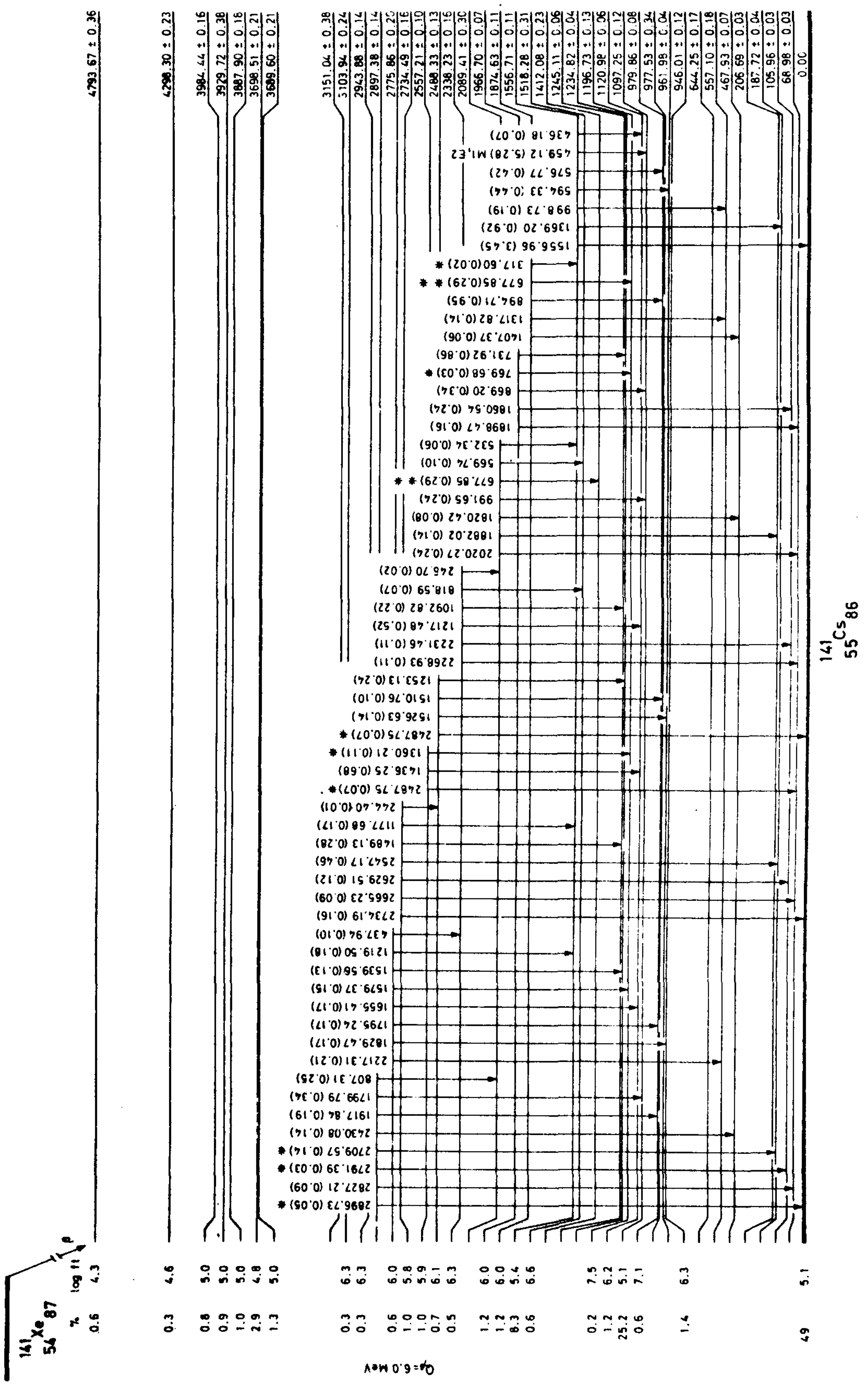

Fig. III.5.1(b) Level scheme of ^{141}Cs (intermediate energy part).

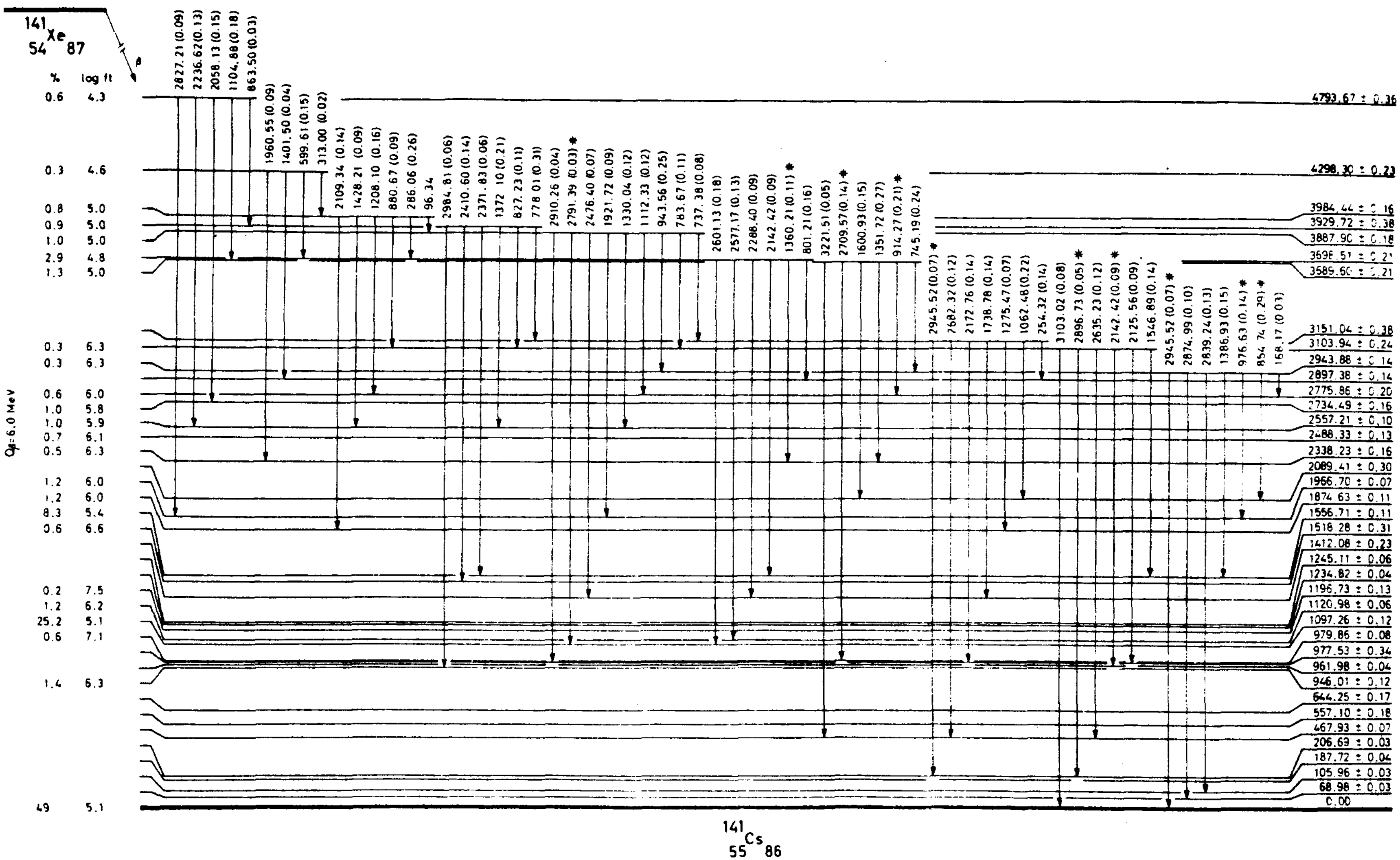

Fig. III.5.1(c) Level scheme of ^{141}Cs (high energy part).

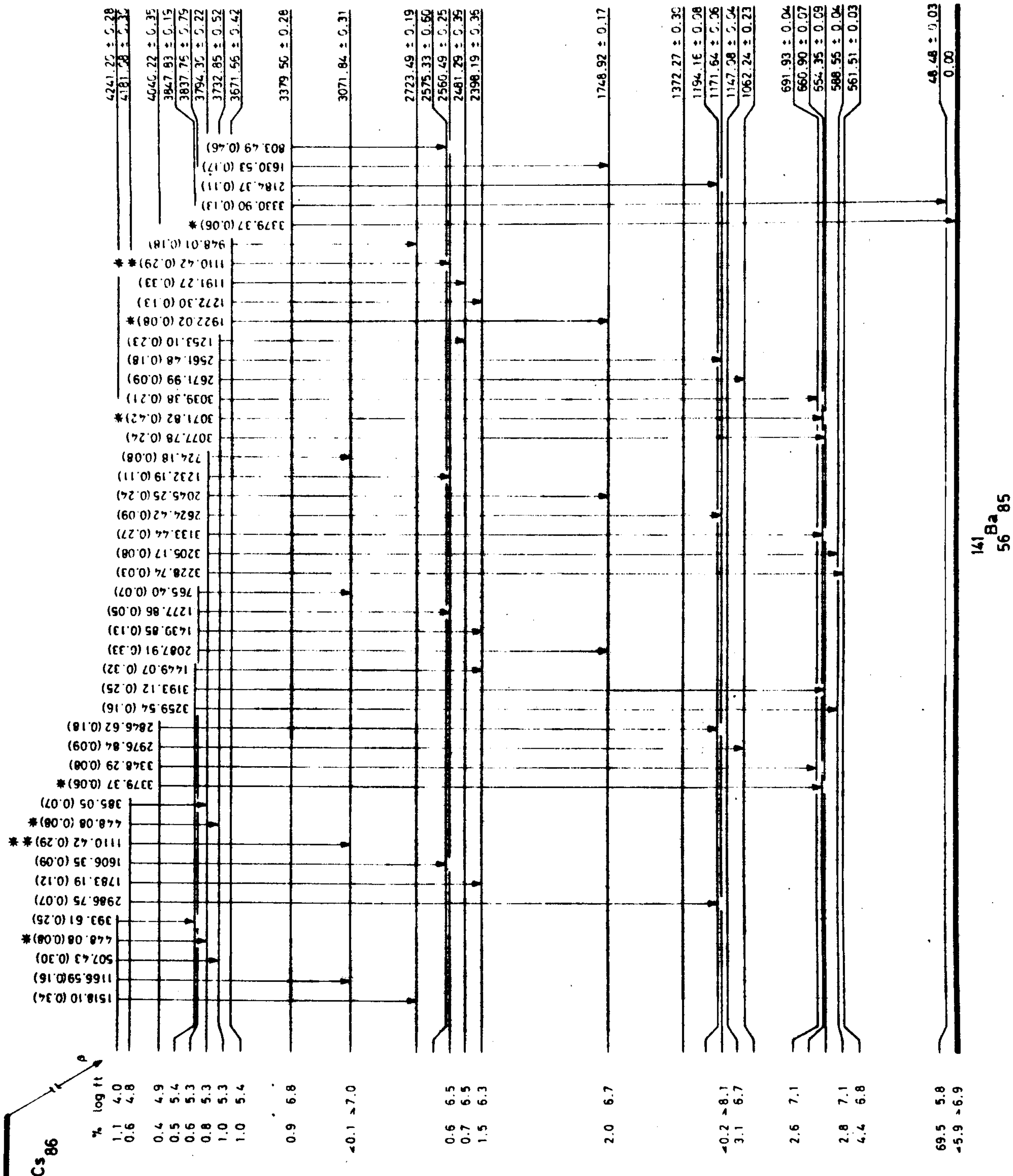

Fig III.5.2(a) Level scheme of ^{141}Ba (low energy part).

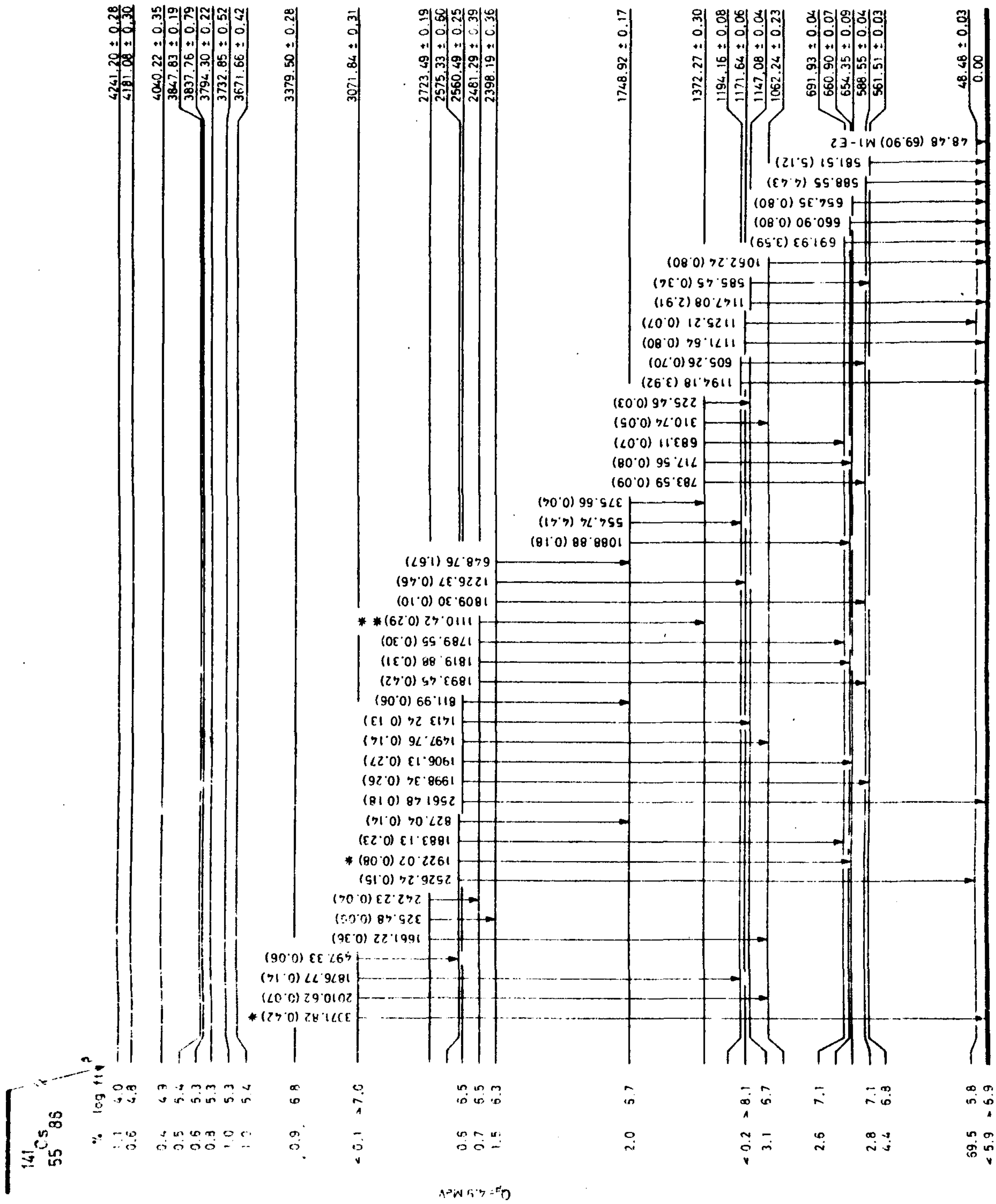

Fig. III.5.2(b) Scheme of ^{141}Ba (low energy part).

III.6. Delayed Neutrons from the A = 141 Chain and Identification of γ-ray Transitions in the A = 143 Chain.

A.N.Proto and D.Otero.

In order to broaden the techniques available for the study of isotopes far from the stability line, a method which allows discrimination of neutrons from γ-rays based on the different time responses of the detector signals, was developed. In our case a hidrogenated plastic within which ZnS(Ag) crystals are dispersed (NE451) was used as the detector. Its efficiency for γ-rays is about 3.5×10^{-6} that of a Ge(Li) detector[1].

The system was tested with the data from the A = 141 chain already published[2]. However, the present measurements indicate that the neutron precursor is ^{141}Xe and not ^{141}Cs as hitherto thought.

In order to explore new research possibilities the γ-radiation emitted in the A = 143 chain was studied, particularly for the less known isotopes ^{143}Xe(0.3 or 0.9 sec), ^{143}Cs(1.7 sec), ^{143}Ba(13.6 sec) and ^{143}La (14.0 min). The results obtained so far allow us to identify the main transitions indicated in Figs. III.6.1 and III.6.2.

A preliminary measurement of the half-life of the ground state of ^{143}Xe favours the value $T_{1/2}$ = 0.3 sec[3] instead of $T_{1/2}$ = 0.9 sec[4]. The possibility that two different isotopes are present can not be ruled out from the measurements made until now because the earlier results were obtained either from an indirect determination or from the observation of β-radiation, while in our case γ-radiation was detected.

---

[1] A.N.Proto, Thesis UNLP (La Plata), Biblioteca Física Nuclear N° 37 (1974).
[2] Nucl. Data Tables 6, (1969) 141.
[3] P.Patzelt, G.Herrman, Proc. Symp. on Phys. and Chem. of Fission, Vol II, Salzburg, Austria, IAEA, Vienna, (1965) p. 243.
[4] S.Amiel et al., Phys. Rev. C5 (1972) 270.

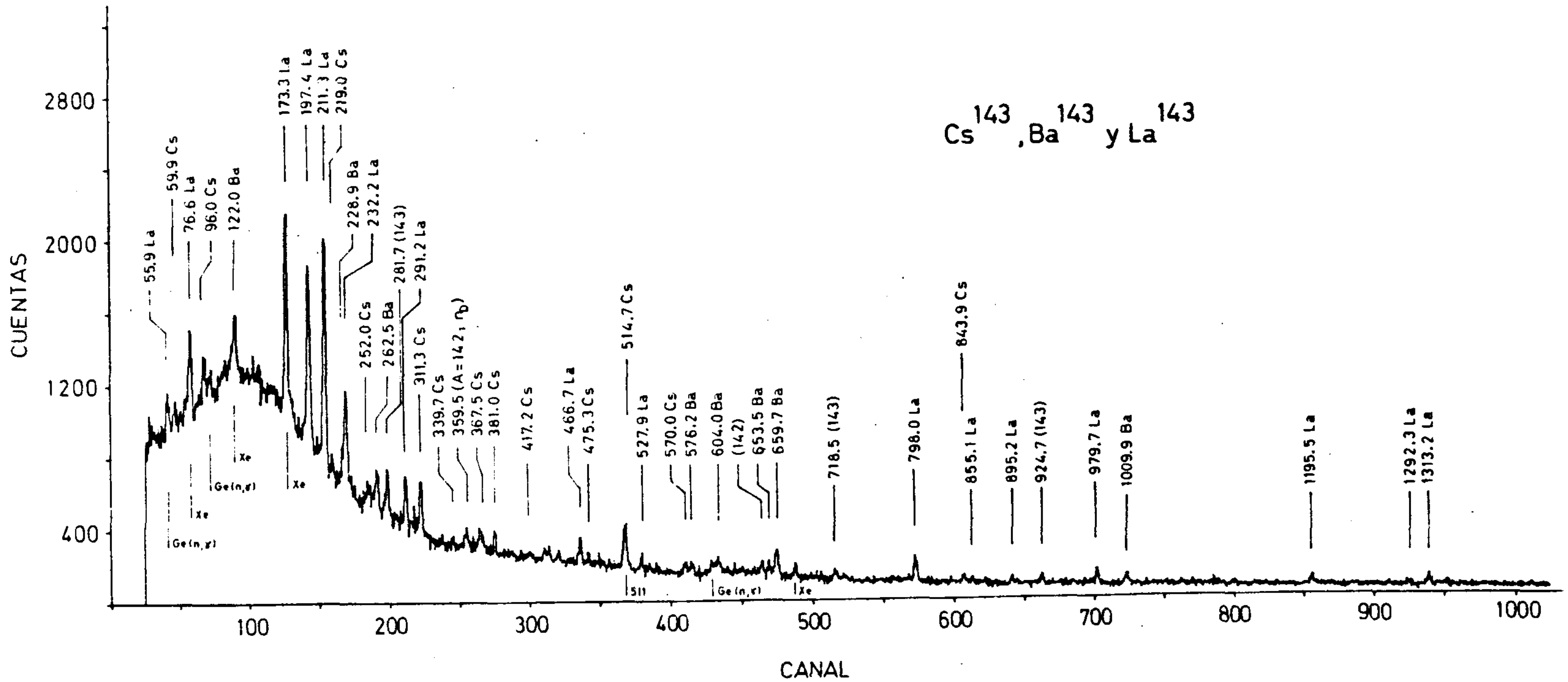

Fig. III.6.1 The top lines indicate transitions from the decay of the isobaric chain A = 143. The bottom lines indicate transitions belonging to ^{143}Xe and background peaks.

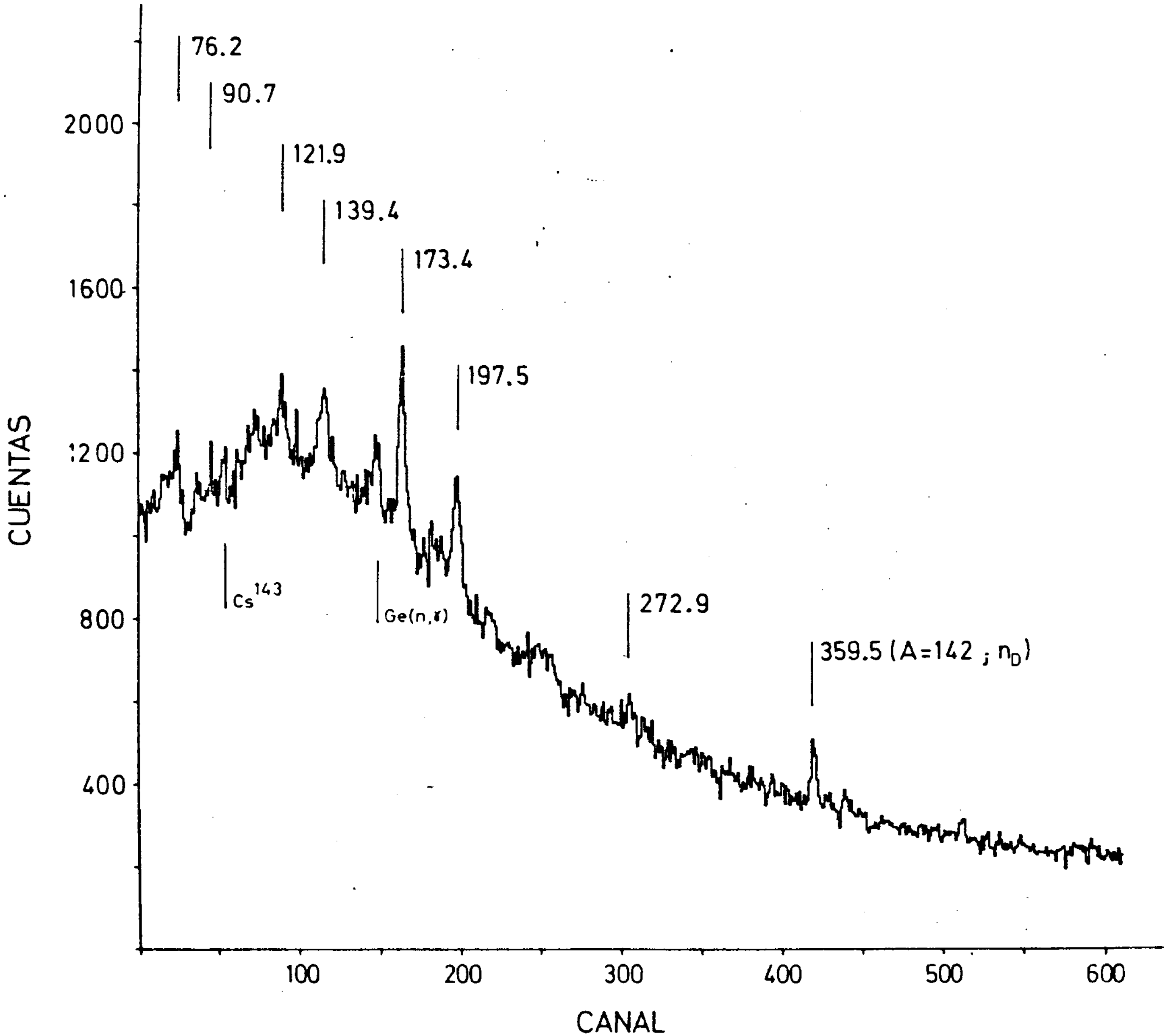

Fig. III.6.2 The top lines indicate transitions from the decay of ^{143}Xe. The 359.5 keV line has been identified as delayed neutron emission.

III.7. Studies of Fission Yields of ^{235}U Products.

D.Otero and A.N.Proto.

The study of the yield of the ^{235}U fission products by on-line techniques depends on the knowledge of their production and emanation properties from the fission chamber. A study of this type was performed using the IALE project facilities described in Sec. III.1. A switching device was installed allowing to deflect the deuteron beam off the neutron-generating target. The time delay for this operation is approximately .03 sec. The mass separator beam can be independently switched off from the collector assembly in about .02 sec.

To study the time dependence of the transport process from the fission chamber to the mass separator ion source, irradiation with a constant neutron flux was performed with the mass separator beam switched off. The deuteron beam was then switched off; the mass separator beam was switched on, and the time evolution of the activity of interest was studied. It was assumed that the process can be described by a set of coupled diffusion equations with a characteristic "diffusion constant", λ_D, describing the transport from the fission chamber to the ion source.

The amount of atoms collected during a saturation irradiation will depend on the constant λ_D. Measurements performed on Xe, Kr, I and Br, showed that this constant is only weakly dependent on the mass of a given element.

Using this method and applying the corrections due to the measured values of λ_D and the respective disintegration constants the accumulated yields for $^{137,138,139,140,141}Xe$ were determined. The yield for ^{141}Xe turned out to be approximately half of that expected[1].

An additional result of the measurement of the temporal behavior of the production of radioactive nuclei was the determination of the half-life of those fission products which are parents of the rare gases and which themselves are retained in the fission chamber. Figs. III.7.1, III.7.2 and III.7.3 show the results for the mass 137 chain. The values obtained for the half-lives in the present work compared to those measured in Ref. 2 are shown in Table III.7.1.

---

1 B.Ehrenberg, S.Amiel, Phys. Rev. C6 (1972) 618.

2 Chart of the Nuclides, Knoll's Atomic Power Laboratory (1972).

Table III.7.1

Half-Lives of A = 137 Nuclei

Isotope	$T_{1/2}$ (sec) present work	$T_{1/2}$ (sec) Ref. 2
^{137}I	25.2 ± 1.2	24.6
^{137}Te	3.0 ± 0.5	3.5
^{137}Sb	2.0 ± 0.6	---

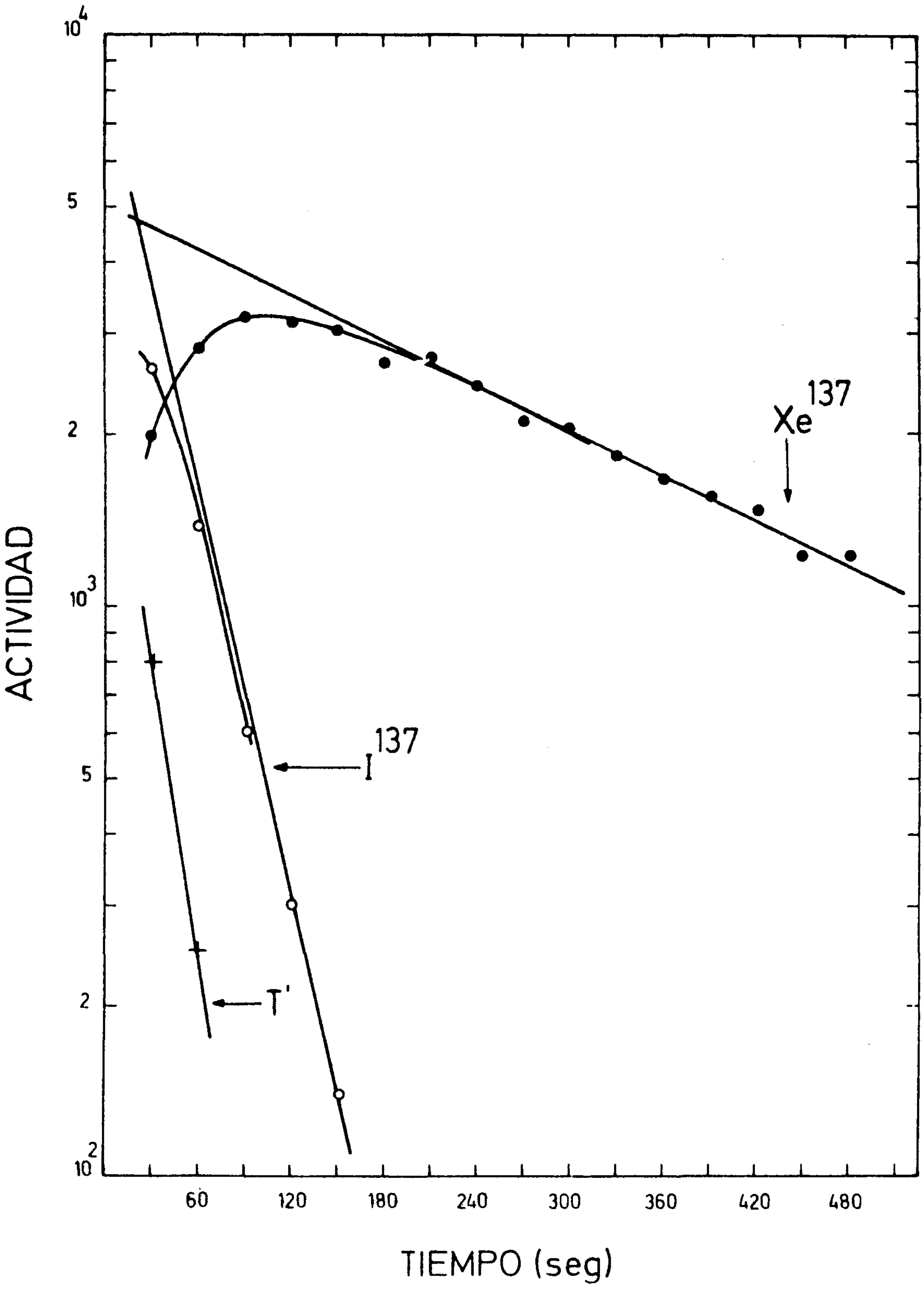

Fig. III.7.1 ^{137}Xe γ-ray activity at the mass-separator collector obtained as a response to a step function of the neutron irradiation.

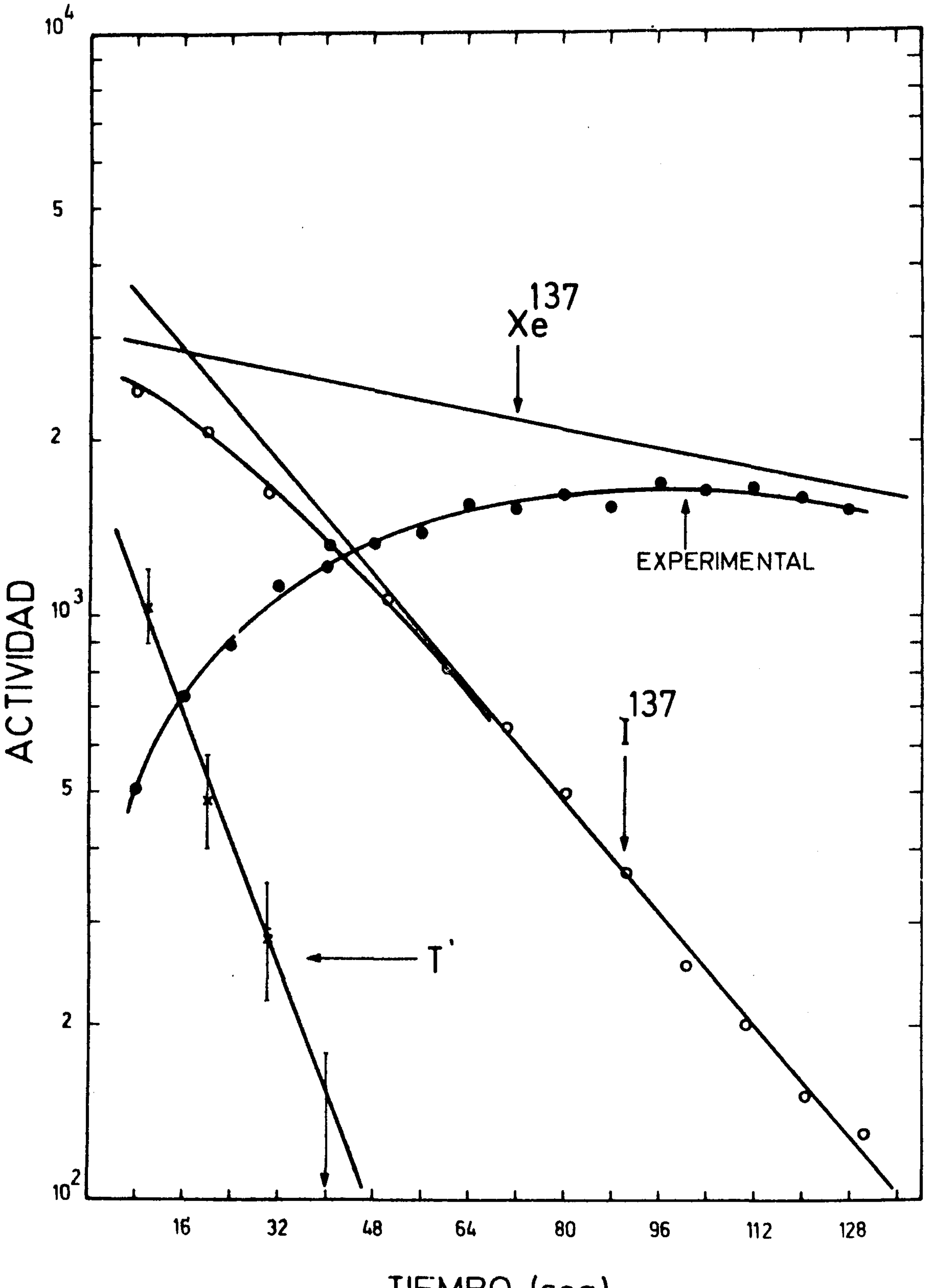

Fig. III.7.2 Same as Fig. III.7.1 (expanded scale).

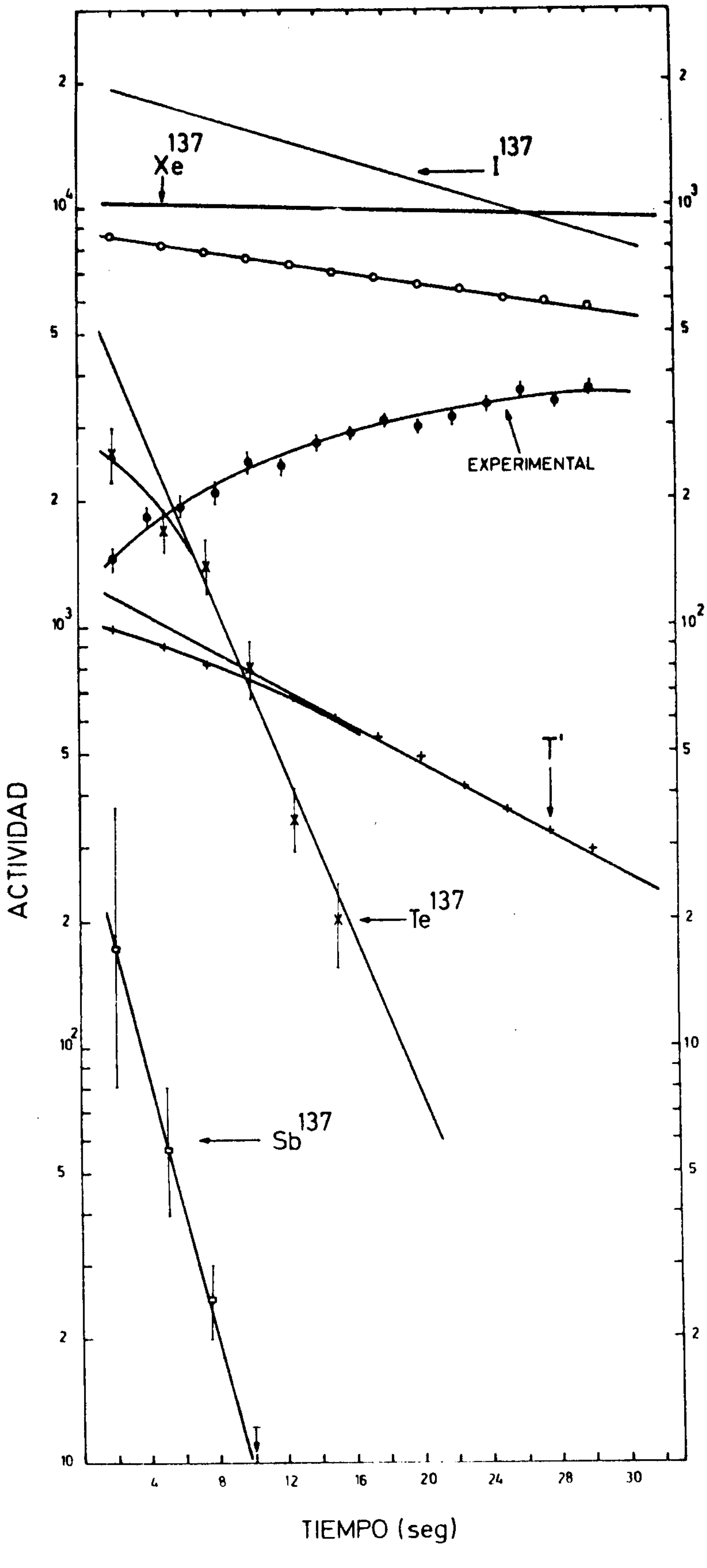

Fig. III.7.3 Same as in Fig. III.7.1 (expanded scale). The scale at the right corresponds to ^{137}Te only.

IV. RADIOACTIVITY

IV.1. The Spin of the 2198 keV Level in ^{74}Ge and Multipole Mixing Ratios of Gamma Transitions in the Decay of ^{74}As.

M.C.Cambiaggio*, G.García Bermudez and M.Behar.

The levels in ^{74}Ge populated by radioactive decay of ^{74}As have been extensively studied by several authors[1,2] and the level scheme shown in Fig. IV.1.1 was proposed. Within the framework of the vibrational model, the 596 level is interpreted as a one-phonon state while the 1204 keV and 1483 keV levels are interpreted as members of the two-phonon triplet.

The situation with the 2198 keV level is contradictory. From decay considerations the appropiate assignment seems to be 2^+ and, consequently, the state could be interpreted as a member of the three-phonon quintuplet. However a direct measurement involving the spin of this level by means of the (p,p'γ) reaction[3] favoured an assignment of 1^- to this level.

The ground state and first two excited states of ^{74}Se are also populated by the decay of ^{74}As. The spin and parities of the ground and first excited state of ^{74}Se are well known. However there are strong discrepancies in the assignments for the 1270 keV level. Kubok et al.[1] established the spin as 0^+ or 4^+; Van Hise et al.[2] suggested $1^{\pm}$ or $2^{\pm}$; and Coban et al.[4] determined the spin as 2^+.

The present experiment was undertaken in order to resolve these discrepancies in ^{74}Ge and ^{74}Se using the γ-γ directional correlation technique. The directional correlation system employed a fixed coaxial Ge(Li) detector and a 5cm × 5cm movable NaI detector. A conventional coincidence system with a TAC was used. Data were collected at seven different angles between the symmetry axis of the detectors. The coincidence counts were normalized and then computer-fitted to a directional correlation function of the form

$$W(\Theta) = \sum_{k=0,2,4} Q_{kk}\, B_k(1)\, A_k(2)\, P_k(\cos\Theta) \qquad (1)$$

Numerals (1) and (2) express the dependence on the properties of the first and second transition in a cascade, respectively. Q_{kk} is the geometrical correction factor.

The spin of the 2198 keV level in ^{74}Ge can be extracted not only from the 994 keV - 1204 keV angular correlation but also from the 994 keV - 608 keV one. The angular correlation coefficients obtained in the first case are only compatible with a 2-2-0 spin sequence as shown in Fig. IV.1.2, where the coefficients $A_{kk} = B_k(1)A_k(2)$ are represented as a function of the mixing ratio δ for different spin sequences. The deduced mixing ratio δ and quadrupole content (Q) for the 994 keV transition are

$$\delta(994) = -2.8 \pm 0.2 \quad \text{and} \quad Q = (89 \pm 2)\%E2$$

From the measurement of the 994 keV - 608 keV cascade one obtains

$$-3.80 \lesssim \delta(994) \lesssim -1.40 \quad \text{and} \quad 93\%E2 \lesssim Q \lesssim 66\%E2$$

The results of both angular correlations agree very well with each other and fix the spin of the 2198 keV level as 2. Furthermore, since a negative parity would give an unlikely high M2 admixture for the 994 keV transition, a positive parity assignment is favoured for this level.

The results of the 635 keV - 635 keV cascade corresponding to levels in ^{74}Se is only compatible with a 2-2-0 spin sequence as shown in Fig. IV.1.2. Although this result agrees with the directional correlation work of Coban et al.[4], there is a difference in the measured mixing ratio; $\delta(635) = -2.6 \pm 0.2$ in the present case whereas the value reported by Coban et al. is $\delta(635) = -(6 \pm ^{2}_{1})$.

The spin assignment of the 2198 keV level and the measured multipolarity of the 994 keV transition (89% E2) enables us to interpret the 2198 keV level in ^{74}Ge as a member of the three-phonon quintuplet. The calculated B(E2) ratios between the 994 keV transition and the gamma rays decaying to the two-phonon, one-phonon and ground state are:

$$\frac{B(E2;994)}{B(E2;715)} = 0.5 \pm 0.2$$

$$\frac{B(E2;994)}{B(E2;1606)} = 38 \pm 10$$

$$\frac{B(E2;994)}{B(E2;2198)} = 83 \pm 15$$

These results show that the 994 keV transition is clearly enhanced compared with the transitions to the one-phonon and ground state; confirming the collective structure of the 2198 keV level in ^{74}Ge.

---

* Universidad Tecnológica Nacional, Buenos Aires, Argentina.

1 A.H.Kuboc, J.D.King and H.W.Taylor, Nucl. Phys. A115 (1968) 625.

2 J.R.Van Hise and C.Paperiello, Nucl. Phys. A188(1972) 148.

3 T.H.Curtis. H.F.Lutz and W.Bartolini, Phys. Rev. C1 (1970) 1418.

4 A.Coban et al., Particles and Nuclei 4 (1972) 108.

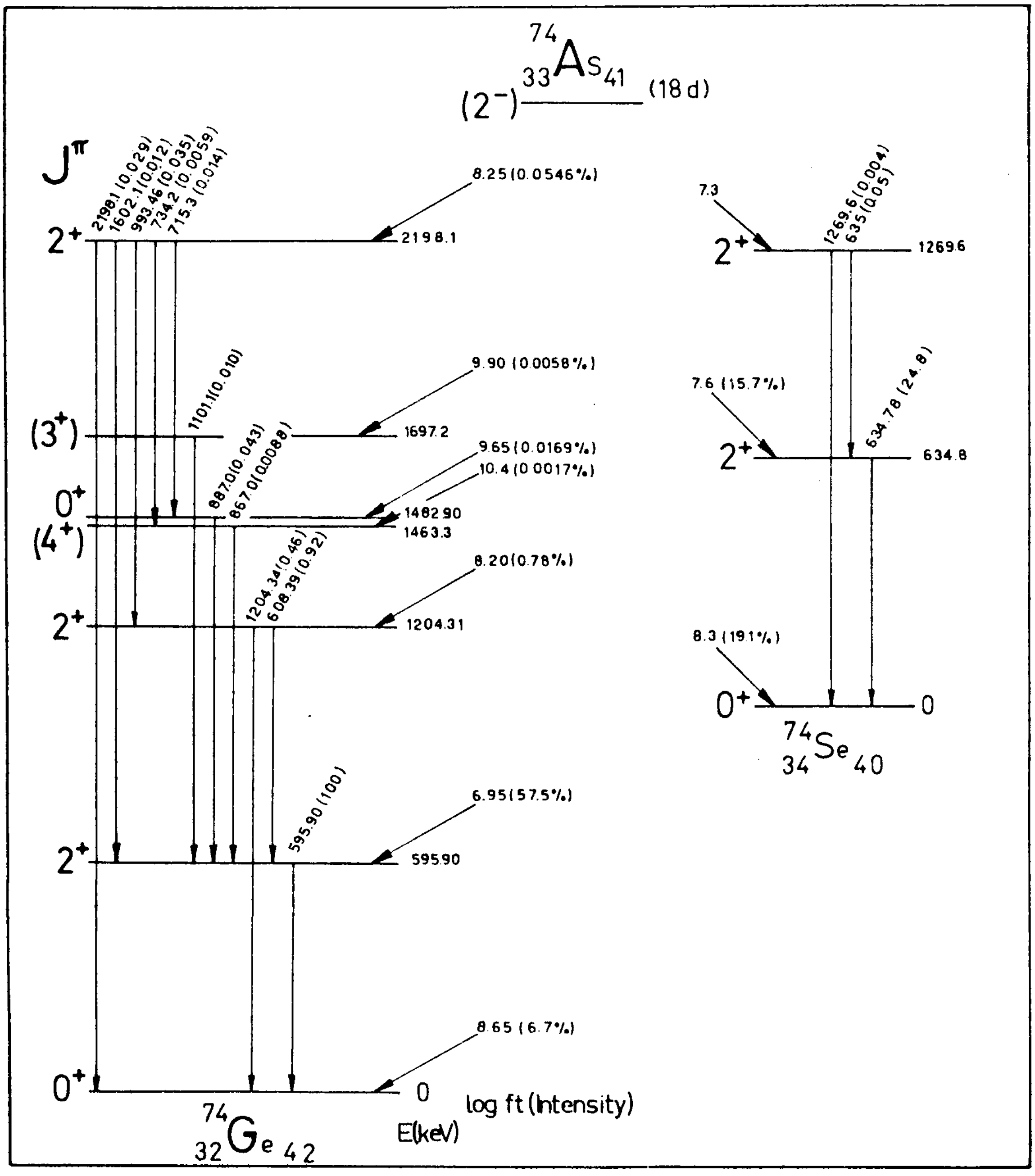

<u>Fig. IV.1.1</u> Decay scheme of ^{74}As.

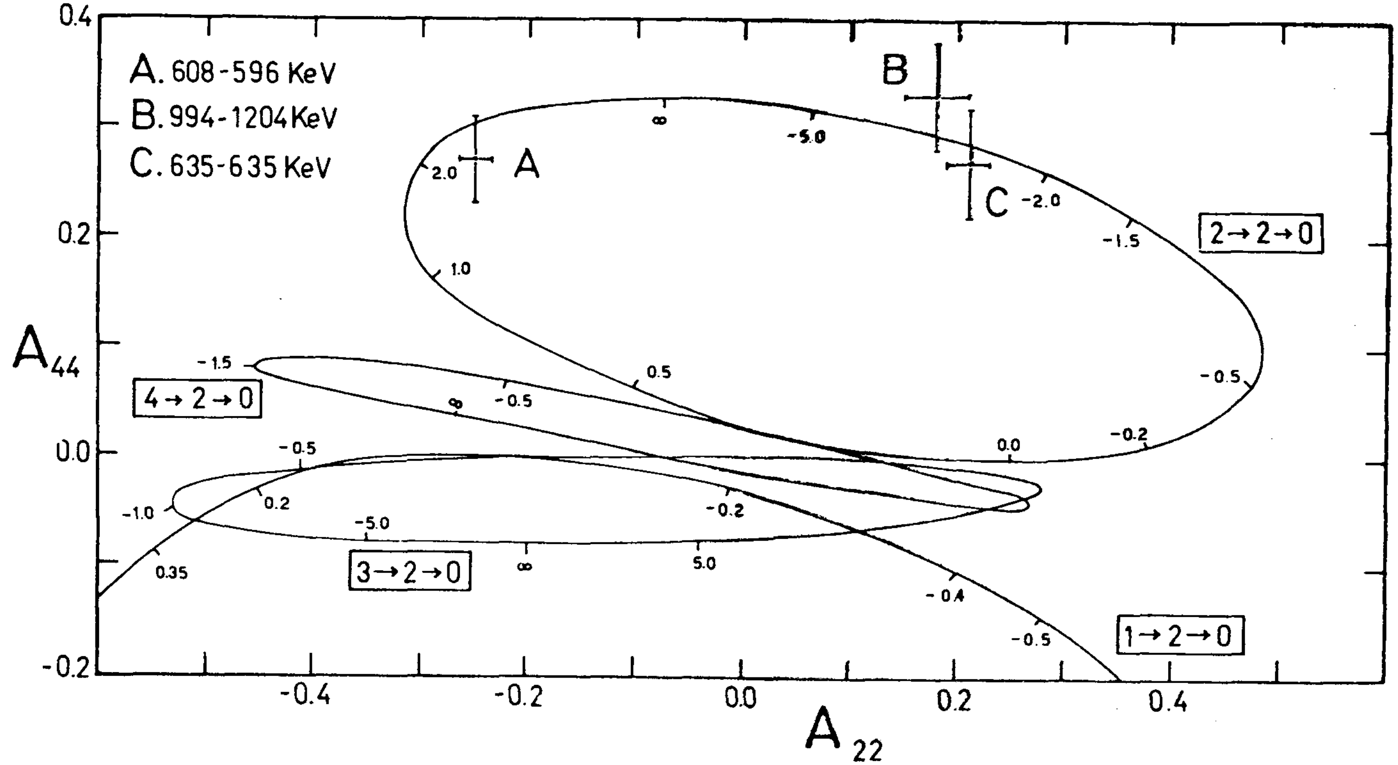

Fig. IV.1.2 Plot of directional correlation coefficients as a function of the mixing parameter δ for various J - 2 - 0 sequences.

IV.2. A gamma-gamma Polarized Directional Correlation Set-Up Using a Planar Ge(Li) Detector as the Polarimeter.

A.Filevich, M.Behar and G.García Bermudez.

In nuclear spectroscopy studies it is often sufficient to measure the directional angular correlation of two subsequent gamma rays and its internal conversion coefficient to obtain the spin and parity of the nuclear levels involved in the cascade. However, there are many cases in which the experimental data do not allow to distinguish between the various spin assignments. For such cases the measurement of the linear polarization of one of the cascade gamma rays, combined with the γ-γ angular correlation measurement, is a method which often allows to resolve the ambiguities mentioned above.

Recently, γ-polarimeters based on a single, thin, Ge(Li) detector[1] and on the anisotropy of the compton effect with respect to the electric vector orientation, have been introduced (see Fig. IV.2.1(a)). In these devices the observed radiation incides perpendicularly to one of the thin edges of the crystal which works both as compton scatterer and absorber.

A γ-ray polarimeter of this type has been constructed using a 25x25x4 mm Ge crystal, mounted in a horizontal cryostat with one of the narrow edges facing a thin aluminium window. Well known γ-ray sources in punctual configuration were used to center the crystal and for efficiency calibration (Fig. IV.2.1(b)). In order to determine the efficiency of the polarimeter, the movable detector was rotated in the 90° - 180° - 270° sequence and the asymmetry was measured. The asymmetry β is related to the efficiency Q by

$$\beta = \frac{N_{\perp}}{N_{//}} = \frac{1 + PQ}{1 - PQ}$$

where PQ is defined as

$$PQ = \frac{W(90°,180°) - W(90°,180°)}{W(90°,180°) + W(90°,180°)}$$

It has been found that Q is approximately constant in the energy range 0.4-1.3 MeV for the present device. The weighted average yields a value Q = 0.154 ± 0.012 (see Fig. IV.2.1b).

In order to decide whether a measurement of the γ-γ(LP) correlation can help to establish spins of nuclear states, the value of the asymmetry β for the cascades more frequently found in spectroscopy studies have been plotted in Figs. IV.2.a and IV.2.3. The first transition in the cascade has a mixing ratio δ (whose sign convention was adopted from Ref. 2), polarization P and electric character. It has been assumed that the second transition is pure.

The solid angle correction is less than 6% for the J = 1-2-0 cascade and less than 3% for all other cases. The asymmetry for the magnetic case can be easily obtained from

$$\beta(\text{mag}) = \beta^{-1}(\text{elec})$$

The tabulated values of the asymmetry β are available upon request.

---

[1] A.E.Litherland, G.T.Ewan and S.T.Lam, Can. J. Phys. 48 (1970) 2320.
[2] K.S.Krane and R.M.Steffen, Phys. Rev. C2 (1970) 724.

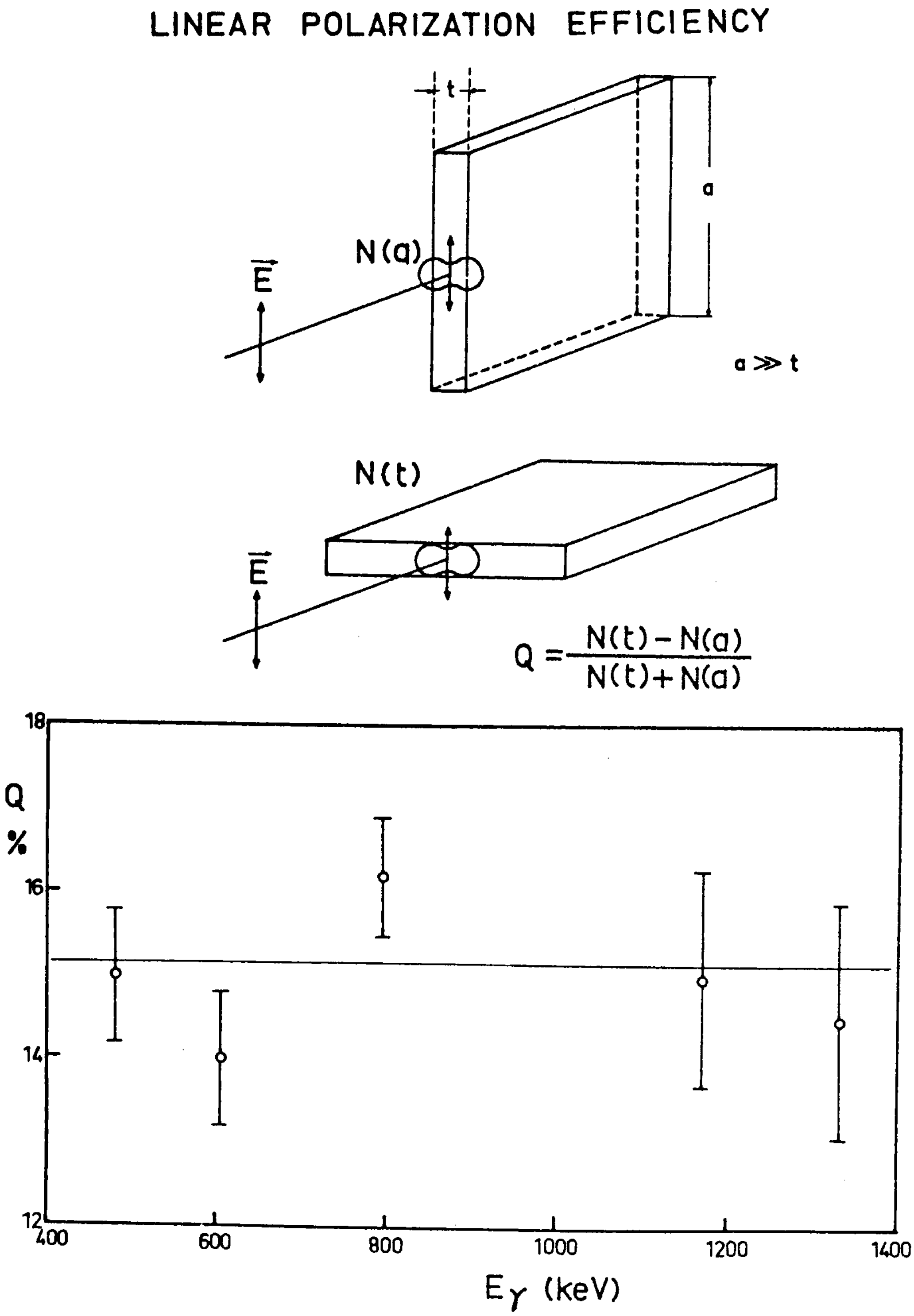

Fig. IV.2.1 (top) Principle of the polarimeter based on a single Ge(Li) crystal.
(bottom) Polarization efficiency measured for the present device.

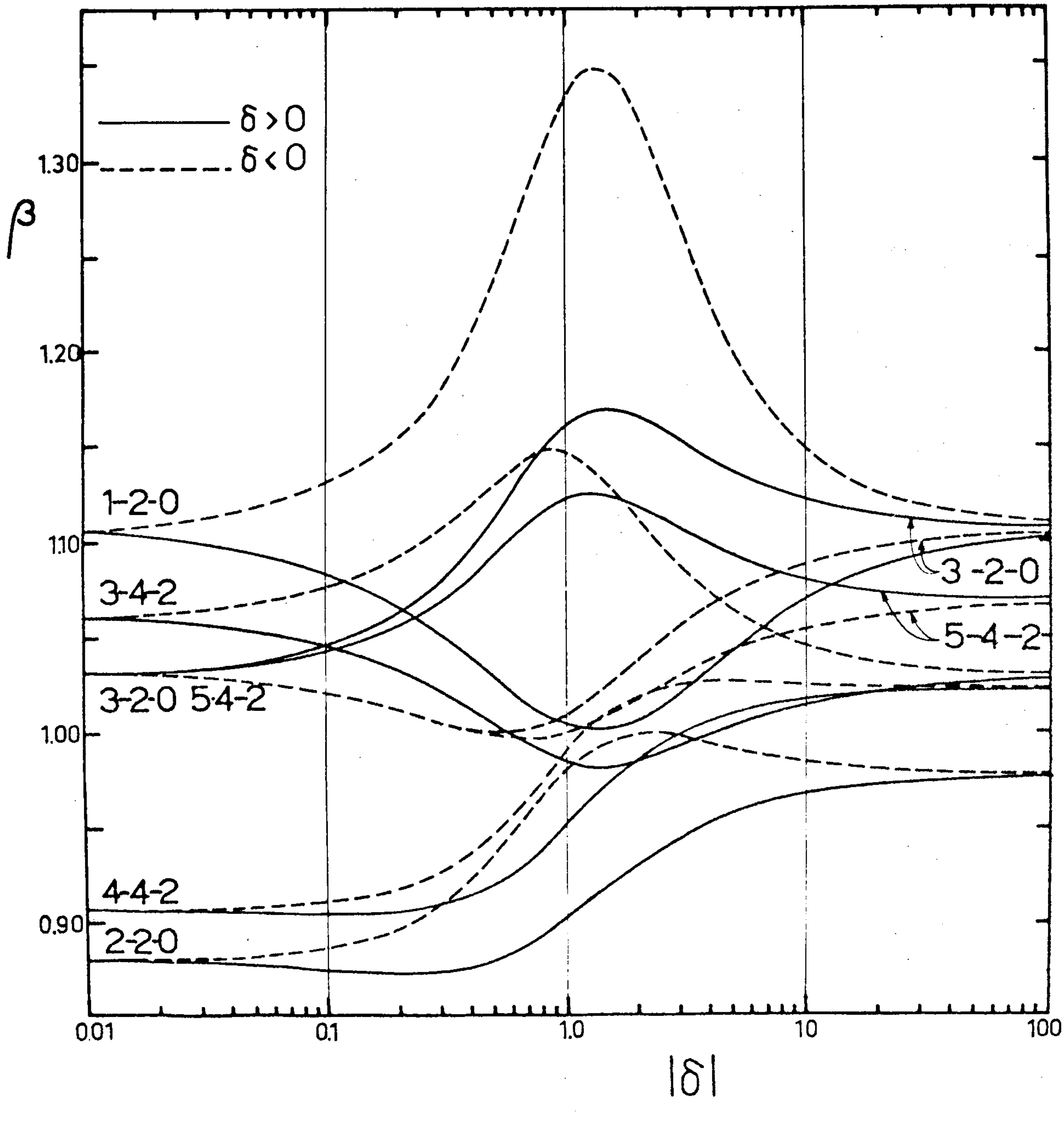

Fig. IV.2.2 Plot of the asymmetry β as a function of mixing ratio δ for different multipolarities (Even transitions).

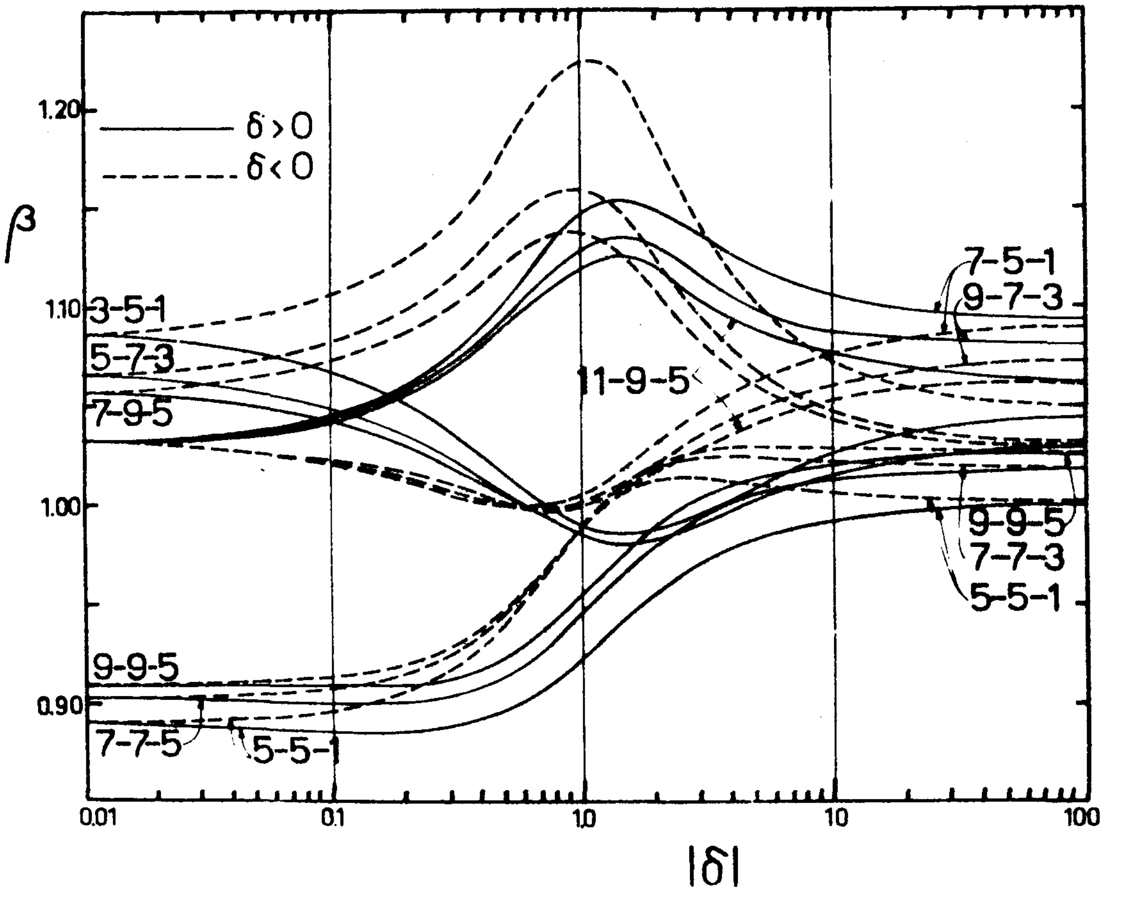

Fig. IV.2.3 Plot of the asymmetry β as a function of mixing ratio δ for different multipolarities (Odd transitions). Levels labelled 11, 9, ..., 1 should read 11/2, 9/2, ..., 1/2.

IV.3. Spin of the 1248 keV and 1958 keV Levels in ^{124}Te Determined from γ-γ Directional and Polarization Directional Correlations.

M.Behar, G.García Bermudez, A.Filevich and M.C.Cambiaggio*.

The nucleus ^{124}Te has been extensively studied and, as a result, a decay scheme has been proposed (Fig. IV.3.1). For certain levels however, the parity assignment is not unique. Such are the cases of the 1958 keV and 1248 states for which the experimental data is compatible[1,2] both with $J^{\pi} = 4^{+}$ and $J^{\pi} = 3^{+}$.

In order to determine the spin and parity of these levels γ-γ directional angular and linearly polarized correlations have been measured, employing the technique described in the preceeding work. For the γ-γ(Θ) correlation the detector angle Θ was varied to 7 different positions. A careful background and chance coincidence substraction was performed.

The results of the measurements of the γ-γ(Θ) correlations do not allow to distinguish between the possible spin assignments of J = 4-2-0 or J = 3-2-0 for the 646-603-keV cascade or J = 4-4-2 or J = 3-4-2 for the 709-646-keV cascade. Even measurements of the conversion coefficient yield contradictory assignments for the multipolarities of these γ-rays.

To resolve these ambiguities the γ-γ(90°LP) correlations were measured by accepting the first transition of the cascades in the polarimeter and the second transition in the movable detector. From the results of this measurement (see Table IV.3.1) it can be concluded without ambiguity that the only spin and parity assignment compatible with experimental data is $J^{\pi} = 4^{+}$ for both the 1958 keV and the 1248 keV levels. These assignments are in good agreement with theoretical predictions. It can be added that on the basis of the present results the 709 keV transition has a pure M1 character.

---

* Universidad Tecnológica Nacional, Buenos Aires, Argentina.

1 R.P.Meyer, W.B.Walters and R.C.Ragaini, Nucl. Phys. A127 (1969) 595.

2 Z.W.Grabowsky, K.S.Krane and R.M.Steffens, Phys. Rev. C3 (1971) 1649.

Table IV.3.1

Results of the γ-γ(90°LP) correlation measurements in ^{124}Te

Cascades	Spin sequence	$\delta = \frac{<L+1>}{<L>}$	β_{theor}	β_{exp}
646 - 603	$3^+ - 2^+ - 0^+$	0.25 ± 0.01	0.930	
	$4^+ - 2^+ - 0^+$	0.00 ± 0.01	1.051	1.055 ± 0.010
709 - 646	$3^+ - 4^+ - 2^+$	-0.43 ± 0.04	0.893	
	$4^+ - 4^+ - 2^+$	0.02 ± 0.06	1.110	1.095 ± 0.030

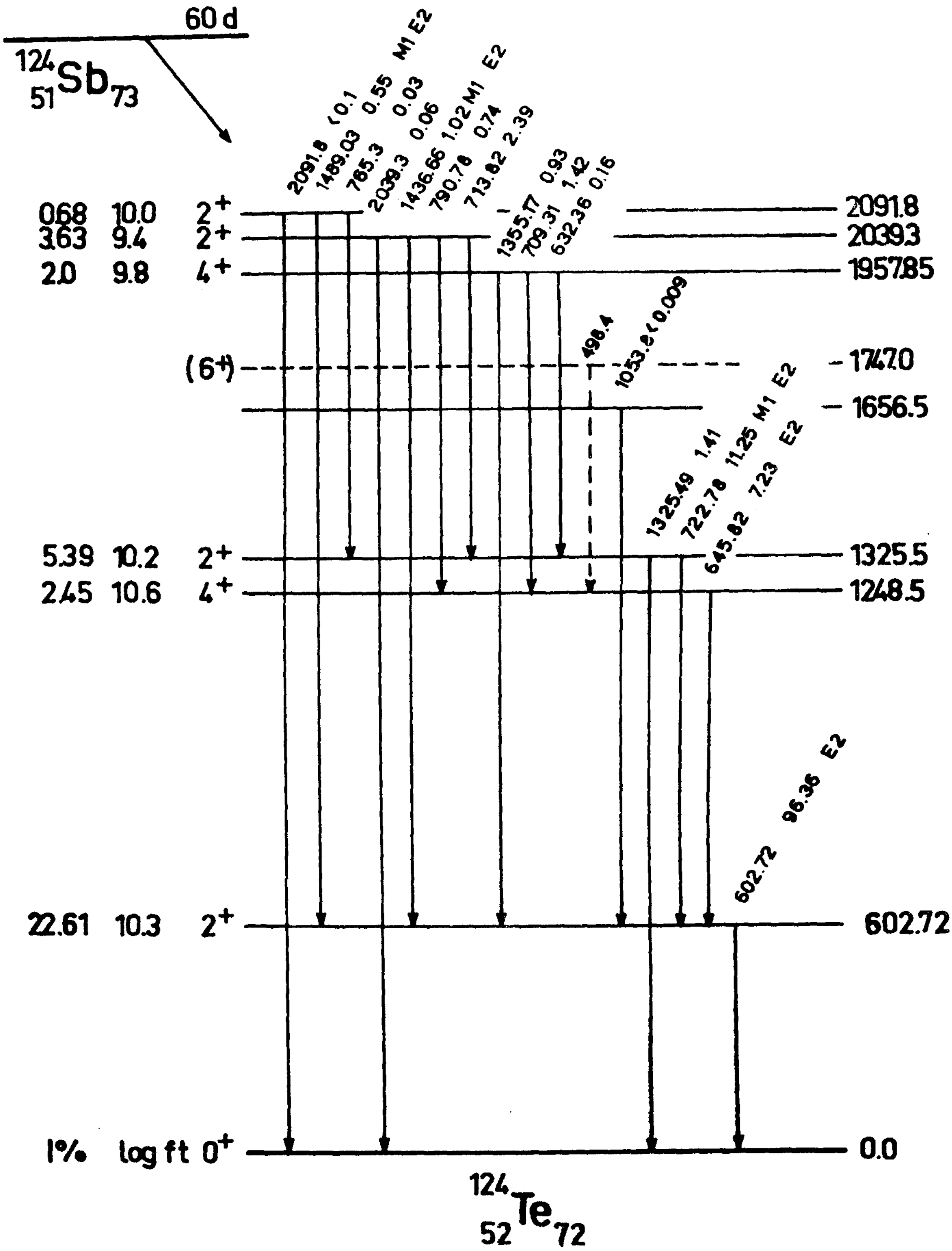

Fig. IV.3.1 Level Scheme of ^{124}Te.

IV.4. Spin of the 2350 keV, 2516 keV and 2547 keV Levels in ^{140}Ce Determined from γ-γ Directional and Polarization Directional Correlations.

G.García Bermudez, A.Filevich and M.Behar.

The nucleus ^{140}Ce has been extensively studied in the past basically because it is one of the seven stable isotones with magic number N = 82. These investigations led to the level scheme shown in Fig. IV.4.1. Spin and parity assignments of almost all the low lying states were made from the studies of the radioactive decay of ^{140}La and from the conversion electron work of Karlsson et al.[2]. However, uncertainties in spin assignments of several levels still subsist. Such is the case of the 2516 keV level where an assignment of $J^{\pi} = 3^{\pm}, 4^{+}$ has been proposed[1,2] and also of the 2547 keV level where the suggested assignment is $J^{\pi} = (1,2)^{+}$. The situation with the respect to the 2350 keV is contradictory. Baer et al.[1] based on the conversion coefficient data of Karlsson et al.[2] made an assignment of $J^{\pi} = 5^{-}$ to this state. However Kalinnikov et al.[3] concluded that the most probable assignment is $J^{\pi} = (4,5)^{+}$.

The present experiment was undertaken in order to clarify this situation by using γ-γ directional correlation and γ-γ polarized directional correlation techniques. The radioactive source ^{140}La was produced by the Buenos Aires RA3 Reactor. The directional correlation system employed a fixed coaxial Ge(Li) (resolution 2.3 keV at 1.33 MeV and 6% efficiency) and a 7.5 cm × 7.5 cm movable NaI detector coupled to a conventional coincidence system using a TAC converter. The window was set on the 1597 keV transition detected in the NaI crystal and the coincidence counting rate was determined for seven different angles. After a straightforward analysis the angular correlation coefficients A_2 and A_4 were obtained for several cascades.

The correlation of the 432 keV transition de-exciting the 2516 keV level has been measured through the triple cascade 432 - (487) - 1597 keV. For this special spin sequence the analysis is reduced to a simple case in which the only possible sequences are J = 3-4-2 and J = 4-4-2. Fig. IV.4.2 shows a parametric plot of A_2 and A_4 for different values of the mixing ratio δ establishing an unique spin determination for the 2516 keV level of J = 4 and a mixing ratio $\delta(432) = 0.54 \pm 0.10$.

The spin of the 2547 keV level was studied through the 951 - 1957 keV cascade. The result, also shown in Fig. IV.4.2, determines a spin of J = 1 and a mixing ratio $\delta(951) = 0.10 \pm 0.03$ for the 951 keV transition.

The spin of the 2350 keV level could not be determined only on the basis of the measurement of the angular correlation of the 267 - 1597 keV cascade, because the experimental results allow different values of the mixing ratio for the 267 keV transition. For this case a measurement of the linear polarization of the 267 keV transition was undertaken using the polarimeter described earlier in Sec. IV.2. The results of this measurement, displayed in Table IV.4.1, determines the spin and parity of the 2350 keV level as $J^{\pi} = 5^{-}$, and the mixing ratio of the 267 keV transition as $\delta(267) = 0.39 \pm 0.05$.

Fig. IV.4.1 shows a partial decay scheme of ^{140}La compared to a shell model calculation of Wildenthal[4].

---

[1] H.W.Baer, J.J.Reidy and M.L.Wiedenbeck, Nucl. Phys. 86 (1966) 332.

[2] S.E.Karlsson, B.Svahn, H.Pettersen and G.Malmsted, Nucl. Phys. A100 (1967) 113.

[3] V.G.Kalinnikov, K.I.Ravn, H.G.Hansen and N.A.Lebedev, Bull. Acad. Sci. USSR, Phys. Ser. 34 (1971) 815.

[4] B.H.Wildenthal, Phys. Rev. Letters 22 (1969) 1118.

Table IV.4.1

Results of the linear polarization measurement in ^{140}Ce

Cascade (keV)	Spin sequence	δ	β_{theor}	β_{exp}
267 - 1597	$4^{-} \rightarrow 4^{+}$	0.13 ± 0.05	0.905	
	$4^{+} \rightarrow 4^{+}$	0.13 ± 0.05	1.104	
	$5^{-} \rightarrow 4^{+}$	0.39 ± 0.05	1.080	1.065 ± 0.029
	$5^{+} \rightarrow 4^{+}$	0.39 ± 0.05	0.926	

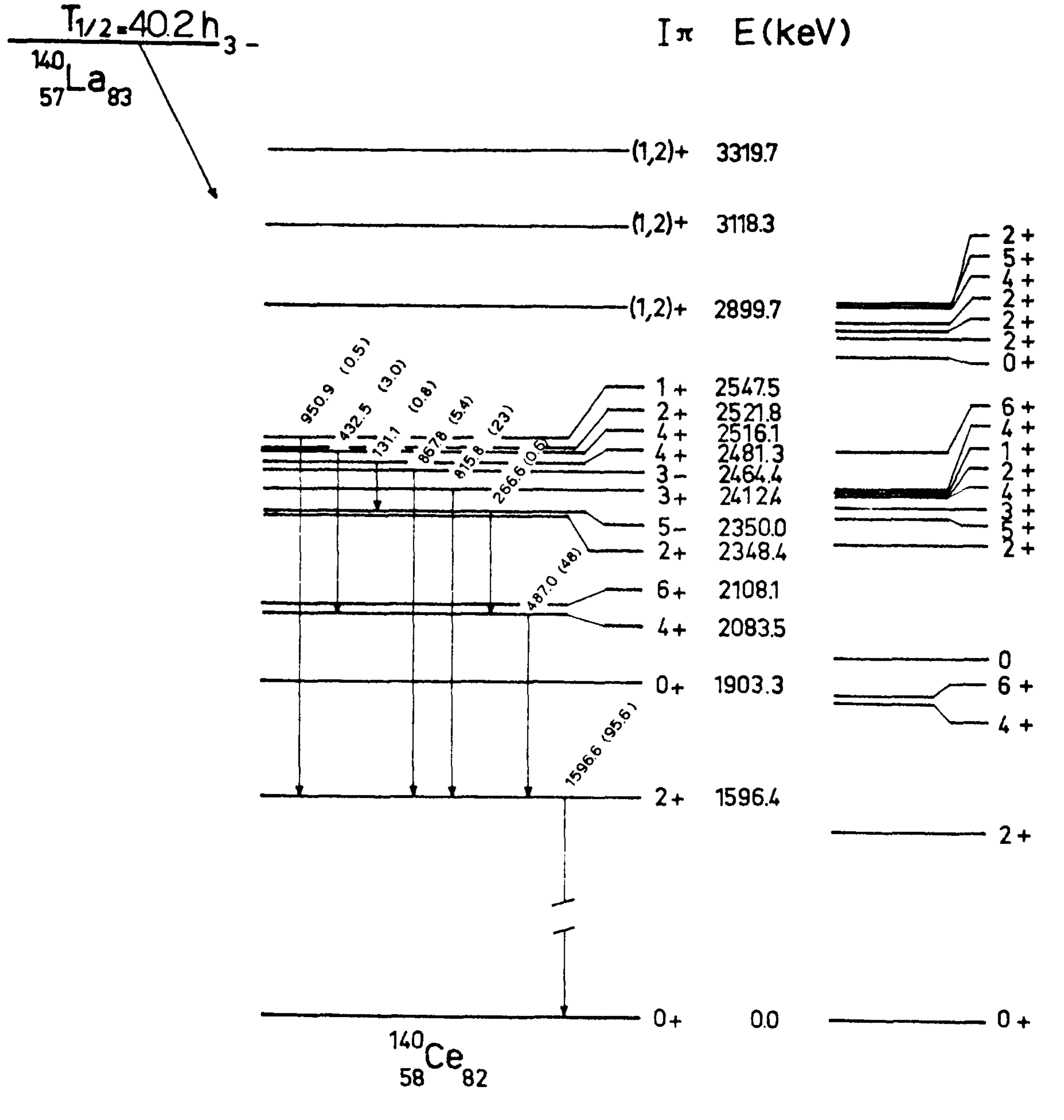

Fig. IV.4.1 Partial decay scheme of ^{140}La compared with the shell model calculation of Ref. 4.

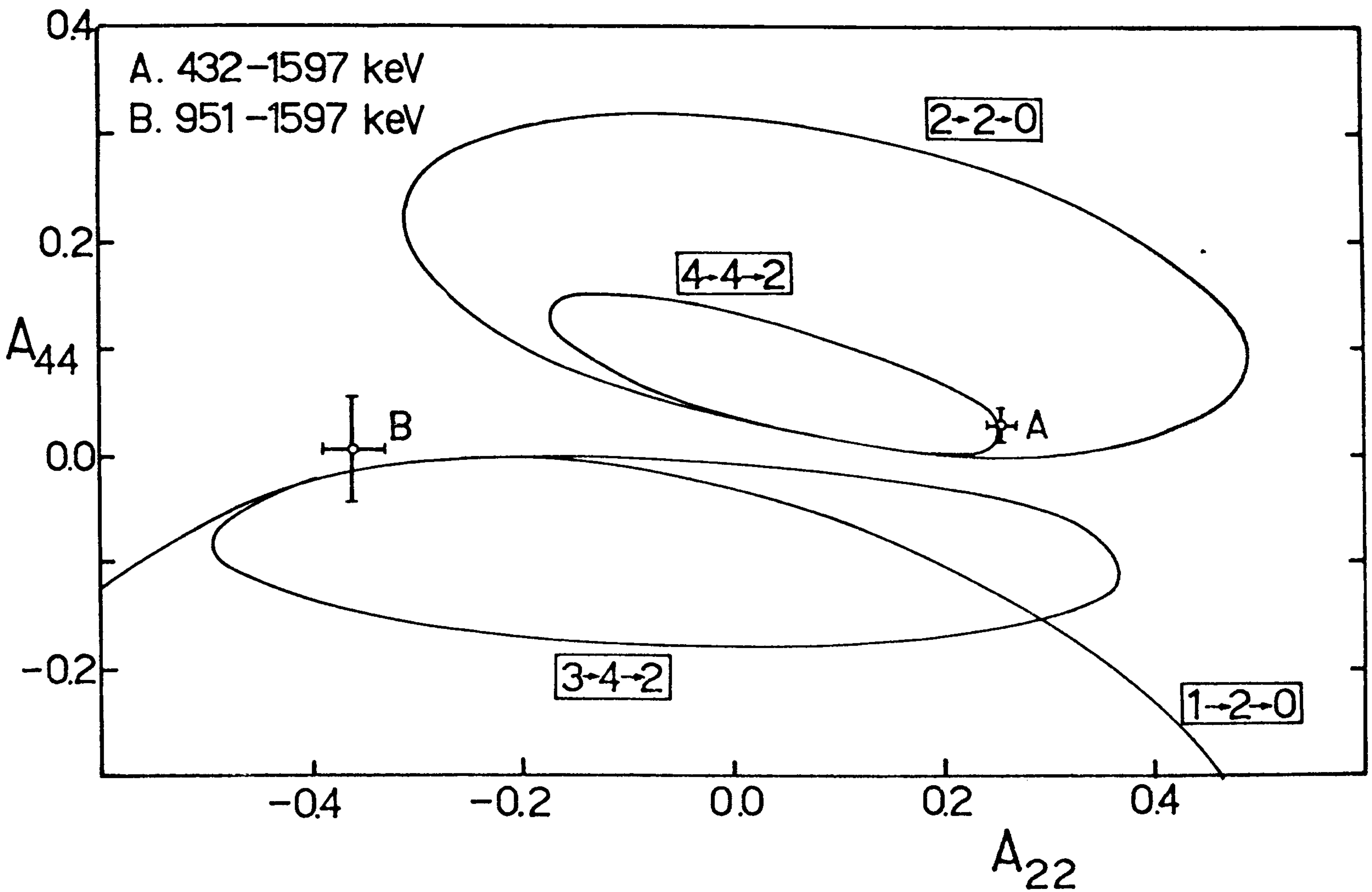

Fig. IV.4.2 Plot of directional correlation coefficients as function of the mixing parameter δ for various spin sequences.

IV.5. Gamma-Gamma Coincidences and Electron Conversion Measurements in ^{141}La.

A.N.Proto, D.Otero and E.Achterberg.

The ^{141}Ba activity was produced at the on-line mass separator and collected in order to perform off-line measurements. After an irradiation period of 20 minutes and a waiting period of 1 minute, the γ-ray spectrum was recorded for another 20 minutes. We measured about 150 sources in this way, in order to record 10^7 events for the 190.40 keV γ-ray transition.

From these measurements we can assign 137 γ-rays to the decay of ^{141}Ba. The intensity of the γ-ray transitions, in percent of β disintegrations, was determined relative to the 1354.52-keV transition of the decay of ^{141}La, whose intensity is well known[1]. This was done by means of a procedure similar to the one described in Ref. 2.

The γ-γ coincidence results obtained after a 50 hour run are summarized in Table IV.5.1. The events collected for the coincidence between the 190.40 and 276.93 keV γ-ray transitions amount to 8×10^4. The quantitative analysis of the results was restricted to the intense transitions although it was possible to identify random coincidences in all cases.

The conversion coefficients are collected in Table IV.5.2. The assigned multipolarities were obtained by comparison with theoretical values of Hager and Seltzer[3].

The level scheme proposed for ^{141}La is shown in Fig. IV.5.1. Twenty two levels are established by γ-γ coincidence results, another 4 levels, placed at 902.51, 2293.69, 2469.45 and 2743.53 keV, are only supported on energy sums and intensity balance, they are connected to other levels by at least 5 transitions, and they were found through the LEVEL program[4].

From the intensity balance for the level at 580 keV, we can place a limit to the conversion coefficient of the 68.07 keV transition to $\alpha < 25$ which implies either E1 or M1/E2 multipolarity assignment.

The consistency of the level scheme is supported by the quantitative analysis of the coincidence results. The numbers shown in parenthesis in the third column of Table IV.5.1 represent the ratio between the coincidence and single intensities normalized to the single intensity of the gating transition. The constancy of these numbers show the validity of the assumed level scheme (Fig. IV.5.1). All numbers in this column are normalized to the 190.40 - 276.93 keV coincidence intensity.

The 12 levels proposed by McIsaac and Murri[5] are confirmed. The levels at 1039.3, 1425.9, 1566.2, 2216.9, 2375.96, 2385.9 and 2440.7 proposed in Ref. 1 are not consistent with our γ-γ coincidences or energy results. The level at

2180.5 keV was not found as we do not detect the γ-rays of 1600.2 and 1877.3 keV. On the other hand we establish new levels at 752.09, 902.51, 1137.15, 1634.20, 2293.69 and 2743.53 keV.

---

[1] R.L.Auble, Nuclear Data A10 (1973) 175.
[2] D.Otero, A.N.Proto, F.C.Iglesias, Phys. Rev. C (to be published).
[3] R.S.Hager and E.C.Seltzer, Nuclear Data A10 (1971) 206.
[4] E.Achterberg, private communication (1974).
[5] L.D.Mc Isaac and E.L.Murri, Nucl. Phys. A156 (1970) 212.

Table IV.5.1

Quantitative coincidence results

(A) Direct Coincidences

Intermediate[a)] level (keV)	Gate (keV)	Coincidences[b)] (keV)
190.34 (54.8)	190.40	276.93 (54.8)[c)], 389.72 (55.3), 457.50 (56.4), 739.09 (55.9), 876.22 (54.8).
304.19 (25.8)	304.18	163.41 (26.5), 343.66 (25.4), 625.14 (27.6), 1197.59 (28.3).
467.19 (32.6)	276.93	113.08 (32.8), 180.82 (29.0), 364.33 (30.7), 462.24 (30.8).
	462.24	467.18 (31.0).
580.18 (2.5)	113.08	349.26, 609.10, 1264.58 : (3.0)[d)]
	389.72	349.26, 609.10, 1264.58, 1346.54 : (2.2)[d)]

(B) Indirect Coincidences

Intermediate[e)] levels (keV)	Gate (keV)	Coincidences[b)] (keV)
467.19 - 190.34 (26.2)	190.40	113.08 (23.6), 180.82 (28.5), 364.33 (28.2), 462.24 (24.9).
580.18 - 190.34 (2.2)	190.40	349.26, 609.10, 1264.58, 1346.54 (2.2)[d)]

a) Total transition intensity which depopulates the level in parenthesis.

b) Quantitative coincidence results in parenthesis, the estimated errors vary between 2 and 20%, depending on the intensity.

c) Normalization value (see text).

d) Average value for the listed coincidence transitions.

e) Intensity connecting initial and final intermediate levels in parenthesis.

Table IV.5.2

K - Conversion-Coefficients of Transitions in ^{141}La

Transition energy (keV)	$\alpha_K \times 10^3$	Multipolarity assignment
113.08	146 ± 30	E1
190.40	172 25	M1 - E2
276.93	53 8	M1 - E2
304.18	34 5	M1 - E2
343.66	22 3	E2 (< 15% M1)
457.50	15 3	M1 - E2
462.24	16 4	M1 - E2
467.18	8 2	E2

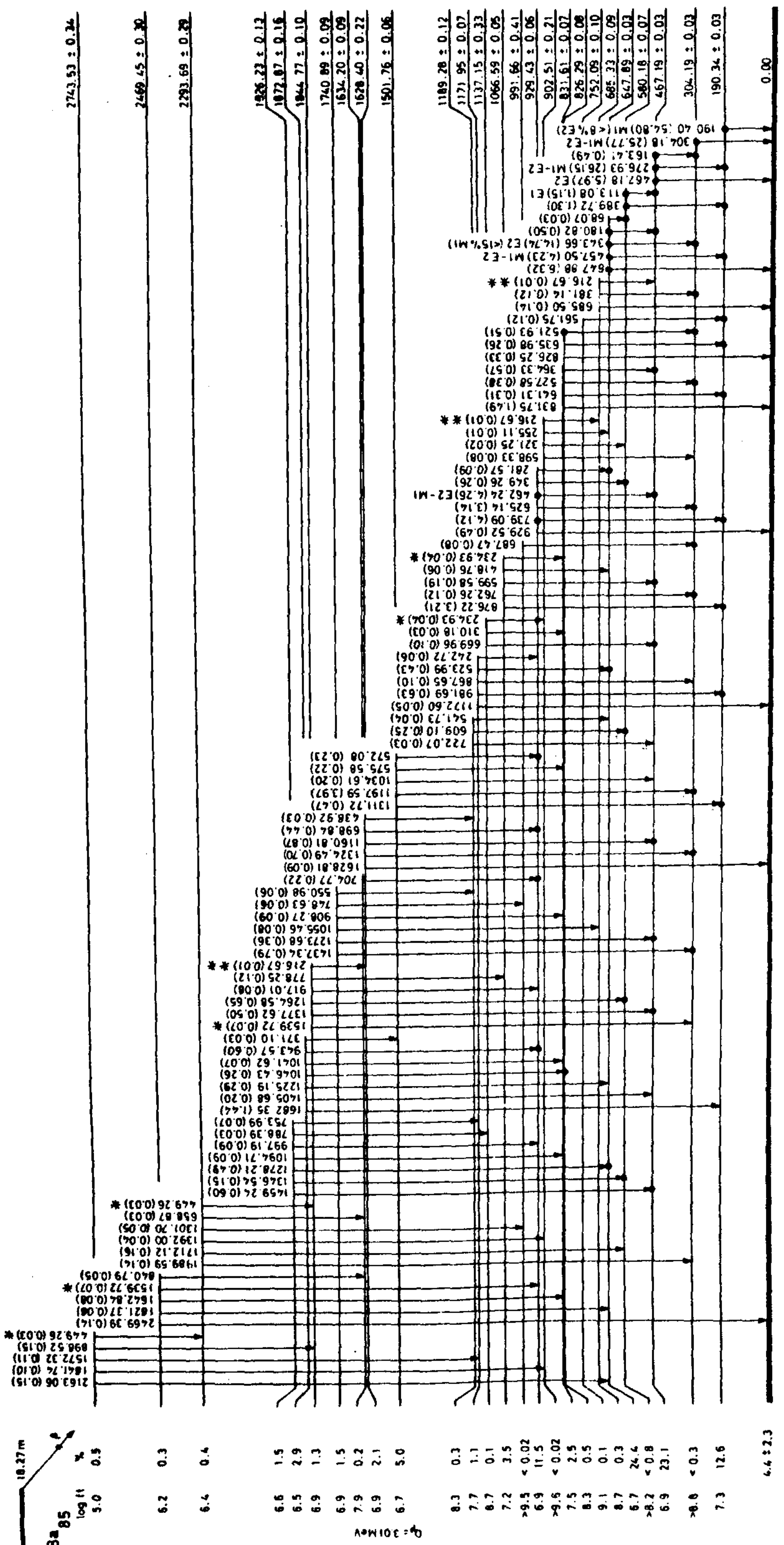

Fig. IV.5.1 Level scheme of ^{141}La.

PART B

THEORETICAL PHYSICS

V. NUCLEAR STRUCTURE

V.1. Shape-Phase Transitioners as Pairing Back-Benders.

R.P.J.Perazzo and S.L.Reich.

Recently[1,2] a considerable effort has been invested in understanding the details of the phase transitions that may be induced by a large enough angular momentum (back-bending of rotational bands). Taking advantage of the close parallelism that can be drawn between the pairing and quadrupole collective descriptions, one can empirically define a "gauge" angular velocity and a pairing moment of inertia as:

$$\omega_p(M) = \frac{E_{M+\Delta M} - E_M}{\Delta M} \quad ; \quad \frac{2\mathcal{J}_p(H)}{\hbar^2} = \frac{2(M - M_0) + 1}{E_{M+1} - E_M} \tag{1}$$

where M is the number of pairs (the closed shell is filled with M_0 pairs) and E_M is defined in terms of the experimental binding energy B_e^{exp}:

$$E_{M - M_0} = - B_e^{exp}(A) + B_e^{exp}(A_0) - \alpha(M - M_0) \tag{2}$$

The parameter α is determined with the condition $E_1 = E_{-1}$. The above empirical distributions of ω_p and $\mathcal{J}_p$ were used to plot several pairing bands (Fig. V.1.1). The Sn isotopes were chosen as an example of a good pairing rotational band, while the Pb isotopes as a good pairing vibrational band. These two features are faithfully reproduced by the corresponding $\mathcal{J}_p$ vs ω_p^2 plots aside from some anomalous behavior of the last members of Pb removal branch. This is in turn consistent with an irregular value of the (t,p) cross sections. The Sm, Nd and Gd bands display the pairing equivalents of the Mottelson-Valatin effect. The "back-bending" pattern arises when the shape-phase transition takes place.

This effect can be phenomenologically interpreted in terms of the hybridization of two bands, one spherical and the other deformed. A calculation along this line has been performed for the Sm case assuming a $E_{sph} = AM^2 + BM$ and $E_{def} = A'M^2 + B'M + C'$ coupled through a -DM term. The free parameters A, B, A', B', C' and D' were adjusted through a χ^2 minimization and the results are displayed in Table V.1.1.

A more complete version of this work has been published[3].

---

1 A.Johnson and Z.Szymansky, Phys. Rev. C7 (1973) 181.

2 R.Sorensen, Rev. Mod. Phys. 45 (1973) 896.

[3] R.P.J.Perazzo and S.L.Reich, Phys. Lett. 55B (1975) 354.
[4] T.Takemasa, M.Sakagami and M.Sato, Phys. Lett. 37 (1971) 473.

Table V.1.1

M	A	g.s.energy theo	exp	exc.energy theo	exp	$u^{a)}$ this calc.	v	$u^{a)}$ ref.4	v
0	144	0.0	0.0	2.835	-	1.000	0.000	-	-
1	146	2.231	1.909	4.180	-	0.999	0.034	-	-
2	148	4.830	4.491	6.084	5.491	0.994	0.108	1.0	0.0
3	150	7.717	7.728	8.627	8.982	0.962	0.274	0.92	0.34
4	152	10.824	10.964	11.876	12.055	0.412	0.911	0.37	0.91
5	154	14.281	14.213	15.703	15.431	0.314	0.950	0.0	1.0
6	156	18.193	18.258	20.001	-	0.279	0.960	-	-

[a] The ground state wave function is $\Psi_{gs} = u|sph\rangle + v|def\rangle$.

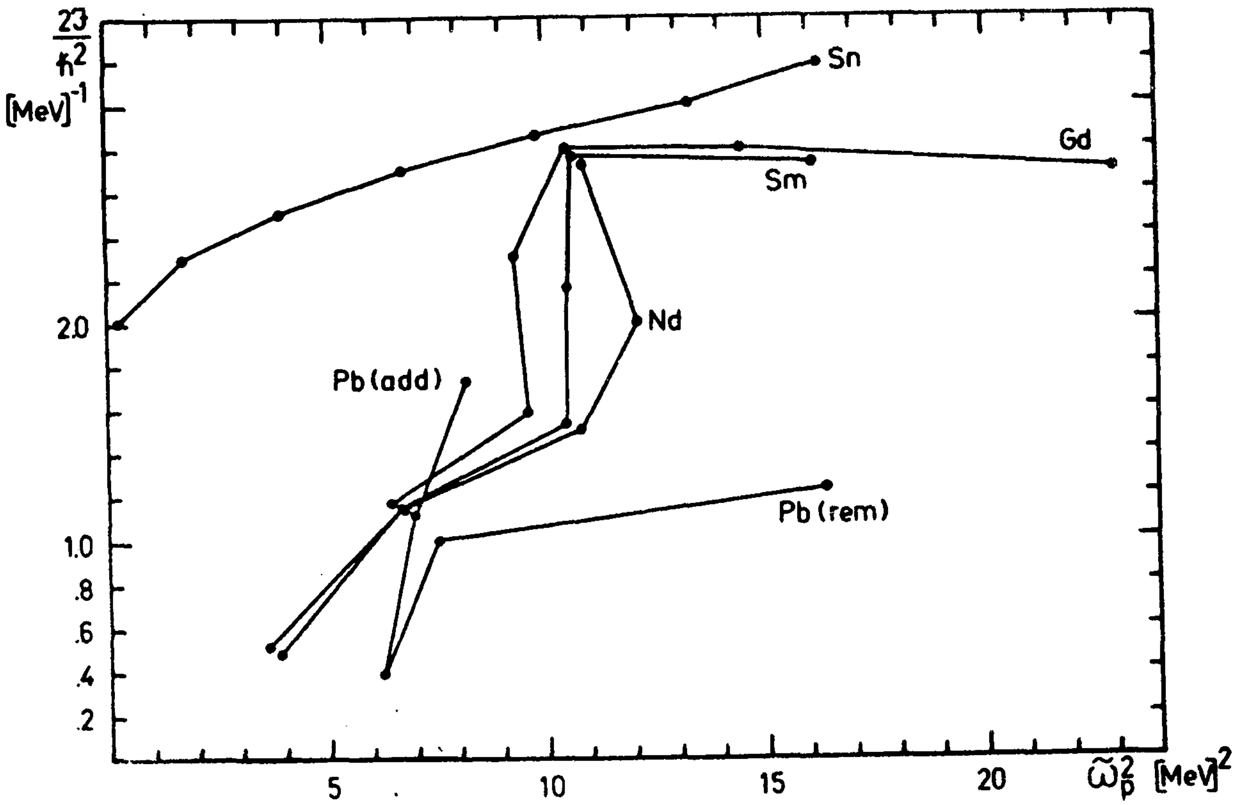

Fig. V.1.1 The pairing moment of inertia J_p as a function of $\tilde{\omega}_p^2$ for various pairing bands. The linear term was defined as described in the text, except for the GD band because $B_e(^{144}Gd)$ and $B_e(^{146}Gd)$ are unknown. In this case the value of α was extrapolated from the known values $\alpha(Z) 56 \leq Z \leq 62$.

V.2. Interplay between Shape and Pairing Deformations in Nuclei.

E.S.Hernández, R.P.J.Perazzo and A.Plastino*.

The finite Fermi systems such as those occurring in Nuclear Physics allow a detailed analysis of the interplay between shape and pairing deformations, and of the phase transitions associated with these degrees of freedom. The purpose of this work is to discuss some of these effects within the framework of a schematic model which allows for investigation of the role of either particle-hole or particle-particle parts of the force near a phase transition.

The model consists of a two single-particle (s.p.) levels with the same shell-degeneracy $\Omega(= j + 1/2)$ and orbital quantum number ℓ[1]. The 2Ω identical nucleons interact through a pairing plus quadrupole (P + Q) force[2]. The properties of the ground-state of such a system can be tackled from several points of view. The simplest approach corresponds to a Nilsson plus BCS (NBCS) calculation[2]. A more involved treatment, which corresponds to a better choice of the s.p. basis, consists of a Hartree-Fock + BCS calculation (HF BCS)[3]. Undoubtedly however, the most correct approximation which considers both parts of the interaction on the same footing, is provided by the Hartree-Fock-Bogoliubov formalism (HFB)[4].

Within the three above mentioned treatments we study the properties of static observables of this many-body system, such as the pairing potential (gap) Δ and the quadrupole moment $\langle Q \rangle$. From examination of the gap as a function of κ (in units of κ_c^o) we observe that (see Fig. V.2.1) a self-consistent treatment that considers the short and long-range part of the interaction on an equal footing results in a large predominance of the quadrupole effects which considerably diminishes the gap from its BCS value. There is an oscillation in Δ near the critical value $\kappa = \kappa_c^o$, which is in correspondence with the appreciable overshooting in $\langle Q \rangle$ (Fig. V.2.2). We can also notice that a wholly self-consistent handling of the interaction (HFB) turns a sharp-phase transition such as the one occurring within NBCS and HFBCS into a smooth one. Furthermore, we realize that self-consistency favours deformation. It is interesting to note that the peaks in Δ and $\langle Q \rangle$ account for a drastic lowering of the ground state energy which is almost a "deformation energy". We may conclude that in the region of the phase transition the interplay between the two forces is decided in favor of the long-range one, as evidenced by the fact that the gap drops almost to zero.

The behavior of Δ as a function of G/G_c^o ($G_c^o = G_c(\kappa = 0)$[5]) can be examined from Fig. V.2.3. We see that a HFB description provides a smooth transition and that for $G > G_c^o$ the absolute value of Δ is lower than the BCS one. The absence of a sharp rising in Δ should then invalidate the concept of a critical coupling strength within a HFB framework. As we look at <Q>, displayed in Fig. V.2.4, we can assert again that self-consistency favors deformation and tends to eliminate discontinuities associated with setting $G = G_c(\kappa)$. The classical competition between shape and pairing deformation appears in the fact that all curves in Fig. V.2.4 approach zero as G grows.

We believe that these results clearly show the importance of a self-consistent handling of the interaction in order to obtain a smooth behavior of the static moments of the nuclear syste.

---

[*] Department of Physics, University of La Plata, La Plata, Argentina.

[1] J.Hoegaasen - Feldman, Nucl. Phys. 28 (1961) 258.
[2] D.R.Bes and R.A.Sorensen, Advances in Nuclear Physics, vol. 2, (Plenum Press, N.York, 1969).
[3] G.Ripka, Advances in Nuclear Physics, vol. 1, (Plenum Press, N.York, 1966).
[4] M.Baranger, Phys. Rev. 122 (1961) 992.
[5] S.T.Belyaev, Mat. Fys. Medd. Dan. Vid. Selsk. 31 (1959) N° 11.

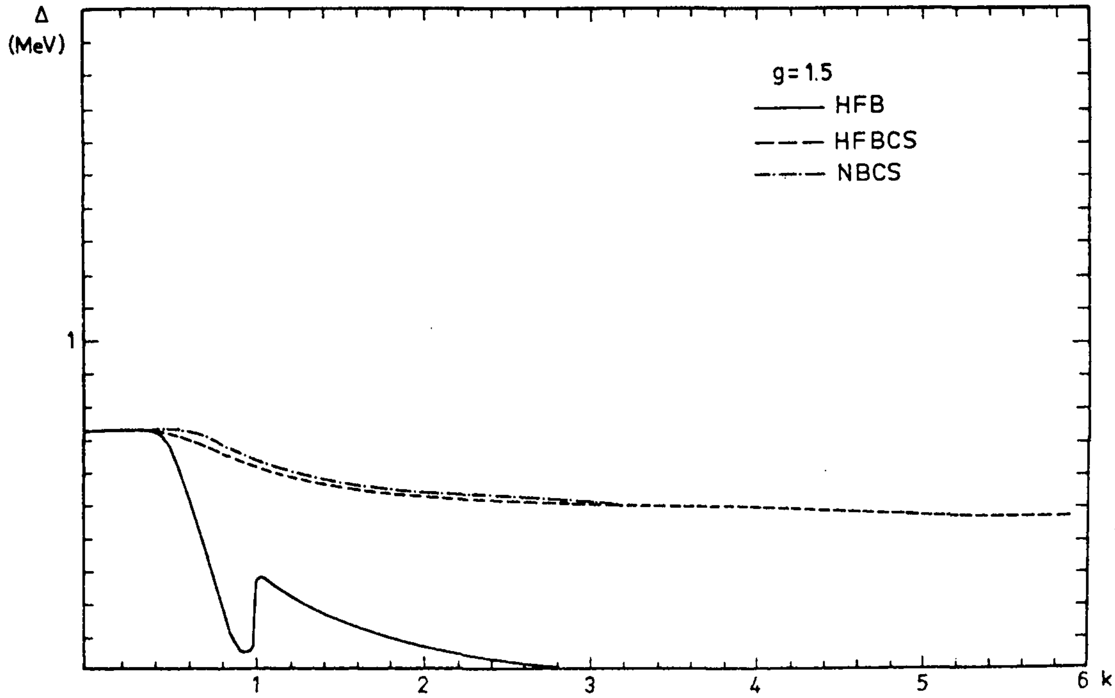

Fig. V.2.1 The absolute value (in MeV) of the pairing moment (gap) Δ against the quadrupole coupling strength $k = \kappa/\kappa_c^o$. The pairing strength $g = G/G_c^o$ has been kept constant at the value 1.5. The units κ_c^o and G_c^o are, respectively, the critical quadrupole and pairing strength, obtained for each force in absence of the other.

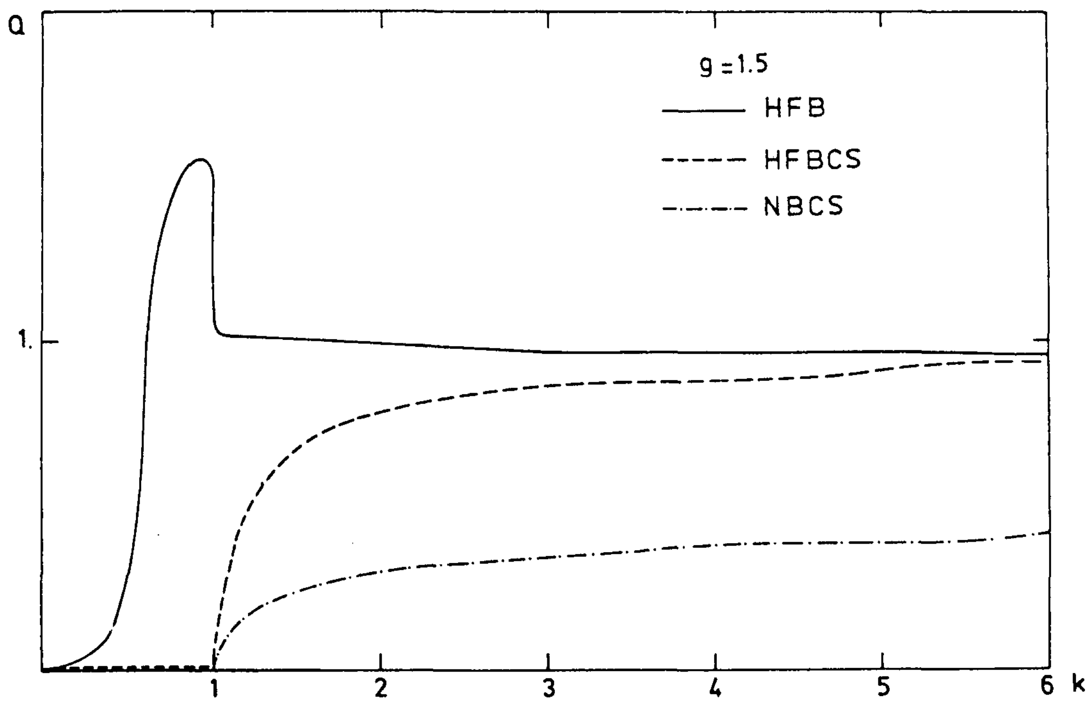

Fig. V.2.2 The same as above but for the absolute value of the quadrupole moment (in arbitrary units).

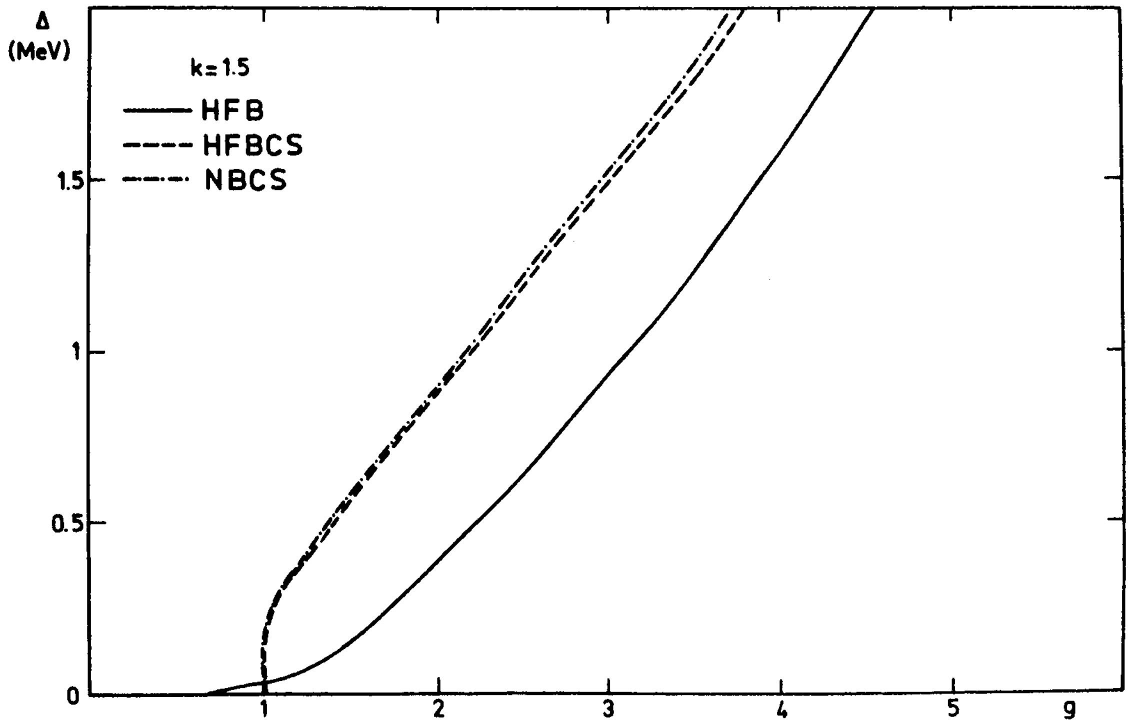

Fig. V.2.3 The absolute value of the pairing moment Δ (in MeV) as a function of the pairing force strength $g = G/G_c^o$. The quadrupole constant $k = \kappa/\kappa_c^o$ has been kept constant at the value 1.5.

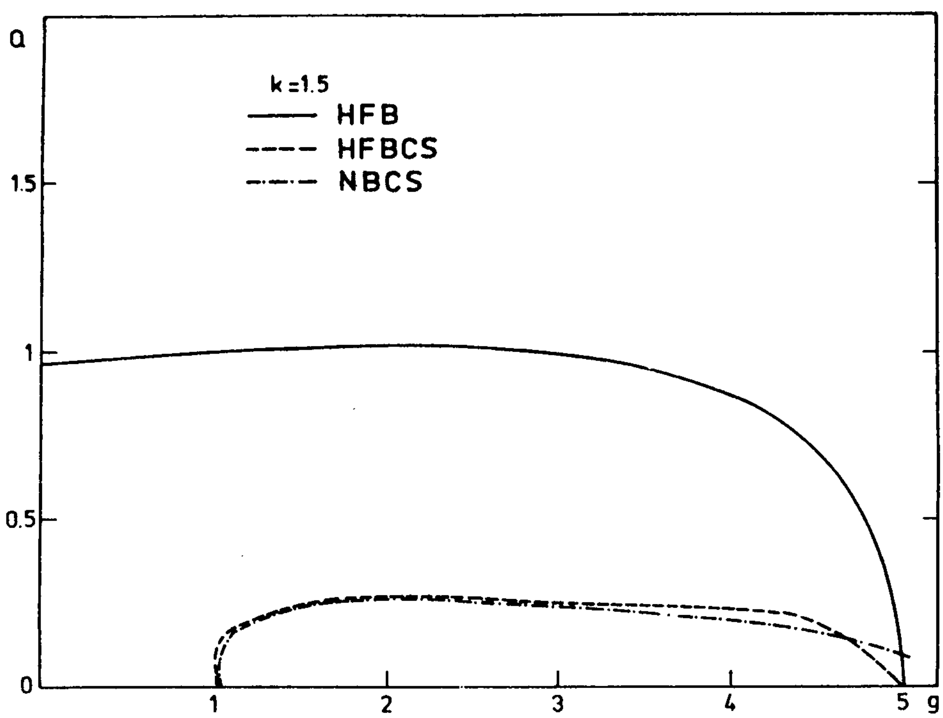

Fig. V.2.4 The same as above but for the absolute value of <Q> (in arbitrary units).

V.3. Properties of Single-Particle States in the ^{208}Pb Region.

S.L.Reich, H.M.Sofía and D.R.Bes.

The properties of single-particle states of ^{207,209}Pb, ^{207}Tl and ^{209}Bi are obtained by subtracting from the empirical values the dressing effects of the multipole particle-hole and pairing phonons.

The difference between the present calculation and a previously reported one[1] lies in the fact that we include the effects associated with the pairing forces. However, effects associated with the continuum are not explicitely taken into account, since harmonic oscillator wave functions are used.

The interaction hamiltonian depends linearly either on the particle-hole or on the pairing collective variables. All possible time-ordering of the vertices appearing diagramatically in perturbation theory[2] up to second order are included. This interaction takes care of violations of the Pauli principle and of spurious effects associated with the overcompletness of the basis. The hamiltonian can be written as:

$$H_{int} = -\sum_{\alpha,\lambda}\Lambda(\alpha,\lambda)\left[\Gamma^{+}(\alpha,\lambda) + (-)^{\lambda}\,\Gamma(-\alpha,\lambda)\right] Q^{+}(\alpha,\lambda)$$

where $\Gamma^{+}(\alpha,\lambda)$ creates a boson ($\alpha = 0$ implies particle-hole and $\alpha = \pm 2$ pairing bosons). The $Q(\alpha,\lambda)$ are the 2^{λ} poles operators connected with the pairing and particle-hole fields. The coupling strengths $\Lambda(\alpha,\lambda)$ are determined by the boson frequencies and single-particle energies through the RPA relations.

In lowest order the corrections of single particle energies are given by the graphs of Fig. V.3.1. A least square fit for the relative excitation energies was performed with the aid of the routine MINUIT. The "bare" energy differencies were used as minimization variables taking as data the experimental single particle plus the collective phonons that appear in the low energy spectrum of ^{208}Pb.

We have studied the modification of the single-particle states which are produced through admixtures with collectives states of normal parity. The amount of this admixtures was checked by calculating the decrease in the cross sections corresponding to one-body transfer processes and by studying the electromagnetic transitions between these states.

A more complete version of this work can be found in Ref. 3.

---

[1] I.Hamamoto, Nucl. Phys. A205 (1973) 225.

[2] B.R.Mottelson, J. Phys. Soc. Japan Suppl. 24 (1968) 87.

[3] S.L.Reich, H.M.Sofía and D.R.Bes, Nucl. Phys. A233 (1974) 105.

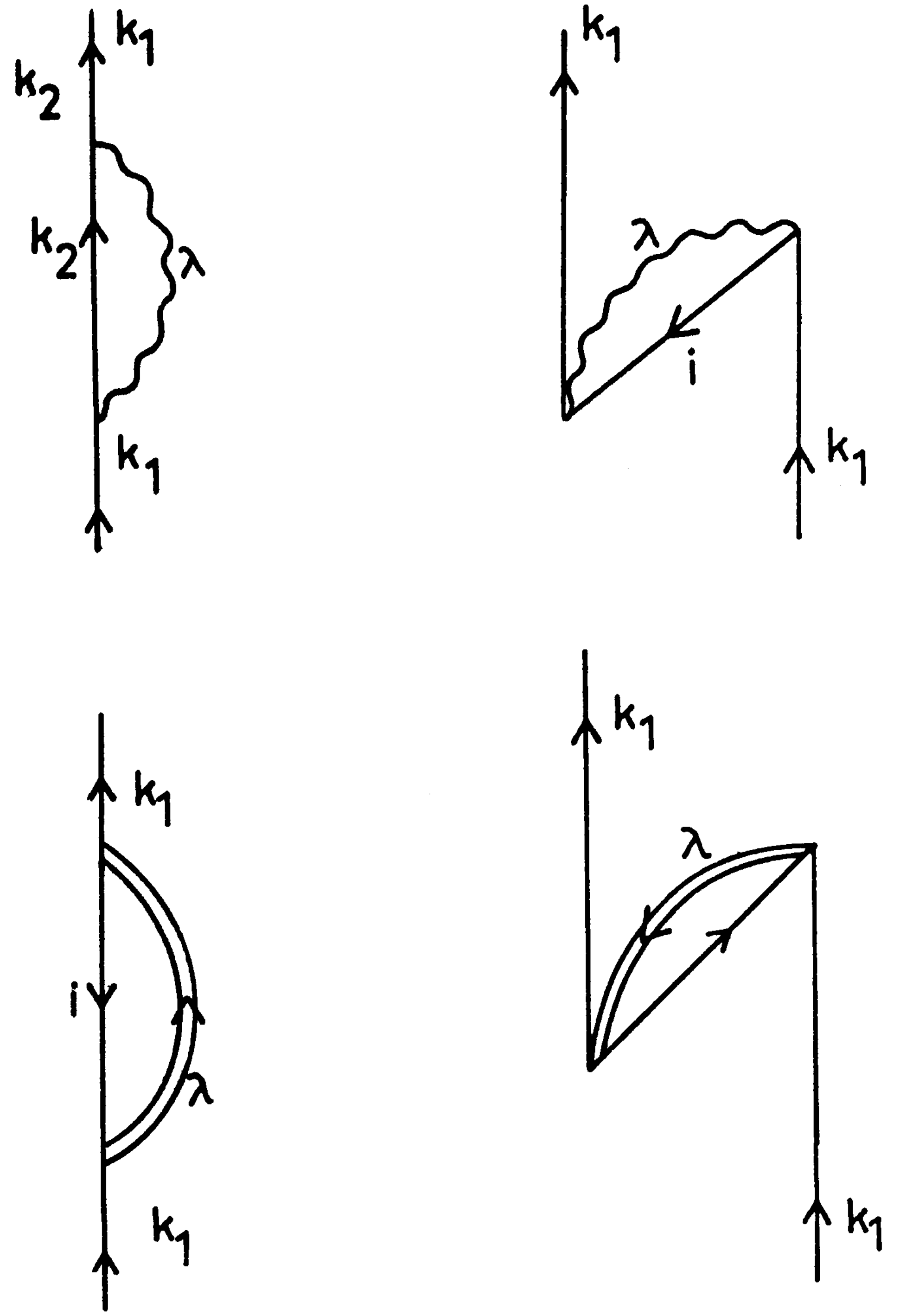

Fig. V.3.1 Graphs representing the four processes giving rise to the corrections of the single-particle energies.

V.4. Nuclear Field Theory

Part of the effort of the Theoretical Nuclear Physics Division was devoted to the establishment of a theory of the particle-vibration coupling or nuclear field theory.

The elementary modes of excitation of nuclei are found to comprise partly collective (boson) excitations associated with pairs of fermions as well as single fermion excitations which are described approximately by independent particle motion.

Both modes of excitation are originated in the fermion degrees of freedom and therefore are not independent. One is thus faced with the problem of explaining the consequences of the Pauli principle associated with the identity of the nucleons that appear in the collective and particle modes as well as the factors resulting from the non-orthogonality of the elementary excitations.

In 1952 Bohr[1] suggested a phenomenological structure for the coupling hamiltonian between both types of excitations involving a linear coupling which conserved the number of particles or holes as shown in Fig. V.4.1(a). In 1968 Mottelson[2] showed that it was necessary to introduce also the extra coupling terms shown in Fig. V.4.1(b) to treat correctly the Pauli principle violations at least in the lowest order of perturbation theory.

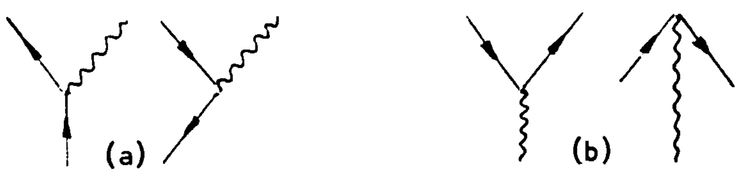

Fig. V.4.1

Important questions related to this approach remained still unanswered at this point, namely whether the Pauli principle was taken into account in higher orders than the first one; the extent to which the initial two-body interaction was taken into account; and whether non-linear couplings with the phonon coordinates were required. To answer these questions the particle-vibration coupling was applied to simple but meaningful models. In each case there was a pure fermion H and a field Hamiltonian H_f given by

$$H = H_{sp} + H_{tb}$$

$$H_f = H'_{sp} + H'_{tb} + H_b + H_{pv}$$

where H_{sp}, H'_{sp} are independent fermion hamiltonians, H_{tb}, H'_{tb} are two body interactions, H_b is an independent boson hamiltonian, and H_{pv} is the particle-vibration interaction. In order to establish equivalence between the results obtained from H and H_f, different prescriptions for the construction of H_f were empirically determined by trial and error. The earlier prescriptions yielded only an approximate equivalence[3]. Finally a complete equivalence was established. This is described in the following pages.

---

[1] A.Bohr, Kgl. Dans. Vid. Sels., Mat. Fys. Medd. 26 (1952) N° 14.
[2] B.Mottelson, Suppl. J. Phys. Soc. Japan 24 (1968) 87.
[3] D.R.Bes, J.A.Evans and N.C.Krauss, J. Phys. A 6 (1973) 6.

V.4.1. Nuclear Field Theory as a Method of Treating the Problem of Overcompletness in Descriptions Involving Elementary Modes of Both Quasi-Particles and Collective Type.

D.R.Bes, G.G.Dussel, R.A.Broglia*, R.Liotta** and B.R.Mottelson†.

It was shown that for a monopole particle-hole force, including only forward vertices, the graphical perturbation treatment of nuclear fields converges to the exact solution. The rules to be used to obtain this agreement are the following:

1. In initial and final states proper diagrams involve collective modes and particle modes; however they do not include a particle configuration that can be replaced by a combination of collective modes.
2. The perturbative hamiltonian must be the two-body fermion hamiltonian plus a fermion-boson hamiltonian derived for this force.
3. The internal lines of diagrams are, however, restricted by the exclusion of diagrams in which a particle-hole is created and subsequently annihilated without having participated in subsequent interactions.
4. The energies of uncoupled particles are given by the H.F. energies and the ones corresponding to the phonon fields by the solutions of the R.P.A. The contributions of the allowed diagrams are evaluated with the usual rules of perturbation theory.

A more extensive version of this work is published in Phys. Lett. 52B (1974) 253.

V.4.2. Simultaneous Treatment of Surface and Pairing Nuclear Fields.
D.R.Bes, R.A.Broglia*, G.G.Dussel and R.Liotta.

The nuclear field treatment was applied when both the surface and pairing nuclear fields were present. In particular the amplitude for the inelastic-surface excitation from a particle state to a particle times particle-hole phonon state and to a hole times a pairing phonon was evaluated in a two level model. For more details see Phys. Lett. 56B (1975) 109.

V.4.3. The Normalization of States in Perturbation Theory.
D.R.Bes, G.G.Dussel and H.M.Sofía.

Since the normalization of the perturbed states is needed in the calculation of transition matrix elements, we developed a simple method to normalize the perturbed states in different perturbation theories. In the Rayleigh-Schroedinger treatment the square of the normalization coefficient is just the derivative of the energy with respect to the unperturbed energy. In the Brillouin-Wigner and Bloch-Horowitz perturbation methods it was also possible to establish a connection between the normalization coefficients and the derivatives of the energy. As consequence, the diagramatic perturbation expansion for the norm of a state is the same as the corresponding expansion for the energy, except for a simple change in the calculation of the energy denominators.

V.4.4. The Nuclear Field Treatment of some Exactly Soluble Models.
D.R.Bes, R.A.Broglia*, G.G.Dussel, R.Liotta and H.M.Sofía.

The nuclear field treatment was applied to simple but physically meaning full models, which are exactly soluble both with the fermion and field treatment. The two methods give identical results if they are carried out to all orders in perturbation theory.

The first model used consisted of degenerate particle-hole excitations and a monopole particle-hole interaction. A detailed discussion of how the Pauli corrections are done was presented for the odd system. These corrections affect not only the energies but also the transition rates and the norms of the states. By partially lifting the particular degeneracies of the model, it was shown that the agreement does not depend on these degeneracies.

The basic set of states is also overcomplete, since we include both particles and phonon degrees of freedom. Even the proper states (to whom the initial and final states are restricted) are too many as compared with the states of the fermion treatment. An example of this situation is discussed in detail for the case of two non-degenerate particle-hole excitations, where there are two proper particle-phonon states with the particle in a fixed state ϕ_e, while there is only one two-particle-one-hole antisymmetric fermion state with the odd particle in the state ϕ_e. One of the states obtained in the field treatment has all the correct properties while the matrix elements populating the second one vanishes. In this way the field treatment corrects for the overcompleteness of the basis. This overcompleteness is increased when pairing phonons are included. The field treatment, however, reproduces the exact results also in this case.

V.4.5 Application of Nuclear Field Theory to Monopole Interactions which Include all the Vertices of a General Force.

D.R.Bes, R.A.Broglia*, G.G.Dussel, R.J.Liotta and H.M.Sofía.

The field treatment was applied to monopole pairing and monopole particle-hole interactions in a two level model of degeneracy 2Ω. The interactions used included not only TDA and RPA vertices but also scattering vertices; therefore the problems treated here have most of the complexities of real nuclei. Yet the model requirements are sufficiently simple making it possible to closely compare the field diagramatic expansion with those of a pure fermion treatment of the residual interaction. We compare magnitudes which are algebraically obtained. In spite of the non existance of a close solution, this is still possible in the present case, since there are only two adimensional parameters in the model that we choose as $1/\Omega$ and the ratio $X = \eta\Omega/\varepsilon$ where η is proportional to the strength of the residual interaction and ε is the splitting between the two levels. Any physical quantity Y can be obtained as

$$Y = \sum_{nm} a_{n,m} X^n \Omega^{-m}$$

A perturbative fermion treatment corresponds to an expansion in powers of X while in the field treatment each graph contributes to a certain order in Ω^{-1}; in particular the RPA is exact in the limit of infinite degeneracy, and thus gives rise to the coefficients $a_{n,o}$ (n arbitrary).

We found agreement between both treatments for the energies of the ground, one-phonon and particle-phonon states as well as the inelastic scattering and two particle transfer matrix element for the even systems up to order Ω^{-2}.

We have also treated the problem of a non-separable interaction by including the exchange components of the force in the construction of the phonon. In this case another rule must be taken into account: if in a given diagram, there is a fermion line and a particle-hole boson line in parallel, we must subtract another diagram in which the phonon is replaced by a pair of (non-interacting) particle-hole lines.

A calculation which includes all the Ω^{-1} diagrams appears to be feasible in actual nuclei, both for schematic and realistic forces. The shell-model degeneracies in actual nuclei are probably sufficiently large so that we may be satisfied by the corrections of order Ω^{-1}. Both the number and the complexities of the diagrams involved in a calculation of order Ω^{-2} become extremely large and such calculations will probably only be performed for very specific cases.

V.4.6. On the Field Treatment of a General Two-Body Interaction

D.R.Bes, R.A.Broglia*, G.G.Dussel, R.J.Liotta and R.P.J.Perazzo.

It is shown that there is a holomorphic mapping between the Feynman diagrams corresponding to the pure fermion Hamiltonian and to the field Hamiltonian. The subset of fermion diagrams which differ only within a particular section and such that this section represents the propagation of a particle-hole pair is replaced by three diagrams within the field treatment. The two diagrams corresponding to the zeroth and first order propagators remain as in the fermion treatment and a single diagram containing a phonon substitutes the remaining elements of the subset.

In addition the fermion Hamiltonian and the field Hamiltonian yield identical values for the two-particle propagators, provided that the phonon frequencies and the strength of the particle-phonon vertices are adequately calculated. The RPA is the most convenient way (but not the most general way) of obtaining these quantities. Similar considerations are made for the vertices corresponding to any external one-body operator.

The field Hamiltonian treats the fermion and phonon degrees of freedom on an equal footing. The product eigenfunctions corresponding to the zero order Hamiltonian constitute an adequate basis for the many body problem, since they take into account an important fraction of the residual two-body interaction. The diagramatic expansion of the residual terms provide a systematic way for correcting all the different errors introduced in the basis: violations of the Pauli principle, overcompleteness of the basis, effects of the two-body interaction which are not included in the zero-order wave functions, etc.

---

* Niels Bohr Institute of Copenhague, Denmark and Physics Department, State University of New York at Stonny Brook.

** Niels Bohr Institute of Copenhague, Denmark.

† NORDITA, Copenhague, Denmark.

VI. NUCLEAR REACTIONS

VI.1. Two-Nucleon Stripping Reactions Populating Isobaric Multiplets.

O.Dragûn, D.R.Bes and E.E.Maqueda.

The direct two-nucleon transfer reactions leading to members of an isobaric multiplet have been subject of detailed studies, particularly in the region $40 \leq A \leq 56$ (ref. 1). Because of invariance under rotations in isospace, the cross sections of the (t,p), (τ,p) and (τ,n) reactions populating states belonging to the same multiplet, should be related by geometrical considerations. The facts that these relations are not fulfilled when usual DWBA procedures are performed[1], and that isospin conservation is such a basic nuclear symmetry, point to difficulties.

We have worked with distorted waves of definite isospin instead of the usual charge-defined basis. In the latter basis the Coulomb potential is diagonal and the isovector potential ("Lane potential") couples the different channels and this coupling is not usually taken into account. In the representation in which the total channel isospin is a good quantum number, the Lane term is diagonal. The coupling terms now result proportional to $|\Delta E_c - V_c^{(-)}(r)|$, the difference between the energy of the analogue states in the target and projectile minus the Coulomb potential of a unit negative charge. There is a large cancellation of this quantity in the nuclear interior[2] and our treatment neglects all terms proportional to it.

In the charge-defined usual treatment one neglects components of the Lane potential which is peaked around the nuclear surface. In our treatments we neglect a quantity small inside the nucleus but that may be significant between the nuclear and matching radius. A CCBA calculation is in progress in order to decide about the adequacy of the different approximations.

Tables VI.1.1 and VI.1.2 summarize the results of our analysis. The symbols r_n, r_p and r are defined as:

$$r_n = \frac{d\sigma(\tau,n)}{d\sigma(t,p)} \quad ; \quad r_p = \frac{d\sigma(\tau,p)}{d\sigma(t,p)} \quad ; \quad r = \frac{d\sigma(\tau,n)}{d\sigma(\tau,p)}$$

The ratios between experimental and DW values of the above defined r's should be equal to one if the concept of analogue states holds. The ratio r_p^{EXP}/r_p^{DW} has an average value of 1.18 ± 0.28 while that of r_n^{EXP}/r_n^{DW} has an average of 1.14 ± 0.34 and r^{EXP}/r^{DW} one of 1.3 ± 0.5, all of them compatible with unity.

The optical model potentials used in our analysis as well as the references for the experimental data are given in a paper to be published in Nuclear Physics.

---

[1] J.D.Garret and O.Hansen, Nucl. Phys. A212 (1973) 600.

[2] D.Robson, Phys. Rev. 137 (1965) B535.

B.Bayman, Proc. Int. School of Physics "Enrico Fermi", Course XL, 1967. Academic Press, New York (1969) p. 380.

Table VI.1.1

Isobaric Multiplet			Config. Form Factor	$d\sigma_{cm}^{EXP}/d\Omega(\Theta)$ in mb/sr			r_n^{DW}	r_p^{DW}	$\frac{r_n^{EXP}}{r_n^{DW}}$	$\frac{r_p^{EXP}}{r_p^{DW}}$
B	T_b			τ,n	τ,p	t,p				
42	1	Ti(0.0)/Sc(0.0)/Ca(0.0)	$f_{7/2}$	3.2	0.93	2.94	0.87	0.32	1.2	1.0
44	2	Ti(9.4)/Sc(2.8)/Ca(0.0)	$f_{7/2}$	0.61	0.90	4.98	0.15	0.23	0.8	0.8
46	3	Ti(14.3)/Sc(5.0)/Ca(0.0)	$f_{7/2}$	0.18	0.64	3.98	0.048	0.13	0.9	1.3
48	2	Cr(8.8)/V(3.0)/Ti(0.0)	$f_{7/2}$	0.54	0.53	1.10	0.40	0.52	1.2	0.9
50	5	Sc(11.2)/Ca(0.0)	$p_{3/2}$		0.3	3.42		0.056		1.6
50	3	V(4.8)/Ti(0.0)	$f_{7/2}$		0.35	0.96		0.38		1.0
50	3	V(8.6)/Ti(3.9)	$p_{3/2}$		0.57	1.24		0.38		1.2
52	4	V(8.8)/Ti(0.0)	$p_{3/2}$		0.61	2.38		0.25		1.0
52	2	Fe(8.5)/Mn(2.9)/Cr(0.0)	$f_{7/2}$	0.23	0.42	0.57	0.42	0.66	1.0	1.1
52	2	Fe(11.1)/Mn(5.5)/Cr(2.7)	$p_{3/2}$	0.21	0.60	0.57	0.40	0.69	1.0	1.5
54	3	Mn(6.1)/Cr(0.0)	$p_{3/2}$		0.97	1.44		0.42		1.6
56	2	Ni(9.9)/Co(3.6)/Fe(0.0)	$p_{3/2}$	0.94	0.60	1.12	0.44	0.69	1.9	0.8
58	3	Co(5.7)/Fe(0.0)	$p_{3/2}$		0.96	1.7		0.37		1.5

Table VI.1.2

Isobaric Doublet			Config. Form Factor	$d\sigma_{cm}^{EXP}/d\Omega(\Theta)$ in mb/sr		r^{DW}	$\frac{r^{EXP}}{r^{DW}}$
B	T_b			(τ,n)	(τ,p)		
50	4	Ti(16.6)/Sc(3.1)	$p_{3/2}$	0.41	0.3	0.87	1.6
54	2	Fe(10.7)/Mn (2.1)	$p_{3/2}$	0.36	0.56	1.00	0.6
56	1	Ni(7.9)/Co(1.4)	$p_{3/2}$	1.43	0.34	2.44	1.7

VI.2. Coupled Channel Analysis of (d,^{6}Li) Reactions.

A.M.J.Ferrero and E.E.Maqueda.

The Coupled Channels Born Approximation (CCBA) has been applied to the ^{24}Mg(d,^{6}Li)^{20}Ne reaction[1] using an improved version of the code MARS[2].

The form factors corresponding to the transfer of four nucleons have been calculated[3] using SU(3) or Nilsson model wave functions.

In the entrance channel the calculations involved the coupling of the 0^+(g.s.), 2^+(1.37 MeV) and 4^+(4.12 MeV) states of ^{24}Mg. For the quadrupole and hexadecapole deformations the values $\beta_2 = 0.39$ and $\beta_4 = 0$ have been adopted[4].

In the exit channel the calculation involved the coupling of the 0^+(g.s.), 2^+(1.63 MeV), 4^+(4.25 MeV), 2^-(4.97 MeV), 3^-(5.62 MeV) and 6^+(8.77 MeV) states of ^{20}Ne alternating between the $0^+ - 2^+ - 2^- - 3^-$ and $0^+ - 2^+ - 4^+ - 6^+$ sets. The parameters β_2 and β_4 have been varied in the range $\beta_2 = 0.14 - 0.35$ and $\beta_4 = 0.03 - 0.09$ to study their effect on angular distributions of the 0^+, 2^+ and 4^+ states. The coupling of the octupole vibration band was taken into account by varying the parameter β_3 between $\beta_3 = 0.17$ and $\beta_3 = -0.17$.

In the case of extended projectiles, such as Lithium, the results obtained for the deformations, using the CCBA, strongly depend on the optical parameters used[1], and therefore they are only valid for each particular case.

The results show[5] that for the CCBA the shapes of the angular distributions corresponding to the excited states are strongly dependent on β_λ. For $\beta_2 = 0.20$, $\beta_4 = 0.09$ and $\beta_3 = -0.08$ the differential cross sections are reasonably reproduced for the 0^+, 2^+, 4^+ and 3^- states of ^{20}Ne. However, in order to obtain a good fit, the relative intensities for the Nilsson case have to be multiplied by factors of 1, 3, 1, and 0.6, respectively.

A DWBA calculation establishes that the 2^- non-natural parity state cannot be populated by a direct process in the (d,^{6}Li) reaction. In the present case one obtains a non-zero cross section, however it is still seven times smaller than the experimental one.

---

1 J.R.Comfort, W.J.Braithwaite, J.R.Durray, W.J.Courtney and H.G.Binghan, Phys. Lett. 40B (1972) 456 and private communication.

2 T.Tamura et al., Phys. Ref. Letters, 25 (1970) 1507.

3 O.Dragún, G.G.Dussel, E.E.Maqueda and R.P.J.Perazzo, Nucl. Phys. A167 (1971) 529.

4 H.Rebel et al.,Nucl. Phys. A182 (1972) 145.

5 A.M.J.Ferrero, Thesis, University of Buenos Aires, (unpublished).

VI.3. Four Nucleon Formfactor for Heavy Ion Reactions.

R.J.Liotta and R.P.J.Perazzo.

The reaction under consideration is:

$$a_1+c_2= (c_1+4n) + c_2 \to (c_2+4n) + c_1= a_2+c_1$$

$$4n= 2 \text{ prot.} + 2 \text{ neut.}$$

The coded expression for the formfactor is the following:

$$g(J'M',JM,c_1a_2,a_1c_2,r)=A\sqrt{4\pi} \sum_{\substack{j_1j_2j_3j_4\\ j_1'j_2'j_3'j_4'}} \sum_{\substack{J_{12}J_{34}\\ J_{12}'J_{34}'}} \sum_{c_1c_2} \times$$

$$\times B^*_{a_2}(I_{a_2},c_2I_{c_2},j_1'j_2'j_3'j_4'J_{12}'J_{34}'J'M')\; B_{a_1}(I_{a_1},c_1I_{c_1},j_1j_2j_3j_4J_{12}J_{34}JM) \times$$

$$\times (-1)^{j_1+j_2+j_3+j_4}(1+(-1)^{\sigma_{12}+\sigma_{1'2'}}+(-1)^{\sigma_{34}+\sigma_{3'4'}}+(-1)^{\sigma_{12}+\sigma_{34}+\sigma_{1'2'}+\sigma_{3'4'}}) \times$$

$$\times \hat{j}_1'\hat{j}_2'\hat{j}_3'\hat{j}_4'\hat{j}_1\hat{j}_2\hat{j}_3\hat{j}_4\hat{J}_{12}'\hat{J}_{34}'\hat{J}_{12}\hat{J}_{34} \sum_{\substack{K_1K_2\\ K_3K_4}} S(K_1\ell_1\ell_1')S(K_2\ell_2\ell_2')S(K_3\ell_3\ell_3')S(K_4\ell_4\ell_4') \times$$

$$\begin{pmatrix} j_1 & j_1' & K_1 \\ -1/2 & 1/2 & 0 \end{pmatrix}\begin{pmatrix} j_2 & j_2' & K_2 \\ -1/2 & 1/2 & 0 \end{pmatrix}\begin{pmatrix} j_3 & j_3' & K_3 \\ -1/2 & 1/2 & 0 \end{pmatrix}\begin{pmatrix} j_4 & j_4' & K_4 \\ -1/2 & 1/2 & 0 \end{pmatrix} P^{K_1K_2K_3K_4}_{1234\;1'2'3'4'}$$

$$\times \sum_{K_{12}K_{34}} \begin{pmatrix} K_1 & K_2 & K_{12} \\ 0 & 0 & 0 \end{pmatrix}\begin{pmatrix} K_3 & K_4 & K_{34} \\ 0 & 0 & 0 \end{pmatrix}\begin{Bmatrix} K_1 & K_2 & K_{12} \\ j_1' & j_2' & J_{12}' \\ j_1 & j_2 & J_{12} \end{Bmatrix}\begin{Bmatrix} K_3 & K_4 & K_{34} \\ j_3' & j_4' & J_{34}' \\ j_3 & j_4 & J_{34} \end{Bmatrix} \times$$

$$\times \sum_L \begin{pmatrix} K_{12} & K_{34} & L \\ 0 & 0 & 0 \end{pmatrix}\begin{Bmatrix} K_{12} & K_{34} & L \\ J_{12}' & J_{34}' & J' \\ J_{12} & J_{34} & J \end{Bmatrix} \hat{L}$$

Where

$$\sigma_{ik} = j_i + j_k + J_{ik} - 1 \; ; \qquad \hat{j} = 2j + 1$$

$$S(K,\ell,\ell') = \begin{cases} 2K+1 & K+\ell+\ell' = \text{even} \\ 0 & K+\ell+\ell' = \text{odd} \end{cases}$$

The operator $A = 1+P_{12}(-)^{\sigma_{1'2'}} + P_{34}(-)^{\sigma_{3'4'}} + P_{12}P_{34}(-)^{\sigma_{1'2'}+\sigma_{3'4'}}$ takes properly into account the antisymmetrization of the entrance and exit channels, P_{ik} interchanges the particle quantum number i and k.

The symbol P is defined as:

$$P^{K_1K_2K_3K_4}_{1234\,1'2'3'4'} = Z^{K_1}_{11'}X^{K_2}_{22'}X^{K_3}_{33'}X^{K_4}_{44'} + X^{K_1}_{11'}Z^{K_2}_{22'}X^{K_3}_{33'}X^{K_4}_{44'} + X^{K_1}_{11'}X^{K_2}_{22'}Z^{K_3}_{33'}X^{K_4}_{44'} + X^{K_1}_{11'}X^{K_2}_{22'}X^{K_3}_{33'}Z^{K_4}_{44'}$$

in terms of the Fourier-Bessel transform integrals:

$$Z^{K}_{n\ell,n'\ell'}(r) = \int k^2\, dk\, \phi^{*}_{n'\ell'}(k)\{\hbar^2k^2/(2m^{*})+|E_{n'\ell'}|+U(r)\}\phi_{n\ell}(k)j_K(kr)$$

$$X^{K}_{n\ell,n'\ell'}(r) = \int k^2\, dk\, \phi^{*}_{n'\ell'}(k)\phi_{n'\ell'}(k)j_K(kr)$$

In the above formulas $\phi_{n\ell}(k)$ stands for the Fourier-Bessel transforms of the single-particle radial wave functions, and U is the optical (Coulomb) potential.

The above expression for the formfactor corresponds to the non-recoil approximation. Throughout it is understood that particles 1 and 2 (1' and 2') are assumed to be protons and 3 and 4 (3' and 4') are assumed to be neutrons. The 4-particle wave function components with respect to cores c_1 and c_2 that are B_{a_2} and B_{a_1} respectively, are given as input. Furthermore both cores are assumed inert and $I_{c_1} = I_{c_2} = 0$ and the summation over c_1 and c_2, representing core configurations, is reduced to only one term.

The program was coded for an IBM/370 computer and later adapted to a UNIVAC 1110 system. The core storage required is approximately 450 K.

Further information can be obtained upon request.

VI.4. Scattering by a Schematic Potential Landscape.

N.C.Nemes*, A.F.R. de Toledo Piza* and R.P.J.Perazzo.

The ion-ion potential that is effective in the collision between two complex nuclei (or in the related phenomena of binary nuclear fission) must be described in terms of potential landscape which involve all the internal degrees of freedom of the colliding fragments together with the main scattering coordinate. One feature that appears to be shared by most of the known situations is the presence of "winding" or "missaligned" valleys. Here we report a study of the qualitative scattering features within a soluble schematic landscape.

The hamiltonian is written as:

$$H_M = H_r + H_x + H_b = \left(\frac{\vec{p}^2}{2n} + V(r) \right) + \left(\frac{\pi^2}{2\mu} + 1/2\mu\omega^2 x^2 \right) + AaF(x)\delta(r-a) \qquad (1)$$

The term H_r is the hamiltonian of relative motion (only S-wave scattering is considered) and $V(r)$ is taken to be a three-dimensional finite square well. H_x qualitative represents an (harmonic) internal degree of freedom that is coupled to the relative motion through H_b. The δ-function barrier strength is modulated by a function $f(x) = 1 - \alpha\exp\{-\rho(x-x_o)^2\}$ of the internal coordinate. The solutions of H_M can be written as:

$$\psi(r,x) = \sum_n u_n(r)\, X_n(x) \qquad (2)$$

The boundary conditions at r = a that couple all the (internal) oscillator channels can be solved by matrix inversion.

The "fussion" calculation is solved with standard boundary conditions of incident waves in a given oscillator channel and outgoing waves in all channels. In order to perform a "fission" calculation a given resonant state in r < a is fed through an independent channel described by a hamiltonian H_1. This is coupled to H_M by

$$H_{1M} = |\upsilon_1\rangle g\, {}^*|\omega_M\rangle = H^+_{M1} \qquad (3)$$

where $|\upsilon_1\rangle$ and $|\omega_M\rangle$ are states in the space of H_1 and H_M, respectively and g is a coupling constant.

Some "fussion" and "fission" calculations were performed with a realistic choice of the parameters. Fig. VI.4.1 shows a spectrum for these calculations as a function of the fragment excitation.

---

* Instituto de Fisica, University of Sao Paulo, Brazil.

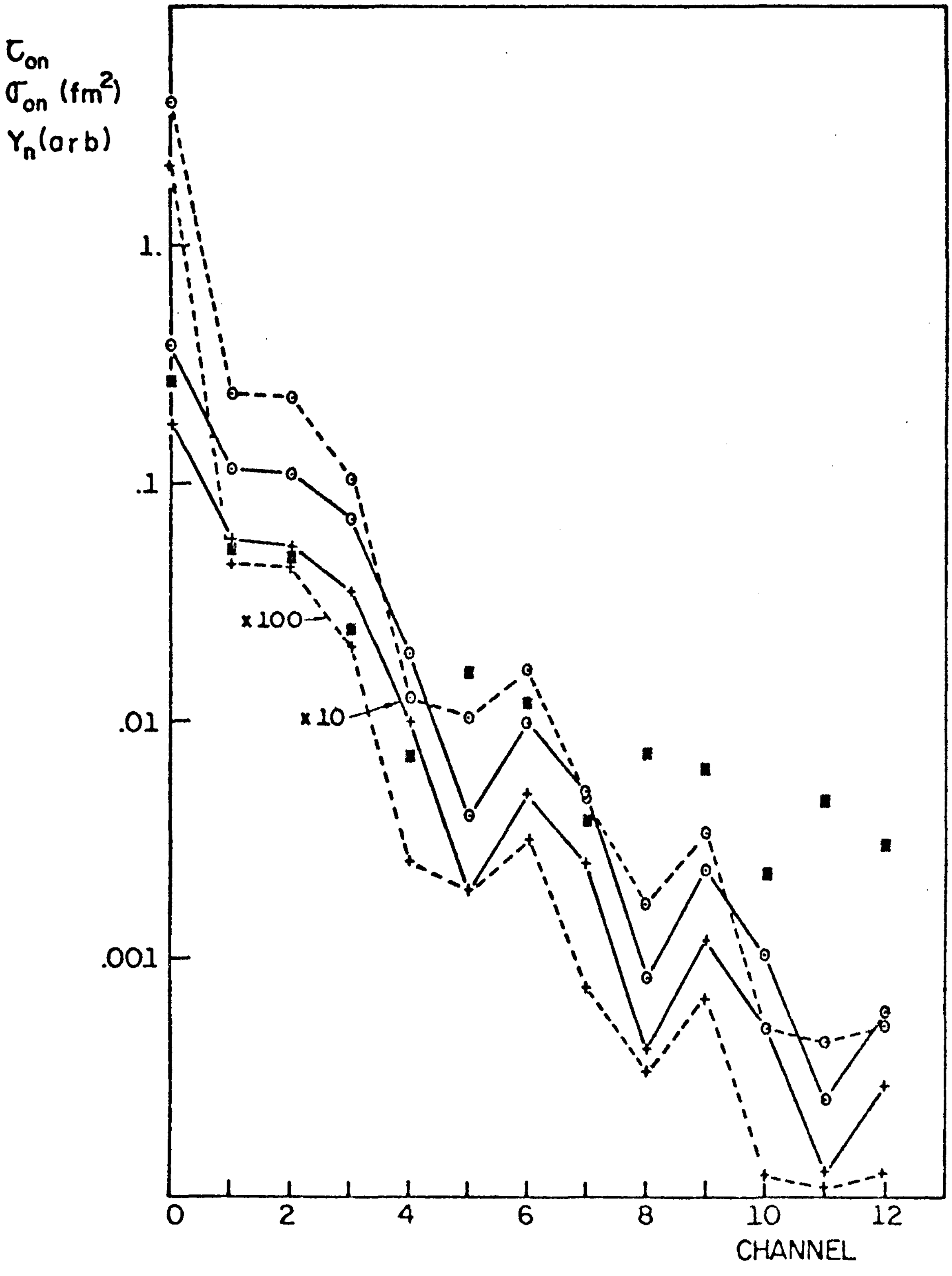

Fig. VI.4.1 Spectra for fussion (circles) and for fission (crosses) calculations. Full curves correspond to "on-resonance" total energy (9.40 MeV). "Off resonance spectra (at 8.6 MeV) are shown in the dashed curves. Black rectangles show values of the "one-dimensional" transmission amplitudes.

PART C

SUPPORTING ACTIVITIES IN APPLIED PHYSICS

VII. ENERGY RELATED STUDIES

VII.1. A Preliminary Analysis on the Utilization of Thorium in Power Reactors.

M.Saraceno.

As part of the support program that this division carries out for other areas in the CNEA a preliminary bibliographic search and assessment of thorium utilization in power reactors has been initiated.

The work is divided in three parts. In the first we review the nuclear physics aspects of the ^{232}Th - ^{233}U cycle and its differences with the ^{238}U - ^{239}Pu cycle. In the second we describe briefly the different schemes that have been proposed for thorium utilization with respect to the fuel cycle, the kind of reactor and reprocessing, with special emphasis on schemes that could be applied to national nuclear plans. In the third we will study strategies for thorium utilization and lines of research presently being pursued in different countries.

The possibility of using thorium as a fertile material in power reactors stems from the following cycle:

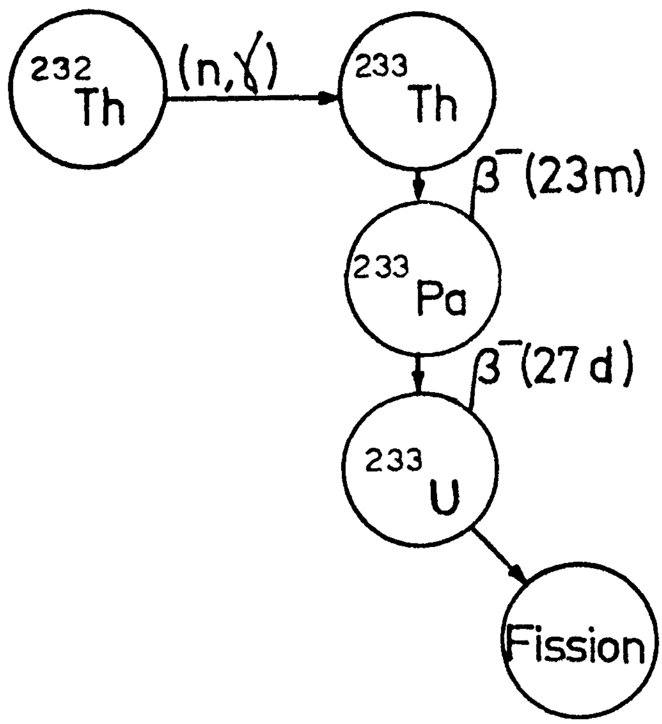

The importance of this cycle comes from the fact that ^{233}U is fissionable by thermal (and fast) neutrons and is potentially a better fuel than ^{235}U and ^{239}Pu.

If ^{233}U is used as a fuel (with ^{232}Th as fertile material) it is possible to breed fresh ^{233}U and therefore only consume ^{232}Th, which is relatively abundant in the earth crust (∿ 4 times as abundant as uranium). The efficiency of conversion of ^{232}Th to ^{233}U is measured by the breeding gain BG, which is defined as

$$BG = \frac{\text{excess n° of } ^{233}U \text{ nuclei created}}{\text{n° of } ^{233}U \text{ consumed}}$$

In terms of nuclear parameters we have

$$BG = \eta - 2 - L$$

where

$$\eta = \frac{\text{n° of created neutrons}}{\text{n° of destroyed neutrons}}$$

and L measures the loss of neutrons in structures, moderator, coolant, intermediate nuclei and fission products.

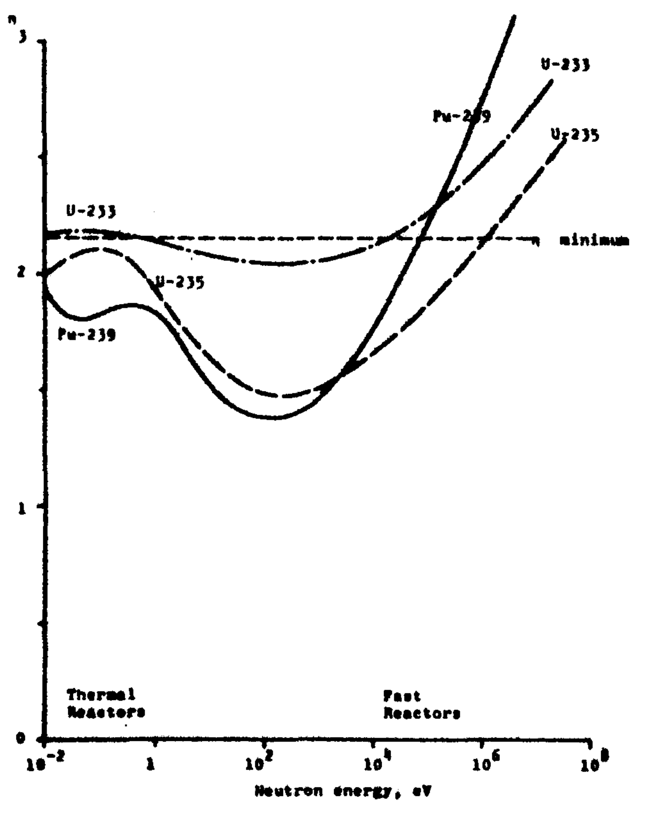

Fig. VII.1.1 Schematic plot of the energy dependence of η for the three fissile nuclei ^{233}U, ^{235}U and ^{239}Pu.

In Fig. VII.1.1 we plot the values of η as a function of energy for the three fissile nuclei ^{233}U, ^{235}U and ^{239}Pu.

We notice that in the thermal region (E < 1 eV) ^{233}U has the highest value of η implying that, even considering losses, we could have BG > 0. This means that more fuel is generated than spent so that thermal breeding using the thorium cycle is feasible while this is not the case for the uranium-plutonium cycle.

VII.2. Utilization of Solar Energy.

J.A.Moragues and W.Scheuer.

Since May 1974, two members of the Department are devoted to solar-energy studies. Their first task was to evaluate the state of the art in the development of technologies for large-scale conversion of solar energy to electricity. To this order, they attended several international meetings and visited a number of laboratories in Europe and the U.S.A. The collection of the necessary information, as well as two parts of the report they are preparing have now been completed; two more parts are being written.

Towards the end of 1975, a technical and economical evaluation of the possibility of solar preheating of the water needed for treatment of the uranium ores in the concentrating plant to be built in Sierra Pintada (Province of Mendoza) was started. Although the process of treatment is yet not completely defined, CNEA's Area of Raw Materials estimates that there will be a daily need of the order of 10^6 liters of water at 70-80 C to be heated. After preliminary calculations a system of shallow solar ponds using large plastic bags, similar to one being tested at the Lawrence Livermore Laboratory, U.S.A. has been preselected. Several PVC plastic bags of 1.4 m^2 and some poliethylene bags are being prepared to explore the best geometry to be used; tests for the selection of appropriate insulator material have started. A computer program for calculating the efficiency of different bag-geometries, produced at the L.L.L., is being adapted to our facilities. A 10 hectare area, about a 1000 m from the concentrating plant, has been defined as apt for the construction of the final pools; solar-radiation-measuring and meteorological instruments to be mounted in this area are being put together and adjusted.

VIII. SERVICES

VIII.1. Use of the Synchrocyclotron for Sample Analysis.

L.Gallacher, A.M.J.Ferrero and M.A.J.Mariscotti.

Several experiments were performed on the Synchrocyclotron of Buenos Aires external beam to study the possibilities of using the existing equipment for various kinds of sample analysis. Measurements can be grouped in four classes:

a) γ-ray spectra produced by α-particle bombardment.

b) X-ray spectra produced by α-particle bombardment.

c) Spectra of Deuterons elastically scattered by thin targets.

d) Spectra of Deuterons elastically scattered by thick targets.

The detectors used were: a Ge(Li) diode (6% efficiency and $\sim$2.5 keV resolution for the ^{60}Co lines), a Ge(Li) X-ray spectrometer (500 eV resolution at 10 keV) and a surface barrier Si(Li) detector 3 mm thick. Trial runs were done with Be, Al, Cu and mylar targets, as well as with real samples of concrete, iron, solid residues from evaporated polluted water (from the Rio de la Plata) and solid pollutants from downtown Buenos Aires air (deposited on a filter by an air current for $\sim$20 hours).

Preliminary conclusions from these experiments are:

(a) γ-ray spectra have the advantage of being insensitive to the thickness of the target and the disadvantage of being heavily populated and therefore difficult to analyze. We plan to put together a catalogue of γ-ray spectra of non enriched elements to help this analysis.

(b) X-ray spectra are instead much simpler to analyze. The background however, has still to be reduced. The method can only determine the presence of heavy elements ($A \gtrsim 30$).

(c) Backscattering of deuterons is a good complement to the X-ray method because it can be used for light elements. At E_d = 27.25 MeV and θ = 135° the intrinsic resolution of the Synchrocyclotron allows the separation of elements with $A \lesssim 25$. However the use of thick targets decreases the sensitivity of this method.

VIII.2. Implantation of ^{140}La in Various Foils.

R.Requejo* and D.Otero.

By request from the Nuclear Physics Group of the University of La Plata, ^{140}La was implanted in Al, Cu, Gd, and Ni foils to study the interaction with the crystal lattice at different temperatures by means of angular correlations. We irradiated seven sources, each for two or three eight-hour periods.

---

* Departamento de Ingeniería (CNEA).

PART D

INSTRUMENTATION AND DEVELOPMENT

IX. MACHINE DEVELOPMENT.

IX.1. Synchrocyclotron.

IX.1.1. Improvements in the Frequency Modulator.

N.A.Fazzini, J.Coralo, J.Garanzini, G.Ietri, A.Morales,
M.Professi and J.C.Rodriguez.

In the frequency modulator, high intensity RF currents flow from the rotating capacitor to ground. Although the machine has been provided with protection devices (grounding capacitors, central axis isolation and a high impedance for RF currents) the erosion of the bearings caused by these currents is strong and the components have to be replaced causing frequent machine openings.

In order to improve the lifetime of the bearings, the inner and outer tracks in each one were short-circuited by three sliding carbon contacts. In this way, the current intensity flowing in each bearing has been decreased and the life-time of these components increased about 80%.

IX.1.2. Automatization of the Internal Target.

N.A.Fazzini, J.Coralo, J.Garanzini, G.Ietri, A.Morales,
M.Professi and J.C.Rodriguez.

In order to introduce and remove the internal target into the accelerator chamber of the synchrocyclotron, a simple servo-system composed of a motor with speed reductor acting on an endless screw was installed. Two microswitches fix the extreme positions allowing the target to be stopped in any intermediate position. Panel lights indicate the operator the state of the system at any time. The system allows the measurement of the internal beam current during irradiation, avoiding the interruptions caused when the target was manually operated.

IX.1.3. Repairs.

N.A.Fazzini, J.Coralo, J.Garanzini, G.Ietri, A.Morales, M.Professi and J.C.Rodriguez.

The main repair performed on the synchrocyclotron in the period 1974 - 1975 has been the replacement of the RF feedthroughs connecting the transmission line both with the active "D" and with the fixed plate in the modulator. In the last position a vacuum leak was observed.

In order to make these replacements the machine had to be almost totally dismantled. To improve the performance of the feedthroughs the surface of the fingers had to be increased. As a result the working temperature of the feedthroughs decreased, and the life expectancy was prolonged.

Several other minor repairs performed in the same period are listed below:

- Replacement of the oscillator tube. The tube socket had to be modified.
- Repair of the internal target vacuun feedthrough.
- Construction and replacement of two coils in the deflecting magnet.
- Repair of the power supply for the quadrupole lenses.
- Replacement of the 1200 liters/sec oil diffussion pump in the beam extracting port.
- Repair of the main magnet current supply.
- Dinamical balance of the frequency modulator.

IX.2. Isotope Separator.

IX.2.1. New Movable Collector.

J.Cava and R.Requejo.

It allows, besides the use of Ge(Li) detectors, the installation of electron solid-state detectors in the vacuum chamber. In this way it is possible to study short-lived isotopes.

IX.2.2. A New Ion-Source.

D.Otero, J.J.Rossi, J.Cava, R.D'Agostino, A.Tersigni and A.Gonzalez.

A new ^{235}U ion-source and electrostatic lens system were designed and constructed. The ^{235}U target is incorporated in the arc-chamber. The system was tested with stable isotopes and then the on-line operation was intended. The efficiency was lower than expected, although isotopes of Br and Rb were observed in addition to those of Kr previously obtained.

A relative improvement in the efficiency was also observed for short-lived isotopes. More work is being presently performed in order to increase the efficiency by incorporating more uranium in the source and increasing the neutron flux from the accelerator.

IX.2.3. Construction of an Arc-Chamber Containing ^{235}U.

J.Cava, R.Requejo and J.Prieto.

Graphite cloth was used to make several discharge chambers for the new ion-source. Several grams of ^{235}U were absorbed and the chambers so prepared were dried in a vacuum oven.

IX.2.4. Electrostatic Deflector for the Ion-Beam Separator.

J.Cava and R.Requejo.

An electrostatic deflector (cylindric capacitor) for the ion-beam has been constructed. The system will permit the deposit of the mass under investigation in three different stations: (1) for β- or γ-ray measurements, (2) for γ-γ angular correlations and (3) for use of a new target incorporating the double-focus spectrometer to the on-line system.

IX.3. Cascade Accelerator.

IX.3.1. Modification of the Lower End of the Accelerator.

A.Tersigni, A.Gorgoschidse and R.Requejo.

The bottom end of the accelerator tube has been modified to allow better focusing of the deuteron beam. New cooled target holders were also constructed.

IX.3.2. Increase of the Neutron Flux.

A.Tersigni, A.Gorgoschidse.

In order to increase the neutron flux produced by the Cockcroft-Walton accelerator, 6 selenium rectifiers were replaced by new Si-type diodes. As a consequence, both the high voltage stability and the maximum atainable voltage have increased.

IX.3.3. Modulator of the Deuteron Beam.

A.Tersigni.

An electromechanical device was designed and installed in order to interrupt the deuteron beam. The system allows pulsing of the neutron flux with a shutting time of approximately 0.05 sec. This is extremely useful to observe the time response of the on-line system and to measure the efficiency of the production of fission byproducts. The effect of stopping the neutron flux has been better than 2.10^{-4} measured on the strongest transitions in A = 140 nuclei.

IX.3.4. Safety System for Beam Deflector.

D.V.Camin, R.D'Agostino and D.Otero.

A new system of protection from isotopic contaminations has been set in operation in the electromagnetic separator. In case of any displacement in the beam position, the vertical deflection of the separator is triggered.

IX.3.5. Uranium Oven.

J.Cava and J.J.Rossi.

A vacuum oven having an internal thermal shielding and a quartz central body was constructed to heat uranium up tp 900 ^0C.

IX.3.6. Changes in the Separator Collector.

J.Cava and J.Vidalle.

The collector pinpoint system was modified to allow a better handling of the beam position control. Operation of an automatic centering device is also permitted.

X. IMPROVEMENTS OF THE EXPERIMENTAL FACILITIES

X.1. Beam Energy Degrader.

A.Kreiner*, N.Fazzini, J.C.Rodriguez, G.Ietri, J.Garanzini, M.Professi and M.A.J.Mariscotti.

This work was the first in a series of projects designed to improve the basic facility of the Buenos Aires Synchrocyclotron with the aim of making it suitable for a research program based on (α,xn) reactions. For this type of studies it is important to be able to vary the beam energy. Because of budget reasons and in order to avoid the interruption of the research activities, the hitherto considered alternative of converting the accelerator into a variable energy machine, was ruled out. Instead, it was decided to build a simple degrader device, as used in other laboratories, in which the beam passes through a foil and looses a certain amount of energy, as a consequence of the inelastic collisions with the electrons, according to the foil thickness.

The device which has been constructed consists in a simple wheel of Al 5 mm thick and 288 mm of diameter with six holes of 60 mm diameter each. Five of these holes are covered with thin Al foils of different thickness. The wheel is located inside a box which is mounted before the first pair of focusing quadrupoles and deflecting magnet.

The thickness of the foils have been chosen so as to have an α-beam with six energy values between 30 and 55 MeV in steps of 5 MeV. The system was calibrated using the $^{197}Au(\alpha,\alpha)^{197}Au$ reaction at θ_{lab} = 30°. As energy references both the non-degraded deuteron and alfa-beam were used (E_d = 27.25 MeV and E_α = 54.5 MeV).

The energy spread shows a small increase as the foil thickness increases; while the beam intensity diminishes significantly and the angular dispersion increases. This information is given in Table X.1.1. The last column shows the ratio between the charge collected at the target position and the Faraday box, about 3.5 m further away from the machine.

The main use and application of the degrader is the determination of excitation functions and the possibility of choosing the optimum energy to study a given reaction. In the energy range provided by this device, (α,xnyp) reactions with x + y ≃ 2 to 4 can be observed and a good number has already been studied. As an example, Fig. X.1.1 shows the curves obtained[1] for γ-rays from the $^{70}Ge(\alpha,np)$ and $^{72}Ge(\alpha,3np)$ reactions, both leading to levels in ^{72}As. Most γ-rays identified (see Sec. II.3) from these curves were not previously known.

* On leave of absence. Present address: Physik Department E17 der Techn. Universität München, 8046 Garching, W.Germany.

[1] M.A.J.Mariscotti, M.Behar, A.Filevich, G.García Bermúdez, A.M.Hernández and C.Kohan, Nucl. Physics (to be published).

Table X.1.1

Thickness (mm)	Beam Energy (MeV)	Target Current (nA)	Target current / Faraday cup current
0	54.5	0.2	1.46
0.18	49.1	0.07	3.81
0.36	43.2	0.04	5.72
0.48	38.9	0.035	12.9
0.60	34.2	0.03	19.5
0.72	29.0	∿0.02	---

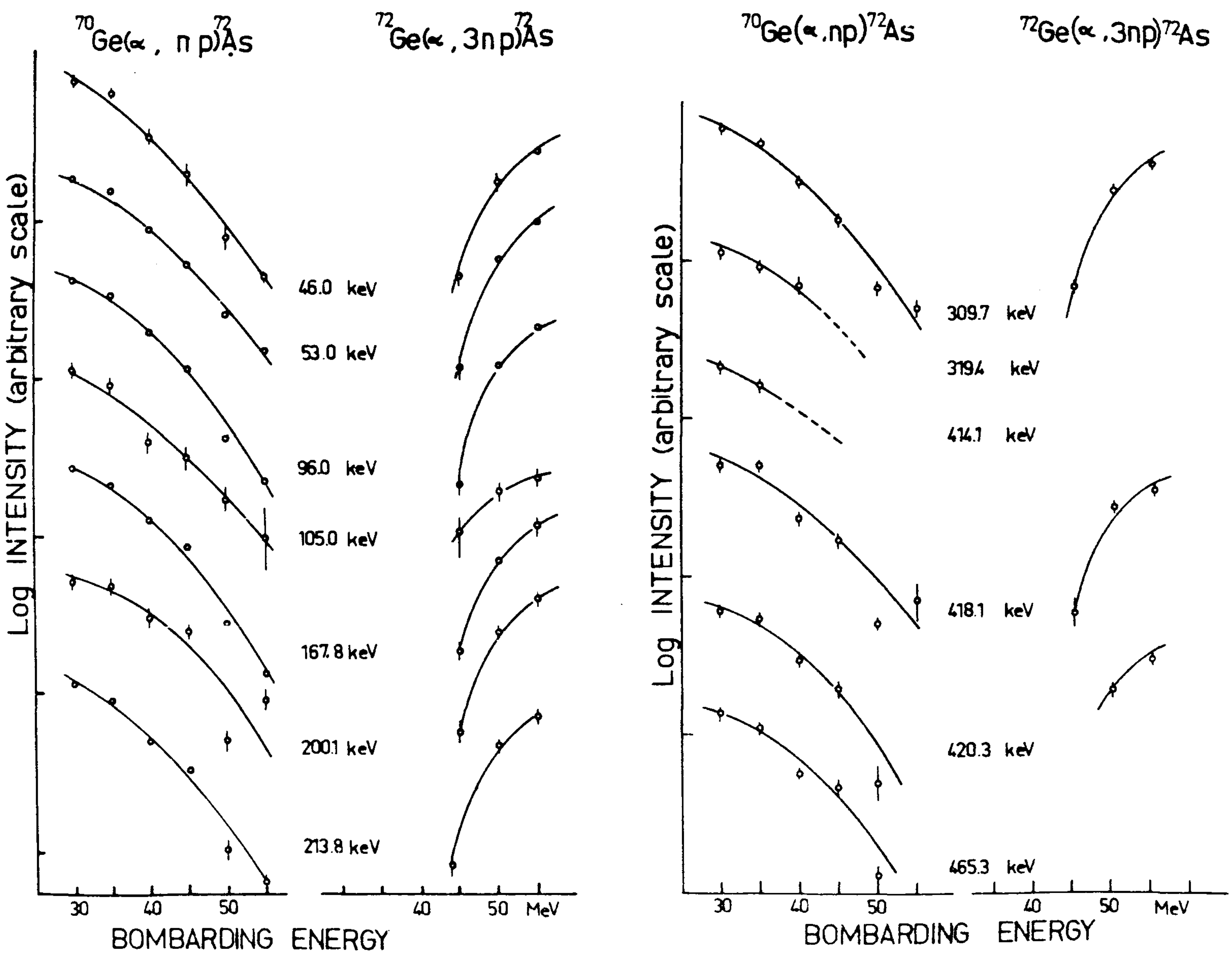

Fig. X.1.1 Excitation functions of γ-rays from the $^{70}Ge(\alpha,np)^{72}As$ and $^{72}Ge(\alpha,3np)^{72}As$ reactions.

X.2. A System for the Determination of Nuclear Half-Lives in the msec-sec Range.

E.Santi*, N.Fazzini, A.Rendina, J.Garanzini, G.Ietri, A.Morales, M.Professi, J.C.Rodriguez, J.Sinderman and M.A.J.Mariscotti.

A system for the determination of nuclear half-lives in the msec-sec range has become available in the Synchrocyclotron facility by means of a mechanical chopper with variable speed. It consists of a circular aluminium plate with two opposite gaps respective to the axis of rotation. The system is located in the beam path, before the first focusing quadrupole; it rotates in the vacuum magnetically coupled to the driving motor through a set of permanent magnets. Fig. X.2.1 shows a sectional view of the chopper parallel to the beam direction. The disk (6) turns around the axis (11) fastened by bearings to a metallic box whose form is a truncated cylinder 40 cm in diameter and 5 cm in height. The coupling of the disk with the motor (29) is made through the magnets (28). There are four magnets on each side: the ones fixed to the disk are capable of holding a weight of up to 1 Kg each, while those attached to the motor hold up to 4 Kg.

Taking into account the beam size, the angular gap was chosen as $\alpha_i = 40°$. The disk can turn from 30 to 3000 rpm allowing the measurement of nuclear half-lives ranging from 1 msec to 1 sec approximately. The time reference signal t_o is obtained with the help of a photo-cell.

Fig. X.2.2 shows the block diagram of the electronic circuit where the principal element is the Intertechnique Generateur Horloge HC41 clock, which generates electric pulses for the time control of the system. The separation between pulses can be adjusted in the range 10^{-5} sec - 10^{5} sec. The pulses generated by this clock, triggered by the signals from the photo-cell, are used to route the data from the γ-ray detector to a different section of the multichannel analyzer. In this way γ-ray spectra as a function of time, can be obtained cyclically starting at $t = t_o$.

Figs. X.2.3 and X.2.4 show the application of the system to the determination of two nuclear half-lives with values situated in the limits of the time range.

Fig. X.2.3 shows the results obtained for γ-rays from the reaction $^{141}Pr(\alpha,3n)^{142}Pm$ which depopulates a 2.1 msec state.

Fig. X.2.4 shows the results corresponding to the isomeric state in ^{197}Tl with $T_{1/2} = 0.54$ sec populated in the $^{197}Au(\alpha,4n)$ reaction.

---

* Research Student.

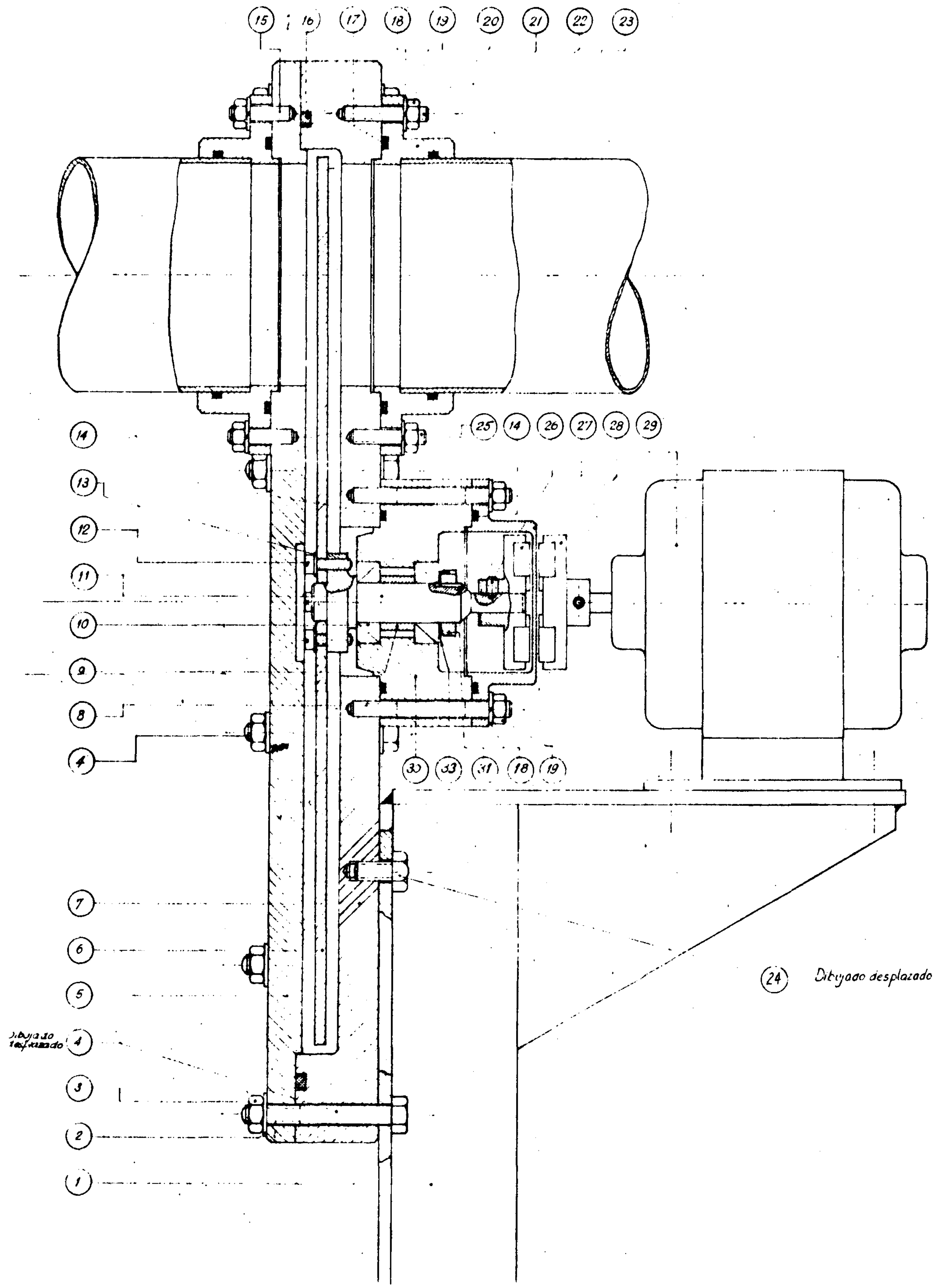

Fig. X.2.1 Sectional view of the chopper parallel to the beam direction.

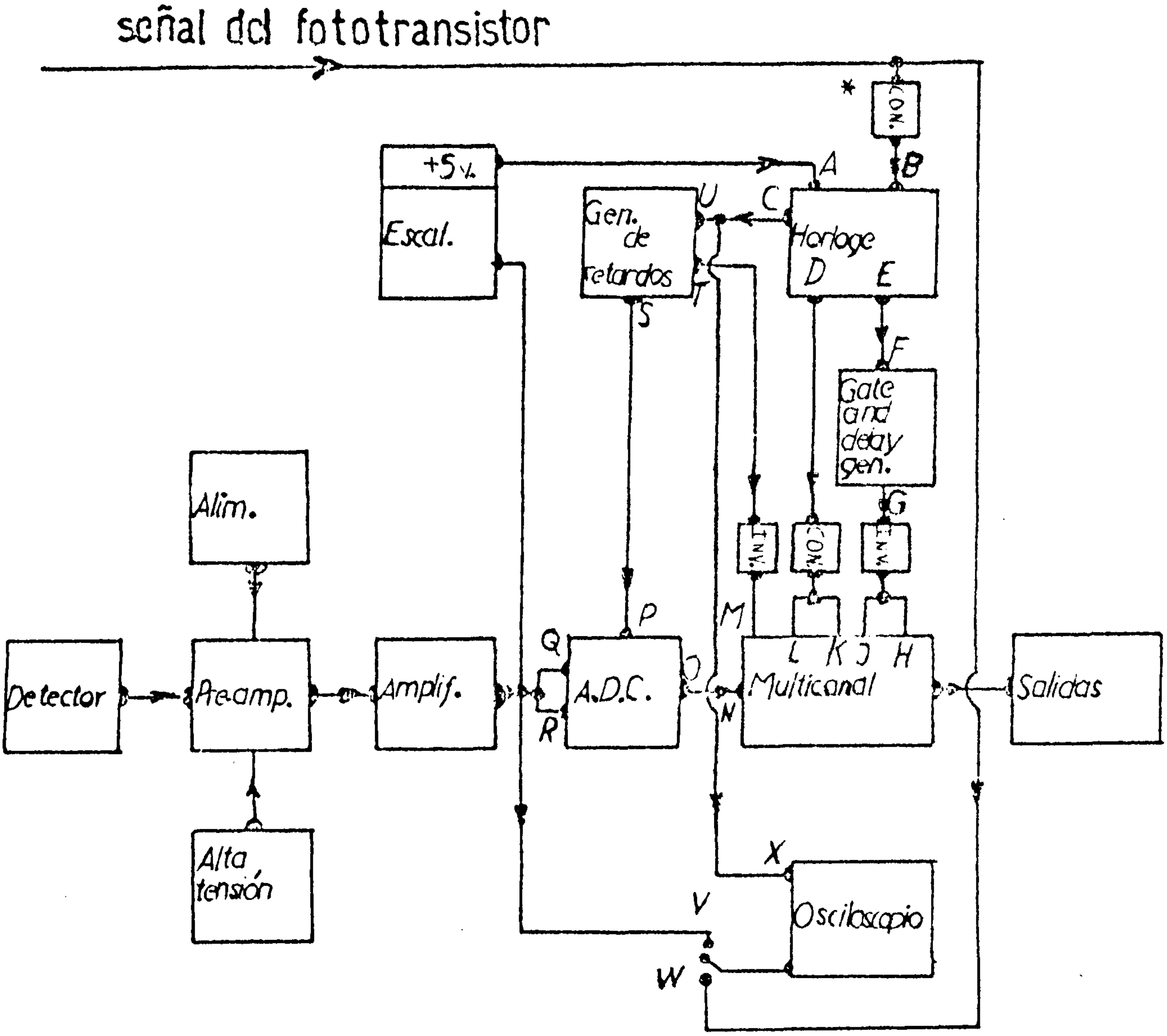

Fig. X.2.2 Block diagram of the electronic circuit.

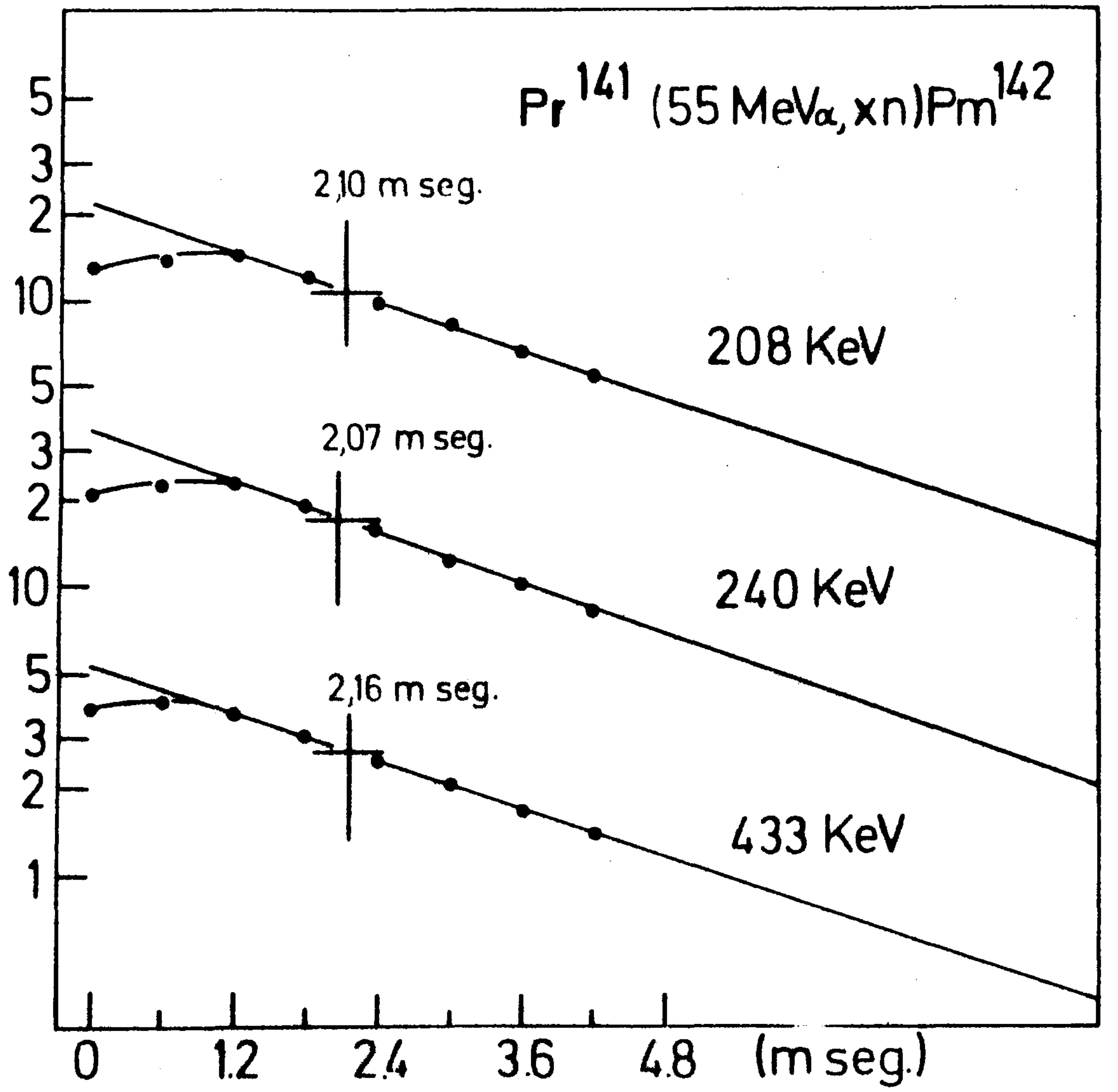

Fig. X.2.3 Determination of the half-life of the 881 keV state in ^{142}Pm.

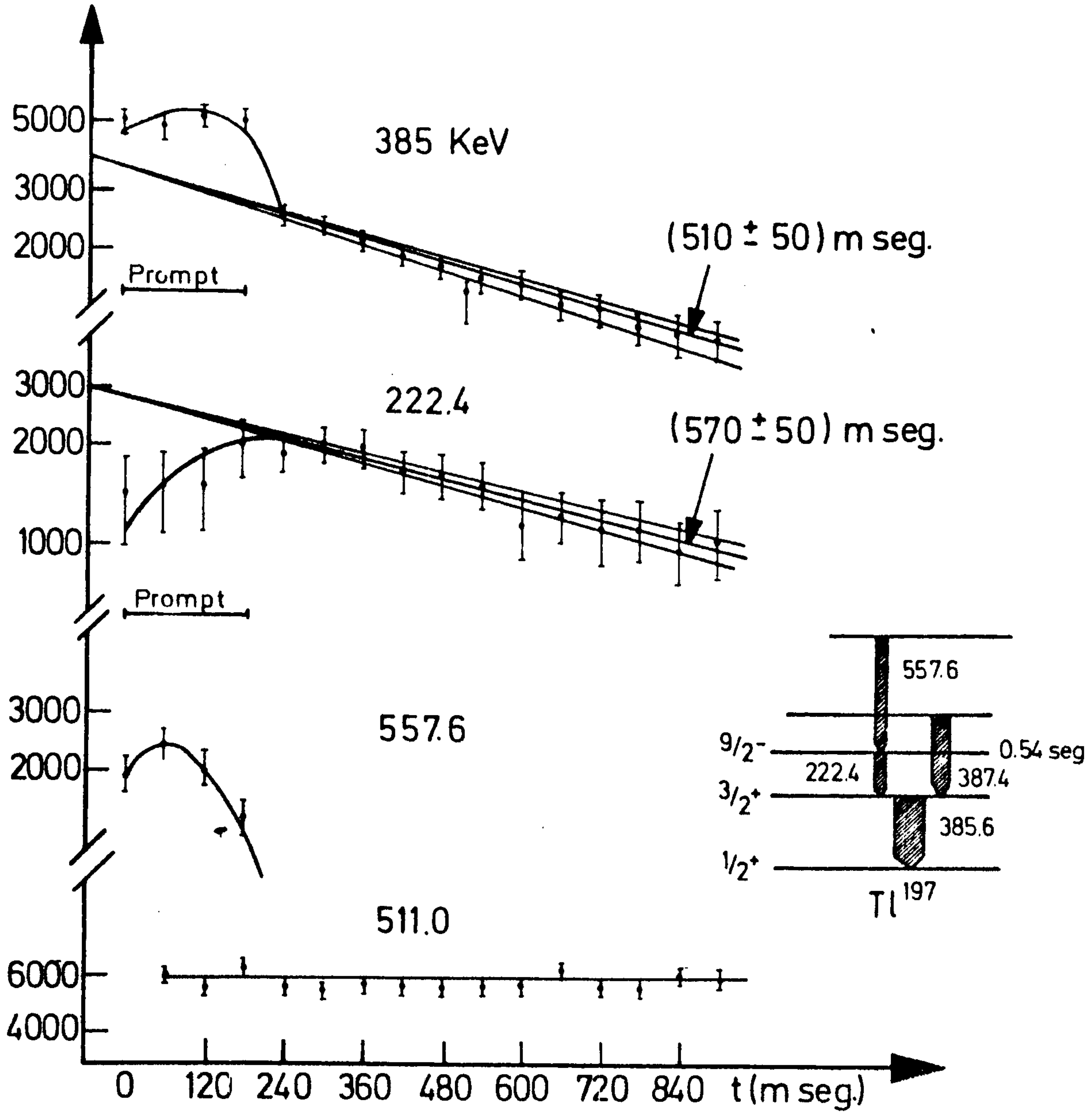

Fig. X.2.4 Illustration of the use of the chopper for the determination of the $T_{1/2}$ = 0.5 sec isomeric state in ^{197}Tl.

X.3. Measurements of Nuclear Half-Lives in the μsec Range.

E.Santi*, J.Sinderman and M.A.J.Mariscotti.

Using the 2000 cycles from the radiofrequency modulator of the Synchrocyclotron, a triggering signal, appropriate for the measurement of nuclear half-lives in the range $50 \lesssim T_{1/2} \lesssim 800$ μsec, was obtained.

The electronic circuit is similar to the one shown in Fig. X.2.2 (see Sec.X.2). The performance of the system is illustrated in Fig. X.3.1 which shows the temporal spectra of γ-rays from the Ce(α,xn) reaction at $E_\alpha = 55$ MeV. The half-life of 640 μsec corresponds to a state of ^{140}Nd. The horizontal distribution shown in the botton of the Fig. X.3.1, corresponds to a 755 keV ray of ^{141}Nd with $T_{1/2} = 63$ sec.

---

* Research Student.

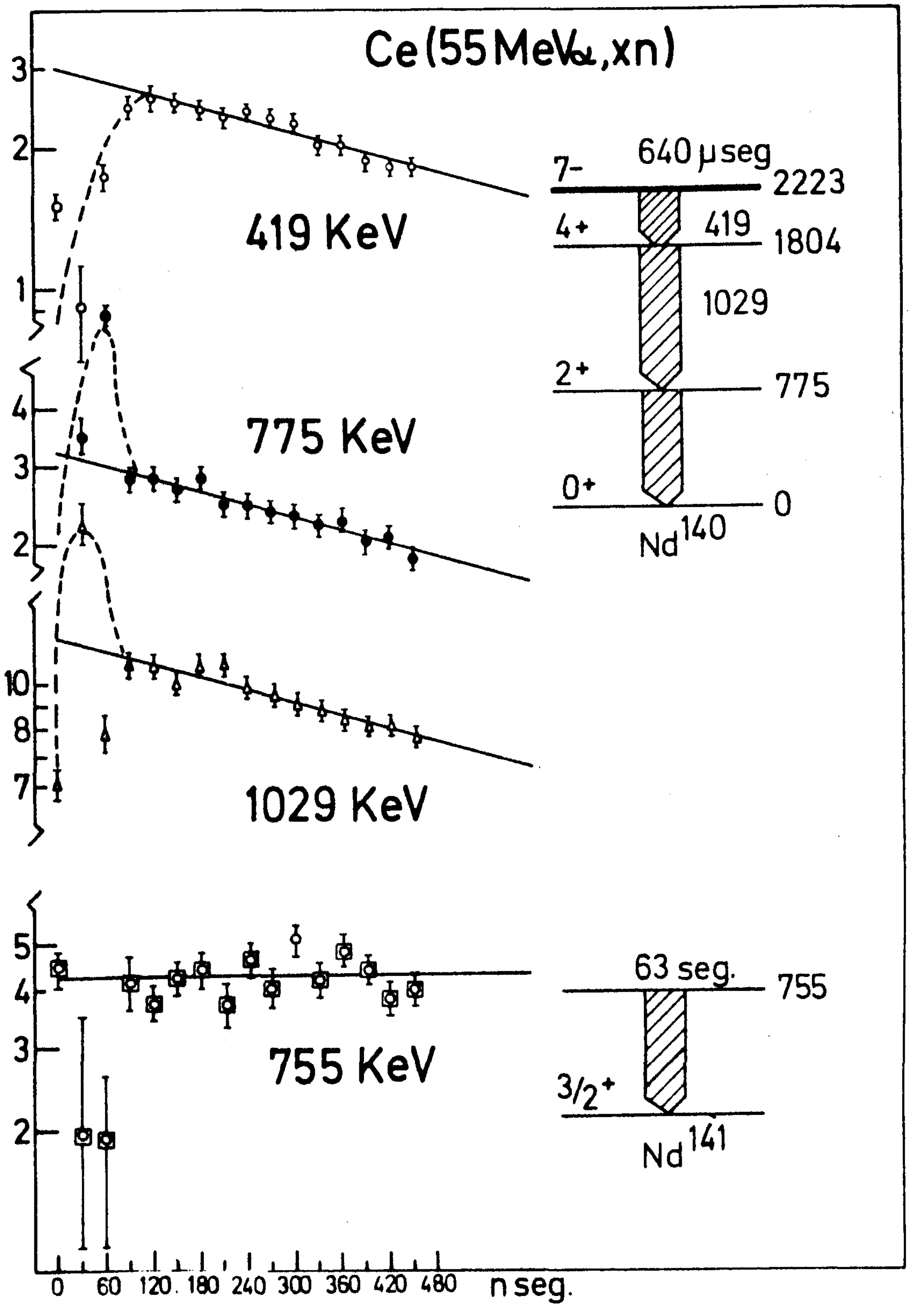

Fig. X.3.1 Determination of a half-life in ^{140}Nd by using the modulation of the Synchrocyclotron radiofrequency.

X.4. Measurements of Nuclear Half-Lives in the nsec Range.

C.Kohan*, P.Thieberger** and M.A.J.Mariscotti.

The present work was carried out in order to obtain an appropriate temporal resolution to measure nuclear half-lives in the range $\sim$ 20 - 150 nsec using the microstructure of the Synchrocyclotron beam, according to the method of Yamazaki and Ewan[1].

The main difficulties stemmed from the radiofrequency noise and the "walk" in the time signal introduced by the modulator circuit.

Fig. X.4.1 shows a comparison between prompt curves obtained with different triggering systems for the energy E_γ = 511 ± 4 keV. The spectra obtained using a plastic scintillator in the beam path to provide the triggering signal is shown at the top of the figure, while the bottom part shows the spectra obtained with a triggereing signal directly from the synchrocyclotron radiofrequency oscillator.

Fig. X.4.2 shows results from the $^{72}Ge(\alpha,np)^{72}As$ reaction at E_α = 35 MeV, obtained with an X-ray Ge(Li) detector. The slope of the prompt distribution is 8 nsec. The half-life $T_{1/2}$ = 17 ± 3 nsec corresponds to a new isomeric state of ^{72}As (see Sec. II.3). The 80 nsec slope indicated for the 46 keV γ-ray corresponds to the half-life of the 3^+ state at 213.8 keV, previously known. A determination using a scintillator crystal instead of a Ge(Li) detector reduced the prompt slope to 3.7 nsec.

---

* Research Student. Present adress: Department of Physics, University of Washington, Seattle, U.S.A.

**Visiting Scholar, Brookhaven National Laboratory, Upton, New York, U.S.A.

1 T.Yamazaki and G.T.Ewan, Phys. Lett. 24B (1967) 378 and Nucl. Instr. and Meth. 62 (1968) 101.

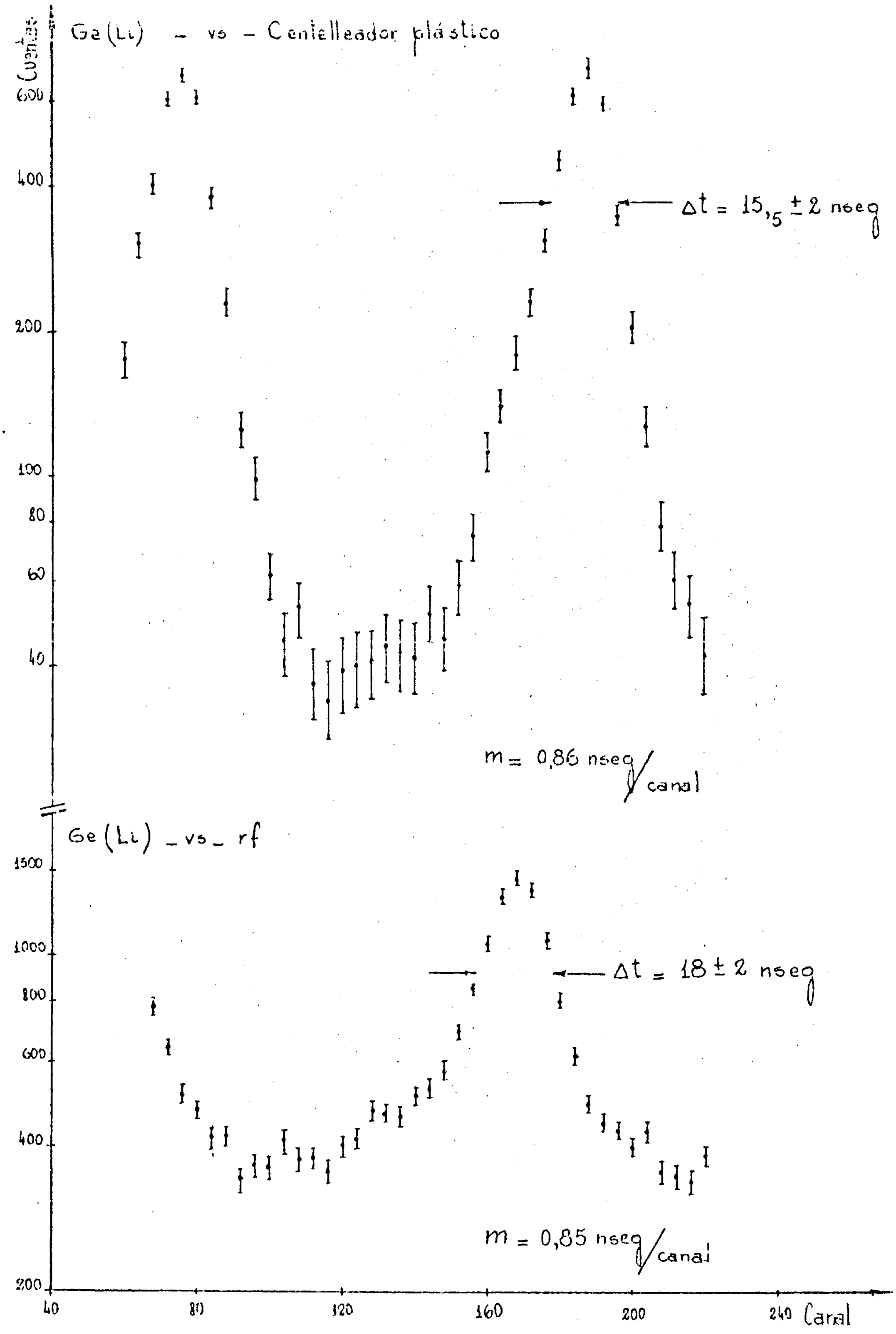

Fig. X.4.1 Prompt curves obtained using a plastic scintillator (top) and the Synchrocyclotron radiofrequency (bottom).

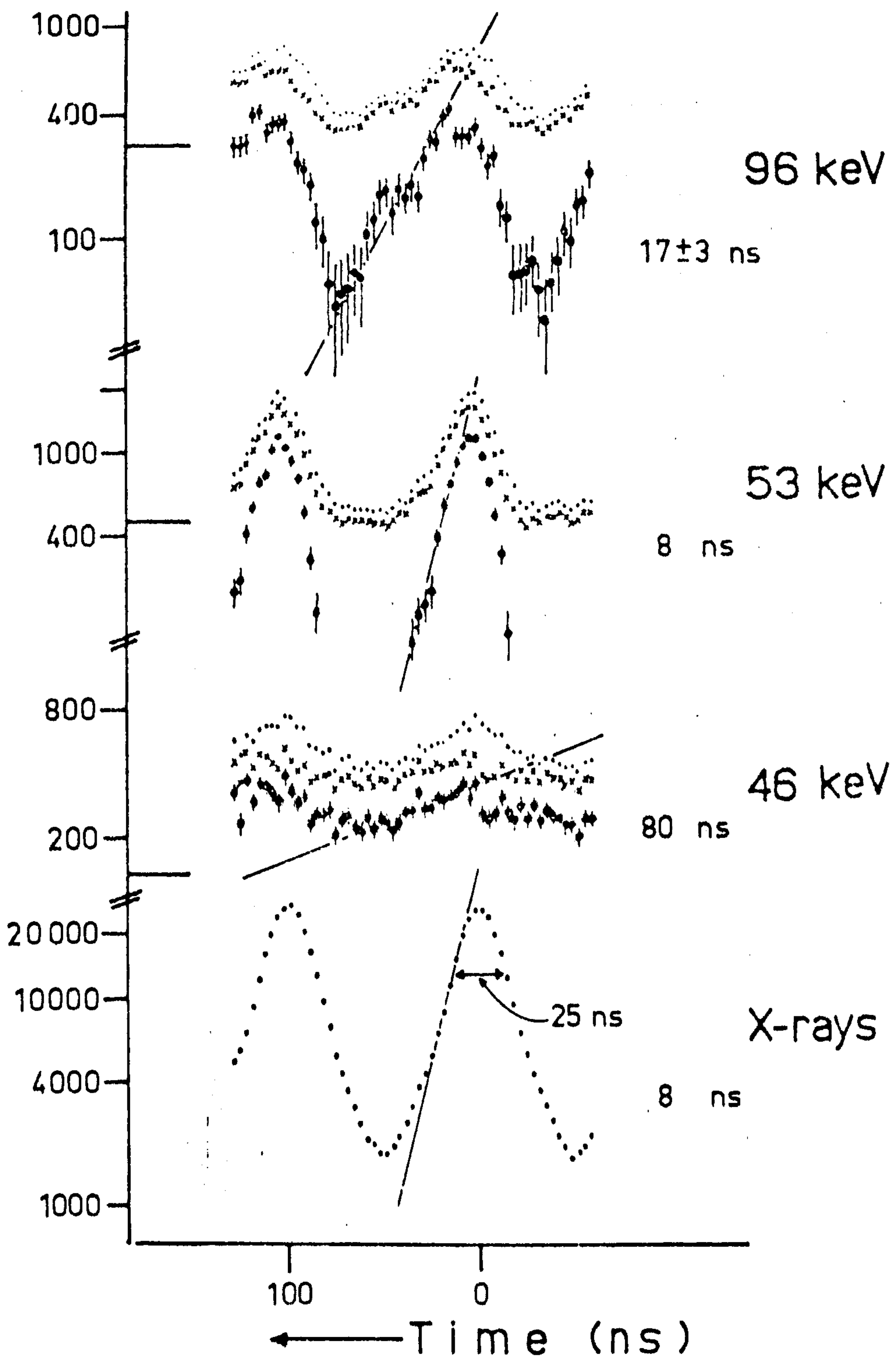

Fig. X.4.2 Time distributions of γ-rays from the $^{70}Ge(\alpha,np)^{72}As$ reaction.

X.5. New Facilities for In-Beam γ-Spectroscopy.

A.Filevich, M.Behar, G.García Bermudez, J.Coralo, A.Morales, J.Prieto and J.C.Rodriguez.

The simple acrylic tube which has been used as a reaction chamber for in-beam (α,xn) experiments has been replaced by a new facilty including (a) a thin wall acrylic chamber 20 cm in diameter and (b) a circular table, 1.2 meters in diameter, which can support Ge(Li) detectors. The detectors can be independently positioned at any angle between 25° and 155° with respect to the beam axis.

The chamber includes two target holders which can be exchanged without breaking the high vacuum. The chamber can be rotated 90° around the beam axis. In this position, the γ-ray detectors can get close to the target in order to perform γ-γ coincidence measurements. The chamber has been designed to accept the pole-pieces of an electromagnet which will permit the study of the interactions between electromagnetic nuclear moments and external fields.

The new chamber and angular correlation table now in operation has been used to perform various experiments, including singles γ-spectra, γ-γ and X-γ coincidences, time distributions and angular distributions.

XI. COMPUTATION

XI.1. Design and Construction of a System for Semiautomatic Analysis of γ-Spectra through an Interphase with an HP-2116B Computer.

R.Pecyner*, A.Filevich, J.Sinderman and M.A.J.Mariscotti.

Due to the lack of appropriate peripherals, one of the principal difficulties in the implementation of the (α,xn) program resides in the data processing. Data are accumulated in a 4096 channel analyzer (Intertechnique), from which the information can be transfered to a fast printer, tape puncher and/or casette recorder which is not IBM compatible. These peripherals are not appropriate to get a fast and efficient transfer of the data to a computer for its subsequent analysis. For this reason, in the first part of this work, an interphase to transfer the data electronically to an HP-2116B computer was constructed[1]. In the second part, a data fitting program was prepared. This program follows conventional ideas[2], but it is adapted to the capacity of the computer and improves on certain characteristics of already existing programs[3].

The availability of a light pen in the multichannel analyzer led us to opt for a semiautomatic procedure. The light pen is used to feed the HP-2116B computer with the following information:

(a) the interval where the peak or multiplet to be analyzed is located;
(b) the appropriate position of the peaks in the interval;
(c) indication of the background;
(d) indicators to differenciate ordinary data from standards (from which the shape parameters are obtained);
(e) indicators of peaks with precisely known energies to be used as energy and intensity references.

With this information the analysis of the spectra is shortened and, in general, better precision is obtained. The peaks are fitted to a gaussian function with an exponential tail on the left side. From the analysis of the above mentioned standard spectra, the shape parameters, namely, the gaussian width and the channel number corresponding to the matching point of the gaussian and the exponential curve, are obtained as a function of energy (or peak position).

The program contains several interesting features which contribute to reduce the computation time. They include the resolution of linear systems (inversion or triangulation of matrices), exponential calculations, truncation of peaks in wide regions o- analysis, substitution of floating point operations by integer tests, procedure for convergence, and optimization of memory and peripherals requirements. The system is able to handle multiplets up to seven peaks. The output is obtained on a teletype and on a calcomp plotter.

Fig. XI.1.1 shows a typical output corresponding to a multiplet of seven peaks from the reaction ^{57}Fe + 30 MeV α[4]. The print includes the positions, heights and areas with their errors. If the calibration option is used, the positions are given in keV and the areas are corrected for efficiency. In order to reduce the processing time the scales and titles have been suppressedin the graph, and only the initial channel is left for identification. The oscilating curve at the bottom of the calcomp plot indicates whether a component not previously considered has been detected. This circumstance is illustrated in Fig. XI.1.2 where a wide and ample oscilation is clearly observed (χ^2 = 2.4). A further analysis shown in Fig. XI.1.2 indicates the presence of an additional peak (χ^2 = 1.2).

The typical processing time for the analysis of ordinary spectra is ≃ 30 sec for each region or interval; this time fluctuates with the number of peaks in the multiplet. The standard spectra take approximately twice as long as the ordinary ones.

---

* Research student. Present address: Department of Physics, University of California, Berkeley, California, U.S.A.

[1] R.Pecyner and J.E.Sinderman, 61st. Meeting of the Argentine Physical Society, Buenos Aires, May, 1975.

[2] M.A.J.Mariscotti, Nucl. Instr. and Meth. 50 (1967) 309 and BNL 10904. T.Routti and S.G.Prussin, Nucl. Instr. and Meth. 72 (1969) 125.

[3] E.Achterberg et al., IEEE Trans. Nucl. Sc. N. S. 19 (1972) 3 and E.Achterberg et al. (to be published) (see also Section XI.3 in this report).

[4] R.Pecyner, Licenciatura Thesis. Fac. Ciencias Exactas y Naturales, Universidad de Buenos Aires, 1975.

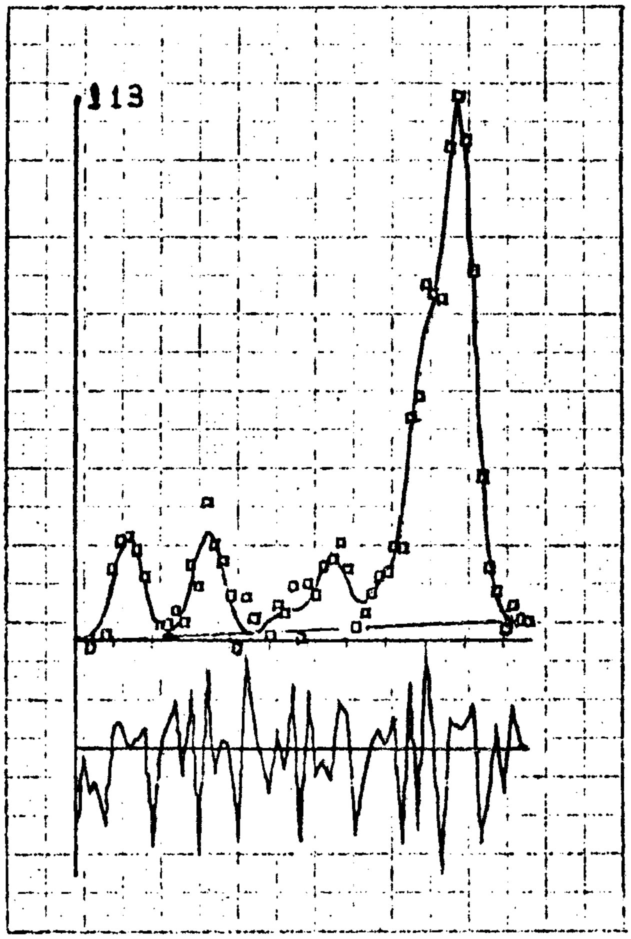

POSICION ERROR ALTURA AREA ERR.%

NORMALIZACION=
1.764121
*EQR

CANALES 113 - 170

POSICION	ERROR	ALTURA	AREA	ERR.%
53.189	.315	245.	.66511E+03	12.77
58.410	.308	252.	.68489E+03	12.47
63.378	.790	56.	.15259E+03	45.55
66.376	.375	184.	.50160E+03	16.31
69.691	.635	95.	.25815E+03	32.02
72.245	.273	606.	.16538E+04	8.47
74.520	.212	1184.	.32302E+04	5.96

JI CUADR./GR.LIB.= 1.2 6 ITERACIONES

Fig. XI.1.1 Typical output corresponding to a multiplet of seven peaks from the reaction ^{57}Fe + 30 MeV α. If the calibration option is used, the positions are given in keV, and the areas are corrected for efficiency.

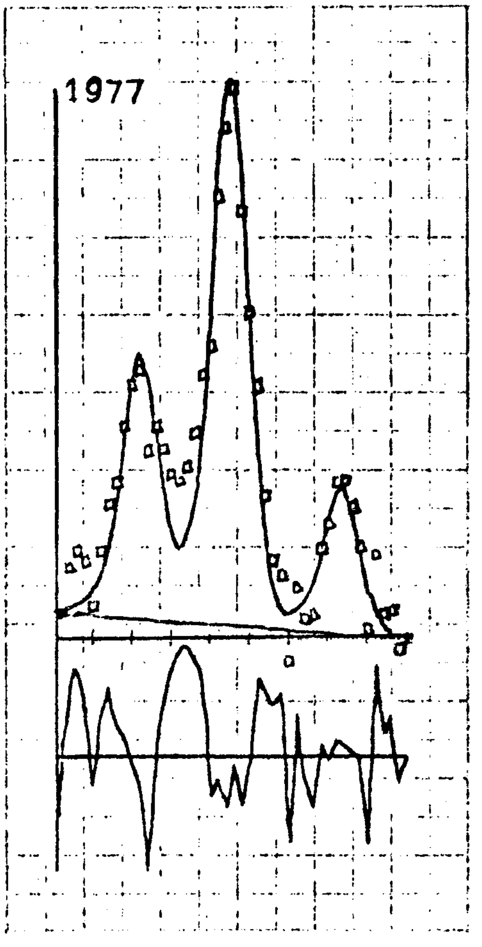

CANALES 1977 - 2021

992.373	.158	174.	.62559E+03	5.69
998.122	.117	372.	.13010E+04	3.45
1005.223	.206	99.	.34764E+03	5.57

JI CUADR./GR.LIB.= 2.4 4 ITERACIONES

CANALES 1977 - 2021

991.965	.195	156.	.52586E+03	7.54
994.953	.366	76.	.21247E+03	13.85
998.250	.127	353.	.12340E+04	3.92
1005.227	.290	99.	.34702E+03	3.59

JI CUADR./GR.LIB.= 1.2 10 ITERACIONES

Fig. XI.1.2 This figure illustrates the case of a peak missing in the analysis as indicated by the oscillating curve at the bottom of the plot. The print out shows the difference before and after including the missing peak.

XI.2 Study of a Program for Automatic Analysis of Spectra by the Method of Numerical Simulation.

A.Díaz Romero.

The method of numerical simulation[1] was applied to the study of a program for automatic analysis of spectra[2] in order to obtain information on its capability to identify and resolve gaussian peaks. This technique can be applied to compare different programs and determine their relative advantages and shortcomings allowing the selection of the most convenient for a given problem.

A FORTRAN program has been wirtten to generate doublets of gaussian shape with variable area, width and separation between peaks. The spectra obtained in this way is then analyzed with the program whose performance one wants to determine. From the comparison of the results of the program with the data of the original simulated spectra the following points, can be deduced:

(a) finding of spurious peaks;

(b) accuracy in the determination of peak areas;

(c) consistency in the resolution of doublets and their mirror image, and doublets and their multipole image;

(d) capability of the program to resolve a doublet with an error in the area less or equal to a given value;

(e) best range of gaussian widths for an efficient use of the program.

In the actual program studied here it was found that it could identify peaks with an area greater than 10 counts (over zero background). The program finds spurious peaks of about 5 counts in the process of resolving a doublet. In addition it shows a non-symmetric behavior in the resolution of mirror doublets.

It is interesting to point out that for doublets that are not well resolved the individual areas are given with large errors but the total number of counts is very well determined.

The results show that an efficient use of the program is obtained for a width range of $\sigma = 2.0$ to $\sigma = 2.5$ channels.

---

1 A.Díaz Romero, Informe CNEA N° 328 (1972), Buenos Aires, Argentina.

2 J.Picard, Rapport CEA R3024 (1966), CEN, Saclay, France.

XI.3. Subroutines Developed for the IALE Facility.

E.Achterberg.

Three main routines for the HP-2116B computer have been completed to process nuclear spectroscopy data. The purpose of this work has been (a) to use the full capacity of the local computing facility, avoiding expensive processing of data in commercial machines, and (b) to allow continuous supervision and control by the user through interactive programming.

The programs which have been developed are:

(a) ANPIK. This is a program for analysis of γ-spectra which is divided in groups. It used non-linear iterative methods for fitiing an empirical function to the region of interest. The determination of errors has been emphasized in order to extract the maximum information from the statistical distribution.
Because of the small available system memory it has been necessary to use calculation routines having a low time efficiency. A number of variables must be recalculated at each iteration, causing a very slow operation of the program.

(b) LEVEL. This routine builds up nuclear levels starting from the γ-ray listing and using the already known levels. The program operates by statistical combination of γ-ray energies and levels, allowing its use in an iterative cycle mode.

(c) SKEMA. The purpose of this program is to determine the best values of the transition energies once the level scheme has been established. Its operation is based on the simultaneous consideration of all relationships established from the γ-rays connecting the obtained levels.

APPENDIX

XII. PERSONNEL OF THE DEPARTMENT OF NUCLEAR PHYSICS

A. Research Staff

Achterberg, E.		
Bes, D. R.*		
Ceballos, A. E.		
Dragun, O. M.		
Dussel, G. G.*		
Erramuspe, H. J.*	(1)	
Ferrero, A. M. J.	(2)	
Filevich, A.	(3)	
Hernández, A. M.	(4)	
Iglesias, F. C.	(5)	
Jech, A. E.*	(6)	
Kreiner, A. J.	(7)	
Liotta, R. J.	(8)	
Maqueda, E. E.*		
Mariscotti, M. A. J.	(9)	(Chairman)
Moragues, J. A.*		
Otero, D.		
Perez Ferreira, E. V.		
Pérez, M. L.*		
Perazzo, R. P. J.*		
Pomar, C.		
Proto, A. N.		
Reich, S. L.		
Rossi, J. J.		
Sametband, M. J.*	(10)	
Saraceno, M.	(11)	
Scheuer, G.		
Soffa, H. M.		
Testoni, J. E.*	(12)	
Ventura, E.	(13)	

* Fellow of the Consejo Nacional de Investigaciones Científicas y Técnicas (CONICET).
(1) During 1974 - 1975 at Centro Atómico Bariloche.
(2) On leave at the Universidad di Milano, Italy.
(3) Appointed June, 1974.
(4) On leave at the Universidad Autónoma de México, México.
(5) Terminated August 1974. Present address: Departamento de Combustibles Nucleares (CNEA).

(6) Terminated August 1975. Present address: Universidad Nacional de Luján, Pcia. de Buenos Aires, Argentina.
(7) Appointed October, 1974. On leave at Physik Department, der Techn. Universität München, Germany.
(8) Appointed December 1974. On leave at Niels Bohr Institute of Copenhague, Denmark.
(9) Appointed December 1974.
(10) Terminated September 1973. Present address: Departamento de Combustibles Nucleares (CNEA).
(11) Fellowship holder. Appointed June 1975.
(12) Terminated October 1975. Present address: Departamento de Reactores (CNEA).
(13) Appointed September, 1975.

B. Research Staff Associated to the Department

Behar, M.*

García Bermúdez, G. J.*

Hernández, E. S.*

C. Research Students

Chimento, L.

De Pino, J. I.

Gallacher, L.

Kalberman, G. R.

Kohan, C.

Lombardi, R.

Mac Donnel, D.

Pecyner, R.

Santi, E. A.

D. Programming Assistant

Díaz Romero, A. M.

E. Engineering Staff

Arizmendi, E. D.

Fazzini, N. A.

Requejo, R.

Sinderman, J.E.

F. Technical Staff

Cava, G.
Coralo, J.
D'Agostino, R.
Garanzini, J.
Gonzalez, H.
Gorgoschidse, A. (14)
Ietri, B. G.
Laffranchi, J.
Morales, A.
Prieto, J.
Professi, M.
Rodriguez, J. C.
Schevenels, L.
Tersigni, A.
Vidalle, J.

G. Secretaries

Corvalan, J.
Neufeld, M.

H. Maintenance Staff

Barzola, G.
De Brasi, O.
Gomez, D. B.

(14) Deceased.

XIII. PUBLICATIONS OF THE DEPARTMENT OF NUCLEAR PHYSICS

A. Papers published or accepted during report period

- Analysis of Two phenomenological Descriptions of Ground-State Bands in Spherical and Closed-Shell Nuclei, J.I.Gorfinkiel, M.A.J.Mariscotti and C.Pomar, Phys. Rev. C9 (1974) 1243.

- The (d,^{6}Li) Reaction in the f-p Shell at E_d=27.2 MeV, A.E.Ceballos, H.J.Erramuspe, A.M.J.Ferrero, M.J.Sametband, J.E.Testoni, D.R.Bes, E.E.Maqueda, R.P.J.Perazzo and S.L.Reich, Nucl. Phys. A228 (1974) 216.

- Levels of ^{91}Rb and ^{91}Sr Fed in the Decays of ^{91}Kr and ^{91}Rb, E.Achterberg, F.C. Iglesias, A.E.Jech, J.A.Moragues, D.Otero, M.L.Pérez, A.N.Proto, J.J.Rossi and W.Scheuer, Phys. Rev. C9 (1974) 299.

- Levels of ^{93}Rb, ^{93}Sr and ^{93}Y Fed in the Decays of ^{93}Kr, ^{93}Rb and ^{93}Sr, E.Achterberg, F.C.Iglesias, A.E.Jech, J.A.Moragues, D.Otero, M.L.Pérez, A.N.Proto, J.J. Rossi and W.Scheuer, Phys. Rev. C10 (1974) 2526.

- On-Line Gamma-Efficiency Calibration Using Fission Produced ^{138}Xe and ^{138}Cs Sources, E.Achterberg, F.C.Iglesias, A.E.Jech, J.A.Moragues, D.Otero, M.L.Pérez, A.N.Proto, J.J.Rossi, and W.Scheuer, Nucl. Instr. and Meth. 116 (1974) 453.

- The Spin of the 2.198 keV Level in ^{74}Ge and Multipole Mixing Ratios of Gamma Transitions in the Decay of ^{74}As, M.C.Cambiaggio, G.García Bermúdez and M. Behar, Z.Physik A275 (1975) 183.

- Multipole Mixing Ratios of Transitions in ^{175}Lu Populated from the Decay of ^{175}Hf, L.M.Quinones, M.Behar, Z.W.Bragowski, M.C.Cambiaggio, G.García Bermúdez and E.S.Hernández, Z.Physik A 274 (1975) 173.

- Spins of the 1248 and 1958 keV Levels in ^{124}Te determined from Gamma-Gamma Directional and Polarization Directional Correlations, M.Behar, G.García Bermúdez, A.Filevich and M.C.Cambiaggio, Phys. Rev. (to be published).

- Levels of ^{141}Cs and ^{141}Ba from the Decays of ^{141}Xe and ^{141}Cs, D.Otero, A.N. Proto and F.C.Iglesias, Phys. Rev. (to be published).

- Level Structure of ^{73}Se from the ^{72}Ge(α,3nγ), M.Behar, G.García Bermúdez, A.M. Hernández and M.A.J.Mariscotti, Nucl. Phys. (to be published)

- Level Structure of ^{72}As Studied with the (α,xnp) Reaction, M.A.J.Mariscotti, M.Behar, A.Filevich, G.García Bermúdez, A.M.Hernández and C.Kohan, Nucl. Phys. (to be published).

- Strength of the Multipole Pairing Coupling Constant, R.A.Broglia, D.R.Bes and B.S.Nilsson, Phys. Lett. 50B (1974) 213.

- Properties of Single-Particle States in the ^{208}Pb Region, S.L.Reich, H.M.Soffa and D.R.Bes, Nucl. Phys. A233 (1974) 105.

- Nuclear Field Theory as a Method of Treating the Problem of Overcompletness in Descriptions Involving Elementary Modes of Both Quasi-Particles and Collective Type, D.R.Bes, G.G.Dussel, R.A.Broglia, R.J.Liotta and B.R.Mottelson, Phys. Lett. 52B (1974) 253.

- Regge Poles and Forward-Angle Anomalies in Transfer Reactions, R.C.Fuller and O.Dragún, Phys. Rev. Lett. 32 (1974) 617.

- Charge Exchange (^{6}Li,^{6}He) and the Two-Step Pickup-Stripping (^{6}Li,^{7}Li) (^{7}Li,^{6}He) Excitation Mode, H.H.Duhm, H.Hafner, R.Renfordt, M.Goldschmidt, O.Dragún and K.I.Kubo, Phys. Lett. 48B (1974) 1

- Shape-Phase Transitioners as Pairing Back-Benders, R.P.J.Perazzo and S.L.Reich, Phys. Lett. 55B (1975) 354.

- Microscopic Description of Isoscalar and Isovector Giant Quadrupole Resonances, D.R.Bes, R.A.Broglia and B.S.Nilsson, Phys. Lett. 16C (1975) 1.

- Simultaneous Treatment of Surface and Pairing Nuclear Fields, D.R.Bes, R.A. Broglia, G.G.Dussel and R.J.Liotta, Phys. Lett. 56B (1975) 109.

- The Normalization of States in Perturbation Theories, D.R.Bes, G.G.Dussel and H.M.Sofía, Am. Journ. Phys. (to be published).

- The Nuclear Field Treatment of Some Exactly Soluble Models, D.R.Bes, R.A.Broglia, G.G.Dussel, R.J.Liotta and H.M.Soffa, Nucl. Phys. (to be published).

- Application of Nuclear Field Theory to Monopole Interactions which include all the Vertices of a General Force, D.R.Bes, R.A.Broglia, G.G.Dussel, R.J.Liotta and H.M.Sofía, Nucl. Phys. (to be published).

- On the Field Treatment of a General Two Body Interaction, D.R.Bes, R.A.Broglia, G.G.Dussel, R.J.Liotta and R.P.J.Perazzo, Nucl. Phys. (to be published).

- Two-Body Stripping Reactions Populating Isobaric Multiplets in the Region $40 \leq A \leq 56$, O.Dragún, D.R.Bes and E.E.Maqueda, Nucl. Phys. (to be published).

B. Papers Presented at Meetings

1. Topical Conference on Problems of Vibrational Nuclei, Zagreb, Yugoslavia, September 24 - 27, 1974.

- Equivalence between Feynman-Goldstone and Particle-Phonon Diagrams for Finite Many-Body Systems, D.R.Bes and R.A.Broglia.

2. Winter Meeting of the German Physical Society, Bochum, Germany, March, 1974.

- Study of the $^{12,13}C(^{6}Li,\alpha)$ Reactions, I.Tserruya, O.Dragún, B.Rosner, S.Kochan and K.Bethge.
- Was Lernt Man aus der $(^{6}Li,^{6}He)$ Reaktion, H.H.Duhm, K.I.Kubo, H.Hafner, O. Dragún and W.Daehnik.

3. Meeting of the Dutch-German Physical Society, La Haya, Holland, April, 1975.

- Ground State Bands in ^{142}Gd and ^{140}Sm, H.Beuscher, W.F.Davidson, R.M.Lieder, A.Neskakis, O.W.B.Schult and M.A.J.Mariscotti.
- Structure of ^{144}Gd, H.Beuscher, W.F.Davidson, R.M.Lieder, A.Neskakis, O.W.B. Schult and M.A.J.Mariscotti.

4. International Conference on Hyperfine Interactions, Lovaine, Belgium, September, 1975.

- Electric Field Gradients Produced by Impurity Atoms in a Cubic Ag Lattice, F. C.Zawislak, R.P.Livi, L.Amaral, J.Schaf and M.Behar.

5. 61a. Reunión de la Asociación Física Argentina, Buenos Aires, Argentina, June, 1975.

- Estudio del Esquema de Niveles del ^{141}La, D.Otero, A.N.Proto, G.Kalberman, F.C.Iglesias.
- Estudio de los Decaimientos β^- del ^{141}Xe y ^{141}Cs, D.Otero, A.N.Proto, F.C. Iglesias.
- Determinación de Momentos Angulares y Parámetros de Mezcla en el Decaimiento del ^{74}As, M.C.Cambiaggio, G.García Bermúdez and M.Behar.
- Estudio del ^{72}As y ^{74}As Mediante Reacciones (α,np) y $(\alpha,3np)$ sobre ^{70}Ge y ^{72}Ge, A.M.Hernández, A.Filevich, M.Behar, G.García Bermúdez and M.A.J.Mariscotti.
- Momento Angular y Paridad del Nivel a 1958 keV en el ^{124}Te, M.C.Cambiaggio, M.Behar, G.García Bermúdez and A.Filevich.

- Sistema para la Medición de Vidas Medias en el Rango mseg-seg en el Sincrociclotrón de Bs. As., E.Santi, N.A.Fazzini, J.E.Sinderman and M.A.J.Mariscotti.
- Estudio del Decaimiento $^{49}Se \rightarrow {}^{49}Ti$, M.T.Bodio, A.M.Hernández and M.A.J.Mariscotti.
- Parametrización del Comportamiento Anómalo del Momento de Inercia Nuclear, A.M.Hernández, J.I.Gorfinkiel and M.A.J.Mariscotti.
- Comportamiento de las Funciones de Excitación en Reacciones con Partículas Alfa sobre Blancos Livianos, C.Pomar, M.A.J.Mariscotti.
- Alimentación de la Banda Yrast en Reacciones (HI,xn), D.Mac Donnell and M.A. J.Mariscotti.
- Sistemática de Vidas Medias de Radio-Nucleídos Deficientes de Neutrones, L.P.Chimento and M.A.J.Mariscotti.
- Interfase Hewlett-Packard-Intertechnique, R.Pecyner and J.E.Sinderman.
- Primera Observación de Estados Excitados del ^{142}Gd, M.A.J.Mariscotti, H.Beuscher, W.F.Davidson, R.M.Lieder, A.Neskakis and O.W.B.Schult.
- Estructura del ^{144}Gd, M.A.J.Mariscotti, H.Beuscher, W.F.Davidson, H.Jager, R.M.Lieder and O.W.B.Schult.

6. <u>62a. Reunión de la Asociación Física Argentina, Rosario, Argentina, December 9 - 11, 1975</u>.

- Teoría de Campos Nuclear, G.G.Dussel, Informe Invitado.
- Estudio del Decaimiento del ^{141}Ba, A.N.Proto and D.Otero.
- Influencia en Reacciones de Transferencia de dos Nucleones de la Dependencia en Isospin del Potencial Optico, O.Dragún, D.R.Bes, E.E.Maqueda.
- La Normalización de Estados en Teorías de Perturbaciones, D.R.Bes, G.G.Dussel and H.M.Sofía.
- La Teoría Nuclear de Campo de algunos Modelos Exactamente Solubles, D.R.Bes, R.A.Broglia, G.G.Dussel, R.J.Liotta and H.M.Sofía.
- Aplicación de la Teoría Nuclear de Campos a Interacciones Monopolares que Incluyen todos los Vértices de una Fuerza General, D.R.Bes, R.A.Broglia, G.G. Dussel, R.J.Liotta and H.M.Sofía.
- Sobre el Tratamiento de Campo de una Interacción General de dos Cuerpos, D.R. Bes, R.A.Broglia, G.G.Dussel, R.J.Liotta and R.P.J.Perazzo.

- Estados Espúreos en Núcleos Impares, D.R.Bes, R.A.Broglia, G.G.Dussel, R.J. Liotta and H.M.Sofía.
- Aproximación Yrast en la Zona del Zr, Mo y Ru, R.P.J.Perazzo and S.L.Reich.
- Observación de dos Nuevas Vidas Medias en ^{72}As, C.Kohan, M.Behar, A.Filevich, G.García Bermúdez, A.M.Hernández and M.A.J.Mariscotti.
- Estudio de los Niveles Nucleares en ^{140}La, G.García Bermúdez, A.Filevich and M.Behar.
- Niveles Excitados en ^{73}Se a partir de la Reacción ^{72}Ge(α,3n), M.Behar, A.Filevich, G.García Bermúdez, A.M.Hernández and M.A.J.Mariscotti.
- ¿"Backbending" en Núcleos Cercanos a Capa Cerrada?, M.A.J.Mariscotti.
- Reacciones ^{64,66}Zn(α,npγ) y Estructura de ^{66}Ga y ^{68}Ga, C.Pomar, M.A.J.Mariscotti, P.Kleinheinz, R.M.Lieder and O.W.B.Schult.
- Descripción Autoconsistente de la Interrelación entre Deformación Cuadrupolar y Deformación de Apareamiento, A.Plastino, E.S.Hernández and R.P.J.Perazzo.

C. Internal Reports

- Sistema de Transporte del Haz Externo del Sincrociclotrón de 28 MeV, M.J.Sametband, A.M.J.Ferrero, A.E.Ceballos, H.J.Erramuspe, H.M.Sofía and N.A.Fazzini, Publicación Interna N° 367 (1974).

D. Ph.D. Theses*

- Dino Otero, Universidad Nacional de La Plata, December, 1974, Estudio de productos de Fisión y Esquema de Niveles pertenecientes al ^{141}Ba.
- Araceli N. Proto, Universidad Nacional de La Plata, December, 1974, Estudio de los Decaimientos β^- del ^{141}Xe y ^{143}Xe.
- Hugo M. Sofía, Universidad de Buenos Aires, March, 1975, Teoría de Campos Nucleares.
- Armando M. J. Ferrero, Universidad de Buenos Aires, March, 1975, Reacciones (d,^{6}Li). Análisis con Canales Acoplados.

* Submitted in partial fulfillment of the requirement for the degree of Doctor en Física.

E. Licenciatura Theses*

- Andrés J. Kreiner, Universidad de Buenos Aires, 1974, Sistema para Variar la Energía del Haz de Partículas Alfa del Sincrociclotrón de Buenos Aires y su Aplicación a las Reacciones (α,xn).
- Douglas Mac Donnell, Universidad de Buenos Aires, 1974, Alimentación de la Banda Yrast en la Reacción Gd(H.I.,xn)Dy.
- Emilio A. Santi, Universidad de Buenos Aires, 1974, Sistema para la Medición de Vidas Medias en el Rango mseg-seg, en el Sincrociclotrón de Buenos Aires.
- Ruben Pecyner, Universidad de Buenos Aires, 1975, Diseño y Realización de un Sistema de Análisis Semiautomático de Espectros γ en el Sincrociclotrón de Buenos Aires y su Aplicación en el Estudio de las Reacciones $^{57}Fe(\alpha,xnyp\gamma)$.
- Carlos A. Kohan, Universidad de Buenos Aires, 1975, Sistema para la Medición de Vidas Medias en el Rango de nseg Utilizando la Microestructura Temporal del Haz de Partículas del Sincrociclotrón de Buenos Aires.
- Jorge I. De Pino, Universidad de Buenos Aires, 1974, Método de Análisis en Base al Modelo Optico Nuclear de Secciones Eficaces Diferenciales de Dispersión Elástica.
- Rina Lombardi, Universidad de Buenos Aires, 1974, Distribución Angular de la Sección Eficaz de Reacción $^{66}Zn(d,^{6}Li)^{62}Ni$ a E_d = 27.25 MeV.

* Submitted in partial fulfillment of the requirement for the degree of Licenciado en Física.